Molecular ordering of ceramide-mediated mitochondrial apoptosis

Amrita Jain

ISBN: 978-94-6295-667-4

About the cover: Destruction of the cell (iStock.com| ID- 623942546)

Printed by: Proefschriftmaken.nl,Vianen

Molecular ordering of ceramide-mediated mitochondrial apoptosis

Moleculaire analyse van ceramiden-gemedieerde mitochondriële apoptose

(met een samenvatting in het Nederlands)

Proefschrift

ter verkrijging van de graad van doctor aan de Universiteit Utrecht
op gezag van de rector magnificus, prof. dr. G.J. van der Zwaan,
ingevolge het besluit van het college voor promoties in het
openbaar te verdedigen
op donderdag 13 juli 2017 des middags te 12:45 uur

door

Amrita Jain

geboren op 1 maart 1988, Khandwa, India

Promotoren: Prof. dr. J.C.M. Holthuis
Prof. dr. J.A. Killian

The research described in this thesis was performed at the Department of Molecular Cell Biology, University of Osnabrück, Germany and funded by the European Union Seventh Framework Program Marie-Curie ITN ‘Sphingonet’ (Grant 289278) and the Deutsche Forschungsgemeinschaft (Sonderforschungsbereich/SFB944-P14).

TABLE OF CONTENTS

Chapter 1

Membrane contact sites, ancient and central hubs of cellular lipid logistics

Amrita Jain[1], Joost C.M. Holthuis[1, 2]

[1]Molecular Cell Biology Division, Department of Biology/Chemistry, University of Osnabrück, D-49076 Osnabrück, Germany; [2]Membrane Biochemistry & Biophysics, Bijvoet Center and Institute of Biomembranes, Utrecht University, 3584 CH Utrecht, The Netherlands

Submitted to BBA - Molecular Cell Research

Membrane contact sites, ancient and central hubs of cellular lipid logistics

Amrita Jain[1] and Joost C.M. Holthuis[1,2]

[1]Molecular Cell Biology Division, Department of Biology/Chemistry, University of Osnabrück, D-49076 Osnabrück, Germany; [2]Membrane Biochemistry & Biophysics, Bijvoet Center and Institute of Biomembranes, Utrecht University, 3584 CH Utrecht, The Netherlands

Corresponding author: Joost C.M. Holthuis, Molecular Cell Biology Division, University of Osnabrück, Barbarastrasse 13, D-49076 Osnabrück, Germany. E-mail: holthuis@uos.de

ABSTRACT

Membrane contact sites (MCSs) are regions where two organelles are closely apposed to facilitate molecular communication and promote a functional integration of compartmentalized cellular processes. There is growing evidence that MCSs play key roles in controlling intracellular lipid flows and distributions. Strikingly, even organelles connected by vesicular trafficking exchange lipids en bulk via lipid transfer proteins that operate at MCSs. Herein, we describe how MCSs developed into central hubs of lipid logistics during the evolution of eukaryotic cells. We then focus on how modern eukaryotes exploit MCSs to help solve a major logistical problem, namely to preserve the unique lipid mixtures of their early and late secretory organelles in the face of extensive vesicular trafficking.

INTRODUCTION

The identity and function of organelles in eukaryotic cells critically rely on the flux of proteins and lipids that they acquire and lose through cytosolic exchange and vesicular trafficking. The repertoire of membrane lipids in eukaryotes typically comprises hundreds of different species (Shevchenko and Simons, 2010). Besides defining the boundary of each organelle, membrane lipids provide specific cues for proteins to support organelles in executing their specialized tasks (Bigay and Antonny, 2012; Jackson et al., 2016). Consequently, the lipid composition of organelles varies dramatically and many lipids are unevenly distributed between the two leaflets of the organellar bilayer (van Meer et al., 2008). How cells monitor and fine-tune the unique lipid mixtures in each organelle to sustain their compartmentalized organization is a major outstanding question in current cell biology.

The non-random lipid distributions in cells cannot be explained by local metabolism alone. For instance, some lipids (e.g. sterols) accumulate and exert their biological activity at locations distant from their site of synthesis. Additionally, enzymes catalyzing sequential steps in pathways of lipid metabolism often reside in membranes of distinct organelles. Spontaneous desorption of a lipid monomer

from a bilayer and its free diffusion through the cytosol is too slow to support any meaningful transport of most lipids (Jones et al., 1990; McLean and Phillips, 1981; Silvius and Leventis, 1993). As lipids are the principal constituents of transport vesicles, bulk amounts of lipids can be moved from one organelle to another by vesicular trafficking. However, various organelles, including mitochondria and plastids, are not connected to the vesicular transport network yet rely on lipid import for proper function. In addition, bulk transport of various lipids between the ER and plasma membrane continues undisrupted when vesicular trafficking is shut off (Baumann et al., 2005; Kaplan and Simoni, 1985; Vance et al., 1991), suggesting that non-vesicular mechanisms play a major role in lipid trafficking along the secretory pathway.

Accumulating evidence indicates that inter-organellar lipid transport is facilitated at membrane contact sites (MCSs), regions where two organelles come within a distance of 30 nm from each other. MCSs are found between almost every pair of organelles (Gatta and Levine, 2017). Despite their heterogeneity, MCSs share some common features. They are typically enriched in proteins involved in lipid metabolism and transport, their formation relies on a tethering of apposing membranes through protein-protein and protein-lipid interactions, and they tend to be dynamic structures that undergo assembly and disassembly in response to changing physiological conditions. While MCSs participate in a wide array of cellular processes including ion homeostasis, organelle inheritance, and apoptosis (De Vos et al., 2012; Iwasawa et al., 2011; Lackner et al., 2013), we here focus on their fundamental role as centers of lipid logistics. There is reason to believe that MCSs are ancient structures that evolved before the establishment of vesicular trafficking. We describe how MCSs may have played a crucial role in the acquisition of bacteria-type lipids from proto-mitochondria by their archeael host, and how mitochondria in modern eukaryotes boost their capacity to acquire essential lipids by creating a variety of MCSs with different organelles of the endomembrane system. We then discuss how lipid transfer proteins operating at ER-Golgi contact sites allow lipids to bypass vesicular connections, and how this arrangement enables cells to build sphingolipid and sterol gradients along the secretory pathway, the maintenance of which is key to a proper functioning of their early and late secretory organelles.

Membrane contact sites and the evolutionary switch in membrane lipid composition

Major events in the evolution of eukaryotic cells included the acquisition of a nucleus, an endomembrane system and mitochondria. The general consensus is that mitochondria arose from endosymbiotic a-proteobacteria in an archaeal host (Yang et al., 1985). However, conflicting views exist on how the merger of two prokaryotes gave rise to cells possessing an elaborate endomembrane system and how the archaeal lipids of the host's cell membrane were replaced by bacterium-type lipids that are characteristic of eukaryotes. Archaeal lipids are composed of glycerol-1-phosphate with ether-linked, methyl-branched isoprenoid chains (Lombard et al., 2012). The structural features of these lipids allow archaea to retain the physical

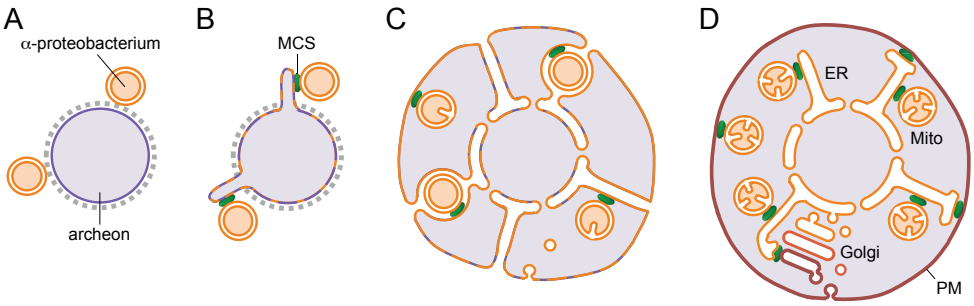

Figure 1. Inside-out model showing the step-wise evolution of eukaryotic cells. (**A**) Free-living α-proteobacteria (proto-mitochondria) form initial contacts with an archaeal host cell (archeon). While α-proteobacteria are surrounded by a double membrane composed of lipids with ester-linked fatty acids (orange), the archeon has a single membrane comprising lipids based on isoprene ethers (purple) and a glycoprotein-rich outer cell wall (grey, dashed). (**B**) Protrusions extending from the archaeal host form primordial membrane contact sites with proto-mitochondria to facilitate an exchange of biomolecules, including lipids. Acquisition of bacterium-type lipids by the host initiates a gradual chemical transition of its membrane. (**C**) Protrusions laterally extend to blebs that increasingly enclose proto-mitochondria. Spaces between the blebs correspond to the lumen of the future ER and nuclear envelope. An increased contact area between the symbionts and translocation of proto-mitochondria into the cytoplasmic compartment of the host allow closer metabolic ties, involving a diversification of MCSs. Acquisition of bacterial lipid biosynthesis machinery by the host results in a further loss of archaeal lipids. The transition from archaeal to bacterial membranes facilitates the development of vesicular trafficking machinery. (**D**) Fusion steps among blebs seal the ER off from the outside world, giving rise to a continuous plasma membrane and promoting the development of a secretory pathway. This is accompanied by the evolution of sphingolipid and sterol biosynthetic/transport machinery and the emergence of the Golgi complex, which serves as a lipid distillation apparatus to keep sphingolipid/sterol levels low in the ER (orange) and high at the plasma membrane (red). Sphingolipid/sterol traffic mediated by lipid transfer proteins at ER-Golgi contact sites bypasses vesicular traffic to exert optimal control over the unique lipid mixtures of the ER and plasma membrane. Figure adapted from (Baum and Baum, 2014).

properties of their membranes over a wide range of temperatures (Chong, 2010). The bulk of bacterial and eukaryotic membrane lipids, on the other hand, are based on glycerol-3-phosphate with unbranched, ester-linked fatty acids. Both eukaryotes and some bacteria, but not archaea, also produce sphingolipids and sterols, which help control membrane fluidity (Desmond and Gribaldo, 2009; Hannich et al., 2011). Contrary to archaeal membranes, bacterial and eukaryotic membranes are adjusted to the phase transition boundary at physiological temperatures. This property is thought to facilitate the dynamic and reversible membrane deformations that are characteristic of eukaryotic cells (Lingwood and Simons, 2010). Many eukaryotic genes involved in lipid metabolism and transport have their closest prokaryotic relatives in a-proteobacteria (Thiergart et al., 2012). While this implies that eukaryotes acquired

their bacterium-type lipids from mitochondria, models of eukaryotic evolution struggle with the question how the dramatic transition from archaeal membranes to bacterium-like membranes may have occurred (Lombard et al., 2012).

A widely favored model is that the nucleus and endoplasmic reticulum (ER) were formed within a prokaryotic cell by invaginations of the limiting membrane, and that proto-mitochondria entered the cell via phagocytosis (Martin et al., 2015; Mast et al., 2014; Molecular biology of the cell, by Bruce Alberts, Dennis Bray, Julian Lewis, Martin Raff, Keith Roberts, and James Watson; Garland Publ. Inc., New York, 1146 pp. $35.95 (U.S), 1986). One problem with this "outside-in" model on the origin of the nucleus, ER and mitochondria is that archaea can form outward protrusions but are not known to undergo processes like endocytosis or phagocytosis. Moreover, scission of endosomes and phagosomes from the plasma membrane requires dynamins, a family of large GTPases that originate from bacteria, not from archaea (Ku et al., 2015). Phagocytosis results in the formation of a food vacuole, which needs to be acidified to allow the breakdown of its contents by acid-activated proteases. Eukaryotic vacuole acidification requires a vacuolar or V-type ATPase. This enzyme stems from an archaeal A-type ATPase whose function in creating ATP from redox-generated ion gradients was reverted to acidify food vacuoles at the expense of cytosolic ATP (Grüber and Marshansky, 2008). Theories that place phagocytosis before the acquisition of mitochondria fail to account for the source of cytosolic ATP required to acidify food vacuoles. Such theories are also hard to reconcile with the notion that the physicochemical properties of membranes based on bacterium-type lipids were a likely prerequisite for the evolution of the dynamic and energy-intensive process of vesicular trafficking.

The above considerations have led to the formulation of alternative models in which the acquisition of mitochondria predates phagocytosis. In their recent "inside-out" model of eukaryotic cell evolution, Baum and Baum (Baum and Baum, 2014) propose that an archaeal host extruded membrane-bound blebs beyond its cell wall that formed intimate contacts with ectosymbiotic proto-mitochondria to facilitate an exchange of biomolecules, including lipids (Fig. 1). Lateral expansion of these blebs eventually trapped populations of proto-mitochondria, with continuous spaces between the blebs giving rise to the nuclear envelope and ER. At some point, proto-mitochondria moved into the cytoplasmic compartment by penetrating the primordial ER membrane, akin to the mechanism by which pathogenic bacteria found within the ER and Golgi of modern eukaryotes gain entry to the cytoplasm (Emelyanov, 2001). Fusion steps among blebs ultimately yielded a continuous plasma membrane, hence separating the ER from the outside world and promoting the development of the secretory pathway. As outlined below, these events were accompanied by a diversification of lipid biosynthetic machinery and allowed the ER and plasma membrane to specialize in carrying out biogenic and barrier functions, respectively.

A key aspect of the "inside-out" model of Baum and Baum is that proto-mitochondria established close metabolic and physical ties with their archaeal host prior to the

formation of the nucleus and the evolution of phagocytosis. Intimate membrane contacts with the ectosymbiotic proto-mitochondria allowed the archaeal host to acquire bacterium-type lipids and initiate a chemical transition of its membranes before bacterial genes for lipid biosynthesis were transferred to its genome (Fig. 1). The transient occurrence of membranes containing a mixture of archaeal and bacterial lipids may have helped core protein machinery of the host (e.g. V-type ATPase, Sec61/SecY translocon, *N*-linked glycosyltransferases) to survive the transformation from archaeal to eukaryotic-type membranes while facilitating the development of a secretory pathway. Under the "inside-out" model, lipid traffic across membrane contacts between proto-mitochondria and their host occurred early on in eukaryotic evolution, before the establishment of the ER. In line with this idea, membrane contacts between mitochondria and ER are ancient (Wideman et al., 2014) and still function as central hubs of lipid traffic in modern eukaryotes (see below).

Diversification of membrane contact sites as platforms of lipid exchange

While mitochondria in modern eukaryotes retain a critical role in lipid biosynthesis and produce some of their own membrane lipids such as cardiolipin, they rely on bulk lipid import for proper function (Fig. 2) (Dimmer and Rapaport, 2017; Flis and Daum, 2013). The ER is the principal supplier of membrane lipids to mitochondria and all other organelles. Newly synthesized lipids are exported from the ER as components of transport vesicles or by lipid transfer proteins (LTPs) that operate at MCSs. Transport by LTPs is crucial for supplying ER lipids to mitochondria as these organelles are not served by vesicular trafficking. LTPs have hydrophobic pockets or clefts that can take up a single lipid molecule upon its partial desorption from a donor membrane. A conformational change might then occur to seal the binding pocket off, protecting the lipid from the aqueous cytoplasm. The reverse process then results in unloading of the lipid at the acceptor membrane. Thus, LTPs act as catalysts of monomeric lipid exchange between membranes, presumably by reducing the energy barrier for dissociating lipid monomers from the membrane (Lalanne and Ponsin, 2000; Lev, 2010; Wirtz and Zilversmit, 1968). Recent estimates of the rate constants for nonvesicular sterol transport in yeast indicate that sterol desorption from the membrane rather than LTP-mediated sterol diffusion through the cytosol is rate limiting (Dittman and Menon, 2017). This implies that there would be no apparent kinetic benefit to having LTP-mediated sterol transfer occur at MCSs. However, combining the action of LTPs with that of tether proteins responsible for creating contacts between a donor and acceptor organelle may offer additional advantages. For instance, restricting transport to subdomains of two organelles may enhance the directness and efficiency of transport for lipid species that are readily consumed in metabolic pathways, prevent deleterious redistribution of toxic lipid species, facilitate the establishment and maintenance of lipid gradients, and provide opportunities for regulatory crosstalk among distinct lipid classes.

Interestingly, work in budding yeast uncovered a protein complex that likely serves a dual role in membrane tethering

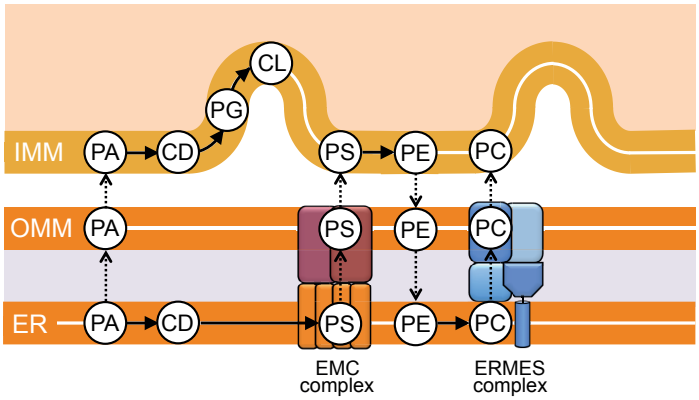

Figure 2. Lipid traffic at ER-mitochondria contact sites. Lipid transport between ER and mitochondria is indicated by dashed arrows. Metabolic conversion of one lipid to another is indicated by a solid arrow. The ERMES and EMC protein complexes have been implicated in PC and PS transport at ER-mitochondria contact sites in yeast, respectively. Note that only the EMC complex is conserved in mammalian cells. While phosphatidylserine (PS) synthesis in yeast involves an enzymatic reaction in which CDP-diacylglycerol (CD) reacts with serine, PS synthesis in mammalian cells relies on a base-exchange reaction in which serine replaces the choline or ethanolamine head group of phosphatidylcholine (PC) and phosphatidylethanolamine (PE), respectively (not shown). OMM, outer mitochondrial membrane; IMM, inner mitochondrial membrane; PA, phosphatidic acid; PG, phosphatidylglycerol; CL, cardiolipin.

and lipid transport at ER-mitochondria contacts. This so-called ER-mitochondrial encounter structure or ERMES complex is composed of four core-subunits: the mitochondrial outer membrane proteins Mdm10 and Mdm34, the integral ER protein Mmm1 and the soluble cytosolic subunit Mdm12 (Kornmann et al., 2009). Three of the four ERMES subunits (i.e. Mdm34, Mdm12, and Mmm1) contain a synaptotagmin-like, mitochondrial and lipid-binding protein (SMP) domain. Proteins with SMP domains typically share two additional characteristics, namely localization to MCSs and the ability to bind and, in some cases, transfer lipids (Saheki et al., 2016). Structural analysis of a complex formed between the SMP domains of Mdm12 and Mmm1 revealed an extended tubular structure traversed by a hydrophobic channel (AhYoung et al., 2015). Biochemical studies showed that the Mdm12-Mmm1 complex preferentially binds phosphatidylcholine (PC), a bulk lipid whose import by mitochondria is essential to sustain their function (Vance, 2014). While these findings support a primary role of ERMES in lipid transport at ER-mitochondria contact sites, direct proof for this is lacking. Phylogenetic analyses revealed that ERMES, though present in the common ancestor of yeast and animals, was lost in the animal lineage (Wideman et al., 2014). Thus, at some point in evolution, ERMES became functionally redundant.

Indeed, the modest changes in mitochondrial lipid composition observed in ERMES mutants suggest that eukaryotes developed alternative pathways for lipid

delivery to mitochondria. For instance, loss of ERMES in yeast enhances formation of mitochondria-vacuole/lysosome contacts, termed vCLAMPs (Elbaz-Alon et al., 2014; Hönscher et al., 2014). Mutations disrupting both ERMES and vCLAMPs render cells nonviable while acute depletion of both complexes causes additive effects in mitochondrial lipid import. As vacuoles are linked to the ER, both directly, through nuclear-vacuolar junctions (NVJs), and indirectly, through vesicular traffic, vCLAMPs may serve as a bypass for lipid exchange between ER and mitochondria. However, the mitochondrial subunit(s) of vCLAMPs remains to be identified, and its other core components do not contain known lipid-binding pockets. Interestingly, Lam6/Ltc1, member of a conserved family of ER-anchored proteins with StART-like lipid transfer domains (Gatta et al., 2015), was found to co-localize with three inter-organellar contacts: ERMES, vCLAMP, and NVJ (Elbaz-Alon et al., 2015; Murley et al., 2015). Overexpression of Lam6/Ltc1 caused an expansion of all three MCSs. Moreover, Lam6/Ltc1 binds sterols *in vitro* and is required for the formation of sterol-enriched vacuolar domains under stress conditions (Murley et al., 2015). Thus, Lam6/Lct1 may coordinate vacuolar and mitochondrial sterol homeostasis. Whether Lam6/Ltc1 and other members of the StART-like LTP family catalyze lipid transfer across membrane contacts remains to be established.

A screen for components influencing mitochondrial import of phosphatidylserine (PS) in yeast yielded a novel ER-mitochondria tether, termed the ER-membrane protein complex (EMC; Fig. 2) (Lahiri et al., 2014). This complex contains six subunits, Emc1-6, and interacts with the outer mitochondrial membrane protein Tom5 at foci that overlap with ERMES. EMC mutants have a reduction in the amount of ER tethered to mitochondria and are defective in PS transport to mitochondria (Lahiri et al., 2014). A notable difference between the EMC and ERMES is that only the EMC is conserved in higher eukaryotes. As EMC subunits have also been implicated in protein folding and quality control in the ER, their role in ER-mitochondria lipid trafficking and tethering may be indirect.

While the concept of ER-mitochondria MCSs as major sites of membrane lipid trafficking first emerged from biochemical studies in mammalian cells more than two decades ago (Rusiñol et al., 1994; Vance, 1990), the identity of functional homologues of ERMES in mammals has yet to be established (Dimmer and Rapaport, 2017; Herrera-Cruz and Simmen, 2017). Work in yeast showed that ERMES and other mitochondria-organelle contacts function as part of a dynamic network, whereby loss of one contact is compensated by reinforcement of another (Elbaz-Alon et al., 2015; Lang et al., 2015). This redundancy in interconnectivity obviously complicates a molecular dissection of mitochondrial lipid delivery pathways but also underscores the significance of membrane contacts as major hubs of lipid traffic in eukaryotic cells. Indeed, a prominent non-vesicular exchange of lipids even occurs at contacts between organelles that, contrary to mitochondria, are integrated into the vesicular transport network. For instance, the ER and Golgi complex exploit similar logistics for lipid transfer as mitochondria by recruiting a variety of LTPs to ER-Golgi contact sites, despite the fact that these organelles already

exchange lipids through intensive bi-directional vesicular trafficking. As discussed below, this arrangement sub-serves a fundamental transition in bulk lipid composition along the secretory pathway.

ER-Golgi contact sites contribute to a fundamental switch in lipid composition along the secretory pathway

Eukaryotes arose from their prokaryotic ancestors through the establishment of two distinct membrane systems, one centered on the ER and the other one on the plasma membrane, allowing specialization in function and lipid composition (Bigay and Antonny, 2012; Holthuis and Menon, 2014; Jackson et al., 2016). This may explain why the advent of eukaryotic cells was accompanied by the evolution of biosynthetic machinery for two entirely new classes of membrane lipids: sphingolipids and sterols (Hannich et al., 2011). Contrary to the bacterium-type glycerophospholipids, sphingolipids primarily contain saturated or *trans*-unsaturated acyl chains linked to a serine backbone. This hydrophobic structure, called ceramide, is the precursor of all major sphingolipids, including sphingomyelin (SM) and glycosphingolipids. The absence of the rigid kinks of *cis*-double bonds, which are common in acyl chains of glycerophospholipids, increases the packing density of sphingolipids in a bilayer. Consequently, at physiological temperatures, an SM bilayer exists in a solid gel phase with tightly packed, immobile chains (Koynova and Caffrey, 1995). However, these membranes become fluid upon addition of sterols. The latter molecules have an apolar inflexible core of four fused rings that interferes with the tight packing of saturated acyl-chains, thus preventing the transition of the membrane to the solid gel phase. At the same time, sterols exert a condensing effect on fluid membranes by reducing the flexibility of the acyl chains (Brown and London, 1998). This, in turn, increases membrane thickness and impermeability to solutes. Thus, sterols allow eukaryotes to drastically reduce unregulated solute movement across their membranes while keeping them fluid over a wide range of temperatures.

Because of their vital properties, eukaryotic cells developed complex mechanisms to control the abundance and subcellular distribution of sterols. The ER is the site of *de novo* sterol production and harbors important sensors of sterol levels (Motamed et al., 2011; Radhakrishnan et al., 2008). However, sterols are rare in the ER (5 mol% of total lipid) but abundant at the plasma membrane (30-40 mol%) (van Meer et al., 2008). This major imbalance in sterol distribution serves a clear purpose. A high concentration of sterols provides the plasma membrane with physicochemical properties that support its barrier function. Conversely, low sterol levels in the ER result in a loosely packed lipid bilayer that facilitates insertion of nascent membrane proteins, thus upholding the biogenic function of this organelle. Indeed, sterol excess inhibits protein import in the ER (Nilsson et al., 2001). This implies that eukaryotes must continuously remove sterols from the ER as they are synthesized, and concentrate them in the plasma membrane. This appears a daunting task, as bi-directional vesicular trafficking along the secretory pathway would constantly

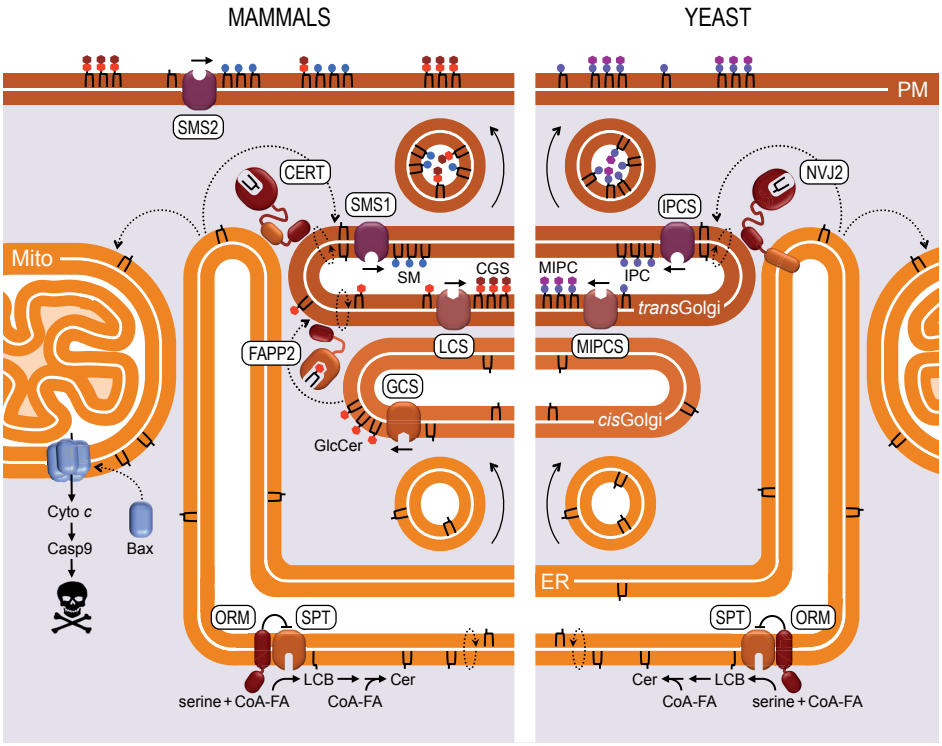

Figure 3. Sphingolipid biosynthesis in mammals and yeast. Sphingolipid synthesis begins on the cytosolic surface of the ER with the condensation of serine and coenzyme A-linked fatty acids (CoA-FA), a reaction catalyzed by serine palmitoyltransferase (SPT) to form long chain bases (LCB). LCBs are subsequently *N*-acylated by ER-resident ceramide synthases to form ceramides (Cer), the precursor of all sphingolipids. In mammals, a portion of newly synthesized ceramides is delivered to the *cis*-Golgi by vesicular trafficking for conversion into glucosylceramide (GlcCer) by glucosylceramide synthase (GCS) on the cytosolic surface. FAPP2 mediates non-vesicular GlcCer transport from the *cis* to the *trans*-Golgi for the production of complex glycosphingolipids (CGS) in the *trans*-Golgi lumen. However, the bulk of newly synthesized ceramides is delivered to the *trans*-Golgi by ceramide transfer protein CERT to form sphingomyelin (SM) by SM synthase SMS1 in the *trans*-Golgi lumen. SM and CGS reach the cell surface by vesicular transport. A second SMS-isoform, SMS2, is primarily active on the cell surface. Yeast lacks structural homologues of SMS but instead contains a functionally analogous enzyme to produce inositol phosphorylceramide (IPC) in the *trans*-Golgi lumen. IPC can be further modified by mannose and phosphoinositol moieties before vesicular transport to the cell surface. In yeast, newly synthesized ceramides can reach the Golgi by vesicular means but also by cytosolic transfer, involving a putative ceramide transfer protein, NVJ2. CERT and NVJ2 also serve a role in preventing the toxic buildup of ceramides in the ER, which may cause a leak of ceramides into mitochondria and trigger apoptosis.

undermine an asymmetric sterol distribution. However, it appears that eukaryotic cells exploit two complementary strategies to tackle this logistic problem.

Sterols preferentially interact with lipids carrying saturated fatty acyl chains and bulky head groups, such as sphingolipids (Slotte, 2013). Contrary to sterols and glycerophospholipids, the bulk of sphingolipids is produced in the lumen of the *trans*-Golgi from ceramide supplied by the ER (Fig. 3; discussed below). Analogous to sterols, sphingolipids are enriched in the plasma membrane while their levels are low in the ER. Thus, sphingolipid production in the Golgi followed by anterograde sphingolipid transport to the cell surface provides a potential means to trap ER-derived sterols and move them up a concentration gradient into the plasma membrane. In line with this idea, retrograde-moving COPI vesicles are relatively depleted of cholesterol and SM in comparison to the Golgi, the organelle from which they bud off (Brugger et al., 2000). Additionally, cell surface SM degradation causes cholesterol to redistribute to the ER (Slotte and Bierman, 1988), leading to downregulation of HMG-CoA reductase, the rate-limiting enzyme in sterol biosynthesis (Gupta and Rudney, 1991). It also deserves mention that glycerophospholipids are more saturated at the plasma membrane than in the ER due to a substantial remodeling of their acyl chains (Fridriksson et al., 1999; Schneiter et al., 1999), which would further promote an asymmetric sterol distribution along the secretory pathway.

Strikingly, sterol transport along the secretory pathway has been shown to be independent of vesicular trafficking (Baumann et al., 2005; Urbani and Simoni, 1990). In stead, recent work suggests that sterol transport is mediated by LTPs that operate at MCSs between the ER and *trans*-Golgi. Thus, two LTPs from the ORP/Osh protein family, Osh4p in yeast and OSBP in mammals, have been implicated in the creation and maintenance of a sterol gradient between early and late secretory organelles (de Saint-Jean et al., 2011; Mesmin et al., 2013). OSBP is the founding member of a large family of proteins named ORPs (OSBP-related proteins) in mammals and Oshs (OSBP homologs) in yeast. As shown in Fig. 4a, OSBP contains an *N*-terminal pleckstrin homology (PH) domain that binds phosphatidylinositol-4-phosphate (PI4P), a phosphoinositide enriched on the cytosolic surface of the *trans*-Golgi in both mammals and yeast. In addition, OSBP possesses a central diphenylalanine-in-an-acidic-tract (FFAT) motif that binds the conserved ER-resident membrane proteins VAP-A and VAP-B, and an oxysterol-related domain (ORD) that, analogous to the ORD domain of Osh4, can bind and transfer cholesterol and PI4P in a mutually exclusive manner (Mesmin et al., 2013; Moser von Filseck et al., 2015). It was shown that OSBP can exchange PI4P for cholesterol while its PH-FATT region mediates recruitment of the protein to ER-Golgi contact sites (Mesmin et al., 2013). This led to a model in which OSBP transfers cholesterol from the ER to the *trans*-Golgi by exchanging it for PI4P (Fig. 4b) (Mesmin and Antonny, 2016). Net transfer of sterols would be energized through dissipation of a PI4P gradient created by the combined actions of PI-4-kinases, which produce PI4P in the *trans*-Golgi, and the PI4P phosphatase Sac1, which converts PI4P to PI in the ER. ER-Golgi contact sites are also the sites where a

PI/PC transfer protein, Nir2, is believed to deliver PI back to the *trans*-Golgi for its conversion to PI4P (Peretti et al., 2008).

However, a conditional yeast mutant lacking all functional Osh proteins, including Osh4p, did not display any major defect in sterol transport between the ER and plasma membrane (Georgiev et al., 2011). Consequently, whether heterotypic lipid exchange fueled by the metabolic energy of PI4P is sufficient to establish a sterol gradient in eukaryotic cells remains to be determined. It appears likely that thermodynamic trapping of sterols by sphingolipids also plays a role. In fact, this may explain why bulk assembly of sphingolipids from ceramides occurs in the *trans*-Golgi, hence spatially separated from bulk glycerophospholipid and sterol production in the ER. The first and rate-limiting step in *de novo* sphingolipid synthesis occurs on the cytosolic surface of the ER, involving the condensation of serine with palmitoyl-CoA by serine palmitoyl transferase (SPT) (Fig. 3). Subsequent reduction of the product yields a long chain base (LCB), which is then *N*-acylated and further reduced by ER-resident ceramide synthases and a desaturase, respectively, to generate ceramide (Levy and Futerman, 2010). In mammals, a portion of newly synthesized ceramides is delivered by a vesicular pathway to the *cis*-Golgi to initiate the production of complex glycosphingolipids, involving glycosyltransferases that are distributed along the Golgi cisternae and a glucosylceramide transfer protein, named FAPP2 (Fig. 3; reviewed in (D'Angelo et al., 2013)). However, the bulk of newly synthesized ceramides is converted to SM by a SM synthase in the lumen of the *trans*-Golgi (Tafesse et al., 2006). Delivery of ER ceramides to the site of SM production requires the ceramide transfer protein CERT (Hanada et al., 2003). Analogous to OSBP, CERT contains a PI4P-binding PH domain, an FFAT motif that interacts with VAPs, and a START domain that binds and transfers ceramide (Fig. 4a). Thus, CERT likely operates alongside OSBP at MCSs between the ER and *trans*-Golgi. This arrangement offers several advantages. To begin with, while CERT exchanges ceramides bi-directionally between the ER and the *trans*-Golgi, metabolic trapping of ceramides by the SM synthase in the latter organelle ensures an efficient one-way transfer. The pool of newly synthesized SM building up in the *trans*-Golgi then provides a thermodynamic trap for sterols (Fig. 4b). This, in turn, would facilitate an exchange of sterols for PI4P by OSBP at the *trans*-Golgi, thus promoting net sterol transfer in the face of sterol excess. The proximity of CERT and OSBP at ER-Golgi MCSs also facilitates regulatory crosstalk to ensure that sphingolipid precursors reach the *trans*-Golgi in harmony with sterols, allowing an efficient implementation of the major switch in lipid composition that marks the adaptation from biogenic to barrier functions (Holthuis and Menon, 2014).

Coordination of sterol and ceramide trafficking at ER-Golgi contact sites

A first 3D reconstruction of the contact sites between the ER and the *trans*-most Golgi cisterna in mammalian cells was reported nearly two decades ago (Ladinsky et al., 1999). While the tethering complexes responsible for creating ER-Golgi contact sites have yet to be identified, CERT and OSBP with their ER and *trans*-Golgi targeting motifs qualify as prime candidate components. Indeed, overexpression of

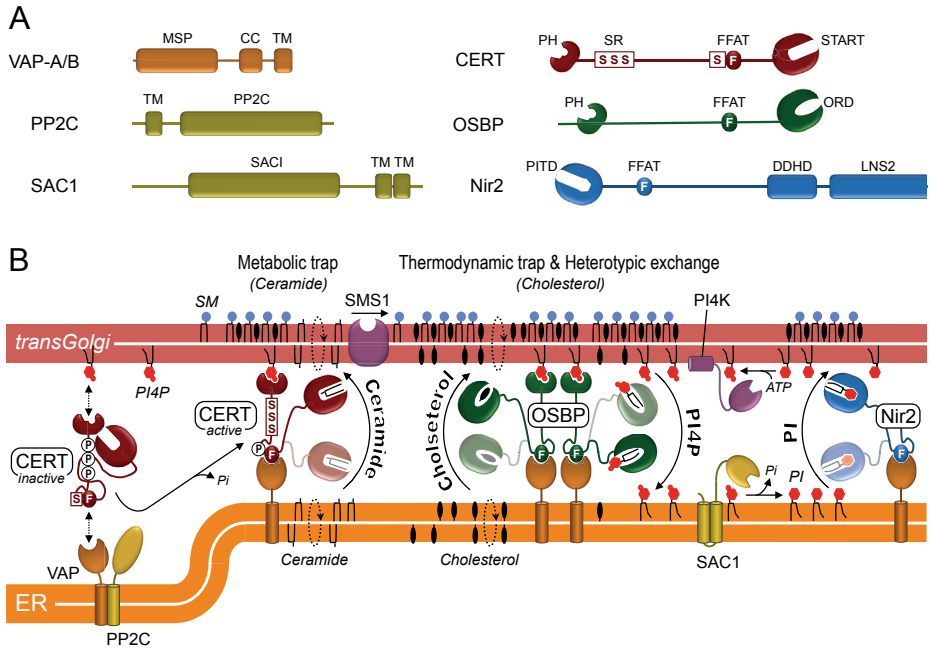

Figure 4. Coordination of LTP-mediated ceramide and sterol traffic at ER-Golgi contact sites. (A) Putative components of ER-Golgi contact sites. VAP-A/B, vesicle-associated membrane protein (VAMP)-associated protein A/B; PP2C, protein phosphatase 2C; SAC1, phosphatidylinositol-4-phosphate (PI4P) phosphatase; CERT, ceramide transfer protein; OSBP, oxysterol binding protein; Nir2, phosphatidylinositol (PI)/phosphatidylcholine (PC) exchange protein; MSP, major sperm protein domain; CC, coiled-coil domain; TM, transmembrane domain; PH, pleckstrin homology domain; FFAT, two phenylalanines in an acidic track motif; SR, serine-rich motif; START, steroidogenic acute regulatory protein-related lipid transfer domain; OSB, oxysterol transfer domain; PITP, phosphotidylinositol transfer protein domain; DDHD, death domain homologous domain; LNS2, lamin/neurexin/sex-hormone-binding domain. **(B)** Coordination of lipid transfer reactions catalyzed by CERT, OSBP, and Nir2. CERT is inactivated through hyperphosphorylation of its SR motif, which results in reciprocal masking of its PH domain and ceramide-binding START domain. On dephosphorylation by PP2C, CERT engages PI4P on the surface of the *trans*-Golgi via its PH domain and ER-resident VAP proteins via its central FFAT motif to catalyze the transfer of ceramides between the cytoplasmic faces of the two organelles. At the *trans*-Golgi, ceramide flips to the luminal side, promoting SM synthesis by SMS1. This metabolic trapping enables continued delivery of ceramide from the ER. Like CERT, OSBP is auto-inhibited and requires VAP proteins to be active and bridge ER-Golgi contact sites via its PH-FFAT motifs. OSBP uses heterotypic lipid exchange to move cholesterol from the ER to the *trans*-Golgi, and PI4P in the opposite direction. Cholesterol build up in the *trans*-Golgi is sustained by ongoing sphingolipid production, which creates a thermodynamic trap for newly arrived cholesterol, and by the maintenance of a steep PI4P gradient, which runs in the opposite direction due to PI4P synthesis in the *trans*-Golgi and PI4P consumption in the ER. A PI transfer protein, Nir2, is required to feed the metabolic cycle of PI4P. Figure adapted from (Mesmin and Antonny, 2016).

VAP-A with CERT or OSBP induces a redistribution of VAP-A to the perinuclear region and, at the EM level, results in the appearance of large contact zones between the ER and Golgi (Kawano et al., 2006; Mesmin et al., 2013). As both LTPs rely on PI4P to bridge the ER and *trans*-Golgi, PI4P plays a central role in controlling the flow of ceramides and sterols across ER-Golgi contact sites. The *trans*-Golgi is enriched in PI4P, achieved by phosphorylation of PI by the PI4 kinase PI4KIIa and PI4KIIIb (Venditti et al., 2016). Interestingly, OSBP-mediated delivery of sterols to the *trans*-Golgi has been proposed to activate PI4KIIa, causing an increase in PI4P levels. This, in turn, enhances recruitment of CERT to promote delivery of ceramide for SM synthesis (Banerji et al., 2010; Perry and Ridgway, 2006). However, the parallel rise in SM and sterol levels in the *trans*-Golgi is curbed by an OSBP-mediated back delivery and consumption of PI4P in the ER. The decline in *trans*-Golgi PI4P levels acts as an intrinsic "OFF"-switch for both OSBP and CERT-mediated lipid transfer. In this way, OSPB may implement a synchronization of sterol and ceramide transport across ER-Golgi contact sites to enable an efficient transition in the functional identify from early to late secretory organelles.

Several lines of evidence indicate that the activity of OSBP and CERT is regulated in coordination with membrane trafficking to the plasma membrane. Protein kinase D (PKD) is a serine/threonine kinase with a critical role in the fission of transport carriers from the *trans*-Golgi (Liljedahl et al., 2001). PKD localizes to the *trans*-Golgi through diacylglycerol (DAG) binding by its C1a domain (Van Lint et al., 2002). Phosphorylation of PI4KIIIb by PKD results in enhanced production of PI4P at the *trans*-Golgi (Hausser et al., 2005), thus providing a platform for the recruitment of OSBP and CERT. Recruitment of CERT stimulates PKD activity, presumably through formation of DAG during SM synthesis (Fugmann et al., 2007). CERT, in turn, is phosphorylated by PKD at a serine, which serves as a priming site for multiple phosphorylations by casein kinase CKIg2 in a serine-rich (SR) motif (Tomishige et al., 2009). Hyperphosphorylation of CERT blocks both the ceramide transfer activity of its START domain and PI4P binding by its PH domain, thus releasing CERT from the Golgi and reducing SM biosynthesis (Kumagai et al., 2007). At the ER, CERT is dephosphorylated by PP2C, a membrane-anchored phosphatase that interacts with VAP-A (Saito et al., 2008). This, in turn, stimulates recruitment of CERT to the *trans*-Golgi and its binding to VAP-A (Fig. 4b). Depletion of SM from the plasma membrane triggers both dephosphorylation of the SR motif and phosphorylation of a serine residue near the FFAT motif to activate CERT, but how this is accomplished remains to be addressed (Kumagai et al., 2007; Kumagai et al., 2014). Besides CERT, PKD also phosphorylates OSBP, causing its release from the Golgi (Nhek et al., 2010). Thus, through activation of PI4KIIIb and subsequent inactivation of CERT and OSBP, PKD may implement continuous rounds of ceramide and cholesterol transfer at ER-Golgi contacts. Moreover, recent work revealed that VAP-dependent association-dissociation dynamics of ER-Golgi contacts are important for creating *trans*-Golgi-derived membrane carriers destined for the plasma membrane (Wakana et al., 2015). This implies that ER-Golgi contact sites not only serve a fundamental

role in membrane maturation but also define the position and timing of membrane fission, analogous to the role of ER contact sites in mitochondria and endosome fission (Friedman et al., 2011; Rowland et al., 2014).

While ER-Golgi contact sites have been well documented in mammalian cells, their occurrence in lower eukaryotes like yeast has been demonstrated only recently. Analogous to mammalian cells, sterol trafficking in yeast occurs independently of vesicular trafficking (Baumann et al., 2005) whereas transport of ceramides to the Golgi is mediated by both vesicular and non-vesicular pathways (Funato and Riezman, 2001). As yeast lacks a CERT homologue, the mechanism by which this organism mediates non-vesicular ceramide transport is unclear. Excess of ER ceramides in mammalian cells is toxic, causing cell cycle arrest and apoptosis (Hannun and Obeid, 2008; Tafesse et al., 2014). Consequently, CERT removal triggers mitochondria-mediated cell death and sensitizes cancer cells to drug-induced apoptosis (Swanton et al., 2007; Tafesse et al., 2014). Ceramide toxicity has also been shown in yeast and may cause an apoptosis-like cell death (Eisenberg and Büttner, 2014). A recent study showed that contacts between the ER and Golgi in yeast increase dramatically during ER stress and when ceramide levels accumulate (Liu et al., 2017). ER-Golgi contact formation requires Nvj2, an ER-resident membrane protein that normally resides at contacts between the nuclear envelope and vacuole (Pan et al., 2000). Nvj2 contains a lipid-binding SMP domain and a PH domain required for Golgi binding. Importantly, Nvj2 was found to facilitate ceramide export from the ER to the Golgi, where Aur1 converts ceramides into inositol phoshorylceramide (IPC), the yeast analogue of SM. Combinatorial loss of Nvj2 and negative regulators of ceramide biosynthesis caused a dramatic accumulation of ceramides and poor growth, even in the absence of ER stress (Liu et al., 2017). Collectively, these results suggest that Nvj2 functions as an inducible ER-Golgi tether that facilitates ceramide export from the ER to prevent the build up of toxic amounts of ceramides. Whether Nvj2 binds and transfers ceramides remains to be established. Mammals contain a structural homologue of Nvj2, HT008, which can partially compensate for the loss of the protein in yeast (Toulmay and Prinz, 2012). Thus, HT008 may act in concert with CERT to promote ceramide export from the ER during stress.

Conclusions and outlook

In here, we have described MCSs as ancient and central hubs of cellular lipid logistics. It is conceivable that MCSs emerged as platforms of non-vesicular lipid exchange already early on during eukaryotic evolution, i.e. when ectosymbiotic proto-mitochondria initiated close metabolic and physical ties with their archaeal host, before the establishment of an endomembrane system and vesicular trafficking. In modern eukaryotes, membrane contacts interconnect mitochondria with the endomembrane system at multiple nodes (Gatta and Levine, 2017). Besides allowing extensive inter-organellar crosstalk and collective regulation, this redundancy in interconnectivity ensures that mitochondria can acquire essential lipids from multiple resources, making them less vulnerable when one particular supply route is compromised.

This redundancy also means that a molecular dissection of the lipid transport machinery operating at mitochondrial contact sites is not straightforward. Several components of MCSs between mitochondria and neighboring organelles possess lipid-binding domains (e.g. Mdm12, Mmm1, Ltc1/Lam6). However, ultimate proof that these candidate LTPs transfer lipids across contact sites remains to be established. For MCS components harboring tethering and lipid transfer activities within one protein, an unambiguous functional analysis may become challenging. Moreover, some LTPs (e.g. Ltc1/Lam6, Nvj2) are found at more than one MCS. There is evidence that these LTPs contribute to MCS dynamics and facilitate cross-talk between different contact sites in response to different physiological conditions (e.g. ER stress, nutrient deprivation; (Elbaz-Alon et al., 2015; Liu et al., 2017). The human genome encodes over one hundred predicted LTPs (Chiapparino et al., 2016), and novel LTPs evolutionary unrelated to previously known LTPs continue to be discovered (Gatta et al., 2015). Consequently, a systematic and unbiased monitoring of interactions between LTPs and their lipid cargo (Maeda et al., 2013) combined with sophisticated genetic and biochemical approaches will be necessary to unravel, in molecular detail, how mitochondria exchange lipids across contact sites with organelles of the endomembrane system.

Strikingly, two of the best-characterized LTPs in mammalian cells, CERT and OSBP, operate at ER-Golgi contact sites. Converging lines of evidence indicate that these LTPs bypass vesicular connections to help create and maintain sphingolipid/sterol gradients between early and late secretory organelles. Vectorial transport of ceramides by CERT is accomplished by metabolic trapping, involving SM synthase in the *trans*-Golgi lumen. OSBP, on the other hand, can move sterols up against their concentration gradient using two additional strategies, namely: i) thermodynamic trapping by sphingolipids produced in the *trans*-Golgi lumen; ii) heterotypic lipid exchange against a steep gradient of PI4P that runs in the opposite direction. By exerting tight control over lipid exchange at ER-Golgi contact sites, these LTPs and their functional homologues allow eukaryotic cells to tackle a fundamental logistical problem, namely to preserve the unique lipid mixtures of the ER and plasma membrane in the face of extensive vesicular trafficking.

An efficient lipid exchange by OSBP and CERT appears to be critically dependent on the ability of their PH-FFAT motifs to tether ER and *trans*-Golgi membranes. Whether these LTPs are also essential for creating ER-Golgi contact sites remains to be established. If this were the case, contact site formation would be critically dependent on PI4P levels in the *trans*-Golgi. Interestingly, both OSBP and CERT are substrates of PKD, which also serves as a master regulator of PI4P levels and membrane fission at the *trans*-Golgi. These and other findings indicate that PKD may tune sterol and sphingolipid levels in the *trans*-Golgi to ensure that only transport carriers with a suitable lipid composition are dispatched for delivery to the plasma membrane. Recent work suggests that ER-Golgi contact sites are dynamic structures (Wakana et al., 2015), in line with the notion that the *trans*-Golgi is not a static compartment but an inducible one that is formed and molded by incoming and

outgoing cargo (De Matteis and Luini, 2008). Thus, future application of advanced approaches in super-resolution live cell imaging will likely reveal major insights into the dynamic organization of LTPs at membrane contacts in relation to vesicular trafficking, organelle homeostasis, and other vital cellular processes.

SCOPE OF THE THESIS

As outlined above, cells exploit LTPs at membrane contact sites to establish and maintain asymmetric lipid distributions among their secretory organelles. A key example is CERT, a ceramide transfer protein that operates at ER-Golgi contact sites to shuttle ceramides synthesized in the ER to the *trans*Golgi for production of sphingomyelin (SM), an abundant and vital component of the plasma membrane. SM is concentrated in the exoplasmic leaflet of the plasma membrane where its high packing density and affinity for sterols help create a rigid barrier to the extracellular environment. Ceramides, on the other hand, serve a dual role as obligatory precursors for the production of SM and as potent mediators of cellular stress, cell cycle arrest and apoptosis. Accordingly, loss of CERT function has two dramatic consequences: i) an increased leakiness of the plasma membrane to ions and other solutes; ii) a toxic build up of ceramides in the ER and subsequent induction of apoptotic cell death. Therefore, a tight regulation of ceramide logistics by CERT and its functional homologues is fundamental to the functional organization and survival of eukaryotic cells.

A deregulation of ceramide levels in the ER has frequently been linked to induction of mitochondrial apoptosis in response to chemotherapeutics, radiation and other anti-cancer regimens. Interventions that suppress ceramide accumulation render cells resistant to these apoptotic stimuli, indicating that ceramides are both necessary and sufficient to trigger mitochondria-mediated cell death. Some studies indicate that ceramides influence this process by sensitizing cells to ER stress and activating apoptotic regulators of the unfolded protein response. However, experiments with isolated mitochondria suggest that ceramides are able to initiate the execution phase of apoptosis by directly promoting permeabilization of the outer mitochondrial membrane to pro-apoptotic intermembrane proteins like cytochrome *c*. While ceramides currently attract wide attention as putative tumor suppressor lipids, where and how these biomolecules exert their apoptogenic activity in cells is poorly understood.

We recently identified SMSr (SAMD8), an ER-resident ceramide phosphoethanolamine synthase, as suppressor of ceramide-mediated cell death. Disruption of SMSr catalytic activity causes a rise in ER ceramides and their mislocalization to mitochondria, triggering a mitochondrial pathway of apoptosis. Blocking *de novo* ceramide synthesis, stimulating ceramide export from the ER or targeting a bacterial ceramidase to mitochondria rescued SMSr-deficient cells from apoptosis. These findings suggested that ER ceramides are authentic transducers of apoptosis and that their arrival in mitochondria is a crucial step in committing cells to death. The key objective of this thesis was to verify these predictions and to develop new approaches to unravel the mechanism by which ceramides trigger apoptotic cell death.

In **Chapter 2,** we analyzed the consequences of targeting newly synthesized ceramides to mitochondria using a ceramide transfer protein equipped with an outer mitochondrial membrane anchor, mitoCERT. We demonstrate that mitoCERT expression activates a ceramide-mediated mitochondrial pathway of apoptosis that requires the pro-apoptotic Bcl-2 protein Bax. Importantly, our findings complement and extend previous *in vitro* studies indicating that ceramides can act directly on mitochondria to promote outer membrane permeabilization, leading to cytochrome *c* release, caspase activation and cell death.

Bax and its structural homolog Bak are thought to directly engage in mitochondrial outer membrane permeabilization by creating proteolipid pores responsible for cytochrome *c* release. To further elucidate the mechanism by which ceramides activate Bax-dependent apoptosis, we developed a switchable version of CERT, sCERT, using FKB-FRBP chemical dimerization technology. In **Chapter 3**, we demonstrate that sCERT can be readily targeted to mitochondria to promote mitochondrial ceramide import in response to rapamycin. Mitochondrial recruitment of sCERT induces Bax translocation to mitochondria. We find that the ability of sCERT to induce mitochondrial translocation of Bax critically relies on its ceramide transfer domain, thus confirming that ceramide arrival in mitochondria specifically activates Bax to trigger apoptosis.

To allow a detailed spatiotemporal analysis of Bax and other active participants in ceramide-induced cell death, we implemented a split-GFP-based Cas9/sgRNA-mediated knockin strategy for GFP tagging of endogenous proteins. In **Chapter 4**, we report on the functional GFP tagging of Bax and additional components of the mitochondrial apoptotic machinery, hence paving the way to dissect the mechanism of ceramide-induced cell death in real time.

In **Chapter 5,** we discuss the general implications of the data presented in this thesis and propose a model on how ceramides might influence Bax cycling between the cytosol and mitochondria at the retro-translocation step to promote assembly of apoptotic pore complexes, leading to cytochrome *c* release, caspase activation and cell death. We also provide some perspectives on how the experimental tools established herein can be exploited to gain further insight into the molecular principles by which ceramides can commit cells to death.

REFERENCES

AhYoung, A. P., Jiang, J., Zhang, J., Khoi Dang, X., Loo, J. A., Zhou, Z. H. and Egea, P. F. (2015). Conserved SMP domains of the ERMES complex bind phospholipids and mediate tether assembly. *Proc. Natl. Acad. Sci. U.S.A.* **112**, E3179–88.

Banerji, S., Ngo, M., Lane, C. F., Robinson, C.-A., Minogue, S. and Ridgway, N. D. (2010). Oxysterol binding protein-dependent activation of sphingomyelin synthesis in the golgi apparatus requires phosphatidylinositol 4-kinase IIα. *Mol. Biol. Cell* **21**, 4141–4150.

Baum, D. A. and Baum, B. (2014). An inside-out origin for the eukaryotic cell. *BMC Biology* **12**, 76.

Baumann, N. A., Sullivan, D. P., Ohvo-Rekilä, H., Simonot, C., Pottekat, A., Klaassen, Z., Beh, C. T. and Menon, A. K. (2005). Transport of newly synthesized sterol to the sterol-enriched plasma membrane occurs via nonvesicular equilibration. *Biochemistry* **44**, 5816–5826.

Bigay, J. and Antonny, B. (2012). Curvature, lipid packing, and electrostatics of membrane organelles: defining cellular territories in determining specificity. *Dev. Cell* **23**, 886–895.

Brown, D. A. and London, E. (1998). Structure and origin of ordered lipid domains in biological membranes. *J. Membr. Biol.* **164**, 103–114.

Brugger, B., Sandhoff, R., Wegehingel, S., Gorgas, K., Malsam, J., Helms, J. B., Lehmann, W. D., Nickel, W. and Wieland, F. T. (2000). Evidence for segregation of sphingomyelin and cholesterol during formation of COPI-coated vesicles. *J. Cell Biol.* **151**, 507–518.

Chiapparino, A., Maeda, K., Turei, D., Saez-Rodriguez, J. and Gavin, A.-C. (2016). The orchestra of lipid-transfer proteins at the crossroads between metabolism and signaling. *Prog. Lipid Res.* **61**, 30–39.

Chong, P. L.-G. (2010). Archaebacterial bipolar tetraether lipids: Physico-chemical and membrane properties. *Chem. Phys. Lipids* **163**, 253–265.

D'Angelo, G., Capasso, S., Sticco, L. and Russo, D. (2013). Glycosphingolipids: synthesis and functions. *FEBS J.* **280**, 6338–6353.

De Matteis, M. A. and Luini, A. (2008). Exiting the Golgi complex. *Nat. Rev. Mol. Cell Biol.* **9**, 273–284.

de Saint-Jean, M., Delfosse, V., Douguet, D., Chicanne, G., Payrastre, B., Bourguet, W., Antonny, B. and Drin, G. (2011). Osh4p exchanges sterols for phosphatidylinositol 4-phosphate between lipid bilayers. *J. Cell Biol.* **195**, 965–978.

De Vos, K. J., Mórotz, G. M., Stoica, R., Tudor, E. L., Lau, K.-F., Ackerley, S., Warley, A., Shaw, C. E. and Miller, C. C. J. (2012). VAPB interacts with the mitochondrial protein PTPIP51 to regulate calcium homeostasis. *Hum. Mol. Genet.* **21**, 1299–1311.

Desmond, E. and Gribaldo, S. (2009). Phylogenomics of sterol synthesis: insights into the origin, evolution, and diversity of a key eukaryotic feature. *Genome Biol Evol* **1**, 364–381.

Dimmer, K. S. and Rapaport, D. (2017). Mitochondrial contact sites as platforms for phospholipid exchange. *Biochim. Biophys. Acta* **1862**, 69–80.

Dittman, J. S. and Menon, A. K. (2017). Speed Limits for Nonvesicular Intracellular Sterol Transport. *Trends Biochem. Sci.* **42**, 90–97.

Eisenberg, T. and Büttner, S. (2014). Lipids and cell death in yeast. *FEMS Yeast Res.* **14**, 179–197.

Elbaz-Alon, Y., Eisenberg-Bord, M., Shinder, V., Stiller, S. B., Shimoni, E., Wiedemann, N., Geiger, T. and Schuldiner, M. (2015). Lam6 Regulates the Extent of Contacts between Organelles. *Cell Rep* **12**, 7–14.

Elbaz-Alon, Y., Rosenfeld-Gur, E., Shinder, V., Futerman, A. H., Geiger, T. and Schuldiner, M. (2014). A dynamic interface between vacuoles and mitochondria in yeast. *Dev. Cell* **30**, 95–102.

Emelyanov, V. V. (2001). Evolutionary relationship of Rickettsiae and mitochondria.

FEBS Lett. **501**, 11–18.

Flis, V. V. and Daum, G. (2013). Lipid transport between the endoplasmic reticulum and mitochondria. *Cold Spring Harb Perspect Biol* **5**, a013235–a013235.

Fridriksson, E. K., Shipkova, P. A., Sheets, E. D., Holowka, D., Baird, B. and McLafferty, F. W. (1999). Quantitative analysis of phospholipids in functionally important membrane domains from RBL-2H3 mast cells using tandem high-resolution mass spectrometry. *Biochemistry* **38**, 8056–8063.

Friedman, J. R., Lackner, L. L., West, M., DiBenedetto, J. R., Nunnari, J. and Voeltz, G. K. (2011). ER tubules mark sites of mitochondrial division. *Science* **334**, 358–362.

Fugmann, T., Hausser, A., Schöffler, P., Schmid, S., Pfizenmaier, K. and Olayioye, M. A. (2007). Regulation of secretory transport by protein kinase D-mediated phosphorylation of the ceramide transfer protein. *J. Cell Biol.* **178**, 15–22.

Funato, K. and Riezman, H. (2001). Vesicular and nonvesicular transport of ceramide from ER to the Golgi apparatus in yeast. *J. Cell Biol.* **155**, 949–959.

Gatta, A. T. and Levine, T. P. (2017). Piecing Together the Patchwork of Contact Sites. *Trends Cell Biol.* **27**, 214–229.

Gatta, A. T., Wong, L. H., Sere, Y. Y., Calderón-Noreña, D. M., Cockcroft, S., Menon, A. K. and Levine, T. P. (2015). A new family of StART domain proteins at membrane contact sites has a role in ER-PM sterol transport. *Elife* **4**, 400.

Georgiev, A. G., Sullivan, D. P., Kersting, M. C., Dittman, J. S., Beh, C. T. and Menon, A. K. (2011). Osh proteins regulate membrane sterol organization but are not required for sterol movement between the ER and PM. *Traffic* **12**, 1341–1355.

Grüber, G. and Marshansky, V. (2008). New insights into structure-function relationships between archeal ATP synthase (A 1A 0) and vacuolar type ATPase (V 1V 0). *BioEssays* **30**, 1096–1109.

Gupta, A. K. and Rudney, H. (1991). Plasma membrane sphingomyelin and the regulation of HMG-CoA reductase activity and cholesterol biosynthesis in cell cultures. *J. Lipid Res.* **32**, 125–136.

Hanada, K., Kumagai, K., Yasuda, S., Miura, Y., Kawano, M., Fukasawa, M. and Nishijima, M. (2003). Molecular machinery for non-vesicular trafficking of ceramide. *Nature* **426**, 803–809.

Hannich, J. T., Umebayashi, K. and Riezman, H. (2011). Distribution and functions of sterols and sphingolipids. *Cold Spring Harb Perspect Biol* **3**, a004762–a004762.

Hannun, Y. A. and Obeid, L. M. (2008). Principles of bioactive lipid signalling: lessons from sphingolipids. *Nat. Rev. Mol. Cell Biol.* **9**, 139–150.

Hausser, A., Storz, P., Märtens, S., Link, G., Toker, A. and Pfizenmaier, K. (2005). Protein kinase D regulates vesicular transport by phosphorylating and activating phosphatidylinositol-4 kinase IIIbeta at the Golgi complex. *Nat. Cell Biol.* **7**, 880–886.

Herrera-Cruz, M. S. and Simmen, T. (2017). Of yeast, mice and men: MAMs come in two flavors. *Biol. Direct* **12**, 3.

Holthuis, J. C. M. and Menon, A. K. (2014). Lipid landscapes and pipelines in membrane homeostasis. *Nature* **510**, 48–57.

Hönscher, C., Mari, M., Auffarth, K., Bohnert, M., Griffith, J., Geerts, W., van der Laan, M., Cabrera, M., Reggiori, F. and Ungermann, C. (2014). Cellular metabolism regulates contact sites between vacuoles and mitochondria. *Dev. Cell* **30**, 86–94.

Iwasawa, R., Mahul-Mellier, A.-L., Datler, C., Pazarentzos, E. and Grimm, S. (2011). Fis1 and Bap31 bridge the mitochondria-ER interface to establish a platform for apoptosis induction. *EMBO J.* **30**, 556–568.

Jackson, C. L., Walch, L. and Verbavatz, J.-M. (2016). Lipids and Their Trafficking: An Integral Part of Cellular Organization. *Dev. Cell* **39**, 139–153.

Jones, J. D., Almeida, P. F. and Thompson, T. E. (1990). Spontaneous interbilayer transfer of hexosylceramides between phospholipid bilayers. *Biochemistry* **29**, 3892–3897.

Kaplan, M. R. and Simoni, R. D. (1985). Intracellular transport of phosphatidylcholine to

the plasma membrane. *J. Cell Biol.* **101**, 441–445.

Kawano, M., Kumagai, K., Nishijima, M. and Hanada, K. (2006). Efficient trafficking of ceramide from the endoplasmic reticulum to the Golgi apparatus requires a VAMP-associated protein-interacting FFAT motif of CERT. *J. Biol. Chem.* **281**, 30279–30288.

Kornmann, B., Currie, E., Collins, S. R., Schuldiner, M., Nunnari, J., Weissman, J. S. and Walter, P. (2009). An ER-mitochondria tethering complex revealed by a synthetic biology screen. *Science* **325**, 477–481.

Koynova, R. and Caffrey, M. (1995). Phases and phase transitions of the sphingolipids. *Biochim. Biophys. Acta* **1255**, 213–236.

Ku, C., Nelson-Sathi, S., Roettger, M., Sousa, F. L., Lockhart, P. J., Bryant, D., Hazkani-Covo, E., McInerney, J. O., Landan, G. and Martin, W. F. (2015). Endosymbiotic origin and differential loss of eukaryotic genes. *Nature* **524**, 427–432.

Kumagai, K., Kawano, M., Shinkai-Ouchi, F., Nishijima, M. and Hanada, K. (2007). Interorganelle trafficking of ceramide is regulated by phosphorylation-dependent cooperativity between the PH and START domains of CERT. *J. Biol. Chem.* **282**, 17758–17766.

Kumagai, K., Kawano-Kawada, M. and Hanada, K. (2014). Phosphoregulation of the ceramide transport protein CERT at serine 315 in the interaction with VAMP-associated protein (VAP) for inter-organelle trafficking of ceramide in mammalian cells. *J. Biol. Chem.* **289**, 10748–10760.

Lackner, L. L., Ping, H., Graef, M., Murley, A. and Nunnari, J. (2013). Endoplasmic reticulum-associated mitochondria-cortex tether functions in the distribution and inheritance of mitochondria. *Proc. Natl. Acad. Sci. U.S.A.* **110**, E458–67.

Ladinsky, M. S., Mastronarde, D. N., McIntosh, J. R., Howell, K. E. and Staehelin, L. A. (1999). Golgi structure in three dimensions: functional insights from the normal rat kidney cell. *J. Cell Biol.* **144**, 1135–1149.

Lahiri, S., Chao, J. T., Tavassoli, S., Wong, A. K. O., Choudhary, V., Young, B. P., Loewen, C. J. R. and Prinz, W. A. (2014). A conserved endoplasmic reticulum membrane protein complex (EMC) facilitates phospholipid transfer from the ER to mitochondria. *PLoS Biol.* **12**, e1001969.

Lalanne, F. and Ponsin, G. (2000). Mechanism of the phospholipid transfer protein-mediated transfer of phospholipids from model lipid vesicles to high density lipoproteins. *Biochim. Biophys. Acta* **1487**, 82–91.

Lang, A. B., John Peter, A. T., Walter, P. and Kornmann, B. (2015). ER-mitochondrial junctions can be bypassed by dominant mutations in the endosomal protein Vps13. *J. Cell Biol.* **210**, 883–890.

Lev, S. (2010). Non-vesicular lipid transport by lipid-transfer proteins and beyond. *Nat. Rev. Mol. Cell Biol.* **11**, 739–750.

Levy, M. and Futerman, A. H. (2010). Mammalian ceramide synthases. *IUBMB Life* **62**, 347–356.

Liljedahl, M., Maeda, Y., Colanzi, A., Ayala, I., Van Lint, J. and Malhotra, V. (2001). Protein kinase D regulates the fission of cell surface destined transport carriers from the trans-Golgi network. *Cell* **104**, 409–420.

Lingwood, D. and Simons, K. (2010). Lipid rafts as a membrane-organizing principle. *Science* **327**, 46–50.

Liu, L.-K., Choudhary, V., Toulmay, A. and Prinz, W. A. (2017). An inducible ER-Golgi tether facilitates ceramide transport to alleviate lipotoxicity. *J. Cell Biol.* **216**, 131–147.

Lombard, J., López-García, P. and Moreira, D. (2012). The early evolution of lipid membranes and the three domains of life. *Nat. Rev. Microbiol.* **10**, 507–515.

Maeda, K., Anand, K., Chiapparino, A., Kumar, A., Poletto, M., Kaksonen, M. and Gavin, A.-C. (2013). Interactome map uncovers phosphatidylserine transport by oxysterol-binding proteins. *Nature* **501**, 257–261.

Martin, W. F., Garg, S. and Zimorski, V. (2015). Endosymbiotic theories for eukaryote origin. *Philos. Trans. R. Soc. Lond., B, Biol. Sci.* **370**, 20140330.

Mast, F. D., Barlow, L. D., Rachubinski, R. A. and Dacks, J. B. (2014). Evolutionary mechanisms for establishing eukaryotic cellular complexity. *Trends Cell Biol.* **24**, 435–442.

McLean, L. R. and Phillips, M. C. (1981). Mechanism of cholesterol and phosphatidylcholine exchange or transfer between unilamellar vesicles. *Biochemistry* **20**, 2893–2900.

Mesmin, B. and Antonny, B. (2016). The counterflow transport of sterols and PI4P. *Biochim. Biophys. Acta* **1861**, 940–951.

Mesmin, B., Bigay, J., Moser von Filseck, J., Lacas-Gervais, S., Drin, G. and Antonny, B. (2013). A four-step cycle driven by PI(4)P hydrolysis directs sterol/PI(4)P exchange by the ER-Golgi tether OSBP. *Cell* **155**, 830–843.

Molecular biology of the cell, by Bruce Alberts, Dennis Bray, Julian Lewis, Martin Raff, Keith Roberts, and James Watson; Garland Publ. Inc., New York, 1146 pp. $35.95 (U.S) (1986). Molecular biology of the cell, by Bruce Alberts, Dennis Bray, Julian Lewis, Martin Raff, Keith Roberts, and James Watson; Garland Publ. Inc., New York, 1146 pp. $35.95 (U.S). *Gamete Research* **13**, 91–91.

Moser von Filseck, J., Vanni, S., Mesmin, B., Antonny, B. and Drin, G. (2015). A phosphatidylinositol-4-phosphate powered exchange mechanism to create a lipid gradient between membranes. *Nat Commun* **6**, 6671.

Motamed, M., Zhang, Y., Wang, M. L., Seemann, J., Kwon, H. J., Goldstein, J. L. and Brown, M. S. (2011). Identification of luminal Loop 1 of Scap protein as the sterol sensor that maintains cholesterol homeostasis. *J. Biol. Chem.* **286**, 18002–18012.

Murley, A., Sarsam, R. D., Toulmay, A., Yamada, J., Prinz, W. A. and Nunnari, J. (2015). Ltc1 is an ER-localized sterol transporter and a component of ER-mitochondria and ER-vacuole contacts. *J. Cell Biol.* **209**, 539–548.

Nhek, S., Ngo, M., Yang, X., Ng, M. M., Field, S. J., Asara, J. M., Ridgway, N. D. and Toker, A. (2010). Regulation of oxysterol-binding protein Golgi localization through protein kinase D-mediated phosphorylation. *Mol. Biol. Cell* **21**, 2327–2337.

Nilsson, I., Ohvo-Rekilä, H., Slotte, J. P., Johnson, A. E. and Heijne, von, G. (2001). Inhibition of protein translocation across the endoplasmic reticulum membrane by sterols. *J. Biol. Chem.* **276**, 41748–41754.

Pan, X., Roberts, P., Chen, Y., Kvam, E., Shulga, N., Huang, K., Lemmon, S. and Goldfarb, D. S. (2000). Nucleus-vacuole junctions in Saccharomyces cerevisiae are formed through the direct interaction of Vac8p with Nvj1p. *Mol. Biol. Cell* **11**, 2445–2457.

Peretti, D., Dahan, N., Shimoni, E., Hirschberg, K. and Lev, S. (2008). Coordinated lipid transfer between the endoplasmic reticulum and the Golgi complex requires the VAP proteins and is essential for Golgi-mediated transport. *Mol. Biol. Cell* **19**, 3871–3884.

Perry, R. J. and Ridgway, N. D. (2006). Oxysterol-binding protein and vesicle-associated membrane protein-associated protein are required for sterol-dependent activation of the ceramide transport protein. *Mol. Biol. Cell* **17**, 2604–2616.

Radhakrishnan, A., Goldstein, J. L., McDonald, J. G. and Brown, M. S. (2008). Switch-like control of SREBP-2 transport triggered by small changes in ER cholesterol: a delicate balance. *Cell Metab.* **8**, 512–521.

Rowland, A. A., Chitwood, P. J., Phillips, M. J. and Voeltz, G. K. (2014). ER contact sites define the position and timing of endosome fission. *Cell* **159**, 1027–1041.

Rusiñol, A. E., Cui, Z., Chen, M. H. and Vance, J. E. (1994). A unique mitochondria-associated membrane fraction from rat liver has a high capacity for lipid synthesis and contains pre-Golgi secretory proteins including nascent lipoproteins. *J. Biol. Chem.* **269**, 27494–27502.

Saheki, Y., Bian, X., Schauder, C. M., Sawaki, Y., Surma, M. A., Klose, C., Pincet, F., Reinisch, K. M. and De Camilli, P. (2016). Control of plasma membrane lipid homeostasis by the extended synaptotagmins. *Nat. Cell Biol.* **18**, 504–515.

Saito, S., Matsui, H., Kawano, M., Kumagai, K., Tomishige, N., Hanada, K., Echigo,

S., Tamura, S. and Kobayashi, T. (2008). Protein phosphatase 2Cepsilon is an endoplasmic reticulum integral membrane protein that dephosphorylates the ceramide transport protein CERT to enhance its association with organelle membranes. *J. Biol. Chem.* **283**, 6584–6593.

Schneiter, R., Brugger, B., Sandhoff, R., Zellnig, G., Leber, A., Lampl, M., Athenstaedt, K., Hrastnik, C., Eder, S., Daum, G., et al. (1999). Electrospray ionization tandem mass spectrometry (ESI-MS/MS) analysis of the lipid molecular species composition of yeast subcellular membranes reveals acyl chain-based sorting/remodeling of distinct molecular species en route to the plasma membrane. *J. Cell Biol.* **146**, 741–754.

Shevchenko, A. and Simons, K. (2010). Lipidomics: coming to grips with lipid diversity. *Nat. Rev. Mol. Cell Biol.* **11**, 593–598.

Silvius, J. R. and Leventis, R. (1993). Spontaneous interbilayer transfer of phospholipids: dependence on acyl chain composition. *Biochemistry* **32**, 13318–13326.

Slotte, J. P. (2013). Biological functions of sphingomyelins. *Prog. Lipid Res.* **52**, 424–437.

Slotte, J. P. and Bierman, E. L. (1988). Depletion of plasma-membrane sphingomyelin rapidly alters the distribution of cholesterol between plasma membranes and intracellular cholesterol pools in cultured fibroblasts. *Biochem. J.* **250**, 653–658.

Swanton, C., Marani, M., Pardo, O., Warne, P. H., Kelly, G., Sahai, E., Elustondo, F., Chang, J., Temple, J., Ahmed, A. A., et al. (2007). Regulators of mitotic arrest and ceramide metabolism are determinants of sensitivity to paclitaxel and other chemotherapeutic drugs. *Cancer Cell* **11**, 498–512.

Tafesse, F. G., Ternes, P. and Holthuis, J. C. M. (2006). The multigenic sphingomyelin synthase family. *J. Biol. Chem.* **281**, 29421–29425.

Tafesse, F. G., Vacaru, A. M., Bosma, E. F., Hermansson, M., Jain, A., Hilderink, A., Somerharju, P. and Holthuis, J. C. M. (2014). Sphingomyelin synthase-related protein SMSr is a suppressor of ceramide-induced mitochondrial apoptosis. *J. Cell. Sci.* **127**, 445–454.

Thiergart, T., Landan, G., Schenk, M., Dagan, T. and Martin, W. F. (2012). An evolutionary network of genes present in the eukaryote common ancestor polls genomes on eukaryotic and mitochondrial origin. *Genome Biol Evol* **4**, 466–485.

Tomishige, N., Kumagai, K., Kusuda, J., Nishijima, M. and Hanada, K. (2009). Casein kinase I{gamma}2 down-regulates trafficking of ceramide in the synthesis of sphingomyelin. *Mol. Biol. Cell* **20**, 348–357.

Toulmay, A. and Prinz, W. A. (2012). A conserved membrane-binding domain targets proteins to organelle contact sites. *J. Cell. Sci.* **125**, 49–58.

Urbani, L. and Simoni, R. D. (1990). Cholesterol and vesicular stomatitis virus G protein take separate routes from the endoplasmic reticulum to the plasma membrane. *J. Biol. Chem.* **265**, 1919–1923.

Van Lint, J., Rykx, A., Maeda, Y., Vantus, T., Sturany, S., Malhotra, V., Vandenheede, J. R. and Seufferlein, T. (2002). Protein kinase D: an intracellular traffic regulator on the move. *Trends Cell Biol.* **12**, 193–200.

van Meer, G., Voelker, D. R. and Feigenson, G. W. (2008). Membrane lipids: where they are and how they behave. *Nat. Rev. Mol. Cell Biol.* **9**, 112–124.

Vance, J. E. (1990). Phospholipid synthesis in a membrane fraction associated with mitochondria. *J. Biol. Chem.* **265**, 7248–7256.

Vance, J. E. (2014). MAM (mitochondria-associated membranes) in mammalian cells: lipids and beyond. *Biochim. Biophys. Acta* **1841**, 595–609.

Vance, J. E., Aasman, E. J. and Szarka, R. (1991). Brefeldin A does not inhibit the movement of phosphatidylethanolamine from its sites for synthesis to the cell surface. *J. Biol. Chem.* **266**, 8241–8247.

Venditti, R., Masone, M. C., Wilson, C. and De Matteis, M. A. (2016). PI(4)P homeostasis: Who controls the controllers? *Adv Biol Regul* **60**, 105–114.

Wakana, Y., Kotake, R., Oyama, N., Murate, M., Kobayashi, T., Arasaki, K., Inoue, H.

and Tagaya, M. (2015). CARTS biogenesis requires VAP-lipid transfer protein complexes functioning at the endoplasmic reticulum-Golgi interface. *Mol. Biol. Cell* **26**, 4686–4699.

Wideman, J. G., Gawryluk, R. M. R., Gray, M. W. and Dacks, J. B. (2014). The Ancient and Widespread Nature of the ER-Mitochondria Encounter Structure. *Molecular Biology and Evolution* **31**, 251–251.

Wirtz, K. W. and Zilversmit, D. B. (1968). Exchange of phospholipids between liver mitochondria and microsomes in vitro. *J. Biol. Chem.* **243**, 3596–3602.

Yang, D., Oyaizu, Y., Oyaizu, H., Olsen, G. J. and Woese, C. R. (1985). Mitochondrial origins. *Proc. Natl. Acad. Sci. U.S.A.* **82**, 4443–4447.

Chapter 2

Diverting CERT-mediated ceramide transport to mitochondria triggers Bax-dependent apoptosis

Amrita Jain[1], Oliver Beutel[1,2], Katharina Ebell[1], Sergey Korneev[1], Joost C.M. Holthuis[1,3]

[1]Molecular Cell Biology Division, Department of Biology/Chemistry, University of Osnabrück, D-49076 Osnabrück, Germany; [2]Max-Planck-Institute for Molecular Cell Biology and Genetics, D-01307Dresden, Germany; [3]Membrane Biochemistry & Biophysics, Bijvoet Center and Institute of Biomembranes, Utrecht University, 3584 CH Utrecht, The Netherlands

J. Cell. Sci. (2017) 130, 360-371

© 2017. Published by The Company of Biologists Ltd | Journal of Cell Science (2017) 130, 360-371 doi:10.1242/jcs.194191

RESEARCH ARTICLE

Diverting CERT-mediated ceramide transport to mitochondria triggers Bax-dependent apoptosis

Amrita Jain[1], Oliver Beutel[1,2], Katharina Ebell[1], Sergey Korneev[1] and Joost C. M. Holthuis[1,3,*]

ABSTRACT

A deregulation of ceramide biosynthesis in the endoplasmic reticulum (ER) is frequently linked to induction of mitochondrial apoptosis. Although *in vitro* studies suggest that ceramides might initiate cell death by acting directly on mitochondria, their actual contribution to the apoptotic response in living cells is unclear. Here, we have analyzed the consequences of targeting the biosynthetic flow of ceramides to mitochondria using a ceramide transfer protein (encoded by *COL4A3BP*) equipped with an OMM anchor, mitoCERT. Cells expressing mitoCERT import ceramides into mitochondria and undergo Bax-dependent apoptosis. Apoptosis induction by mitoCERT was abolished through (i) removal of its ceramide transfer domain, (ii) disruption of its interaction with VAMP-associated proteins (VAPs) in the ER, (iii) addition of antagonistic CERT inhibitor HPA12, (iv) blocking *de novo* ceramide synthesis and (v) targeting of a bacterial ceramidase to mitochondria. Our data provide the first demonstration that translocation of ER ceramides to mitochondria specifically commits cells to death and establish mitoCERT as a valuable new tool to unravel the molecular principles underlying ceramide-mediated apoptosis.

KEY WORDS: Bcl-2 proteins, Ceramide transfer protein, Cytochrome *c*, Endoplasmic reticulum, Membrane contact sites, Mitochondrial apoptosis, VAP receptor

INTRODUCTION

Apoptosis is a form of programmed cell death with a crucial role in organismal development and tissue homeostasis. Perturbations in apoptosis contribute to human diseases including cancer and autoimmunity. The role of mitochondria in apoptosis that is triggered by diverse stress stimuli (e.g. DNA damage, cytokines) has been well established and provides an attractive target of therapeutic interventions (Czabotar et al., 2014; Tait and Green, 2013). Permeabilization of the mitochondrial outer membrane (MOM), allowing passage of intermembrane space proteins such as cytochrome *c*, is considered a point of no return in the suicide program, leading to activation of caspases that execute an ordered cellular self-destruction. MOM permeabilization (MOMP) is controlled by the B-cell lymphoma 2 (Bcl-2) protein family, which includes pro- and anti-apoptotic members that collectively determine the balance between cell death and survival (Luna-Vargas and Chipuk, 2016; Moldoveanu et al., 2014). The principal function of the anti-apoptotic Bcl-2 proteins is to antagonize the pro-apoptotic activities of the Bcl-2 proteins Bax and Bak (also known as BAK1), which are thought to directly engage in MOMP by creating proteolipid pores responsible for cytochrome *c* release (Kuwana et al., 2002; Salvador-Gallego et al., 2016; Wei et al., 2001).

Although apoptosis research has primarily focused on the role of Bcl-2 proteins, a growing body of evidence supports a crucial role for lipids. Notably, ceramides – central intermediates of sphingolipid metabolism – have frequently been implicated as potential mediators of mitochondrial apoptosis (Hannun and Obeid, 2008; Patwardhan et al., 2016). Numerous studies have revealed that cellular ceramide levels rise concomitantly with apoptosis induction in response to a variety of apoptotic stimuli, including tumor necrosis factor α (TNFα) (García-Ruiz et al., 2003; Luberto et al., 2002), chemotherapeutic agents (Alphonse et al., 2004; Bose et al., 1995) and radiation (Deng et al., 2008; Mesicek et al., 2010), through activation of sphingomyelinases, stimulation of *de novo* ceramide synthesis, or both. Interventions that suppress ceramide accumulation render cells resistant to these apoptotic stimuli, indicating that ceramides are necessary and sufficient to trigger mitochondrial apoptosis. Consequently, the potential of ceramide-based therapeutics in the treatment of cancer has become a major focus of interest. However, where and how ceramides exert their apoptogenic activity in cells is not well understood.

Some reports indicate that ceramides can promote apoptotic cell death by inhibiting phosphoinositide-3 kinase (PI3K) and Akt/PKB signaling, resulting in dephosphorylation and subsequent activation of the pro-apoptotic Bcl-2-family protein Bad (Bourbon et al., 2002; Zhu et al., 2011). Short-chain ceramides can activate protein phosphatase 2A (PP2A), which dephosphorylates and inactivates the anti-apoptotic protein BCL2 (Dobrowsky et al., 1993; Mukhopadhyay et al., 2009). An upregulation of ceramide levels has also been reported to sensitize cells to endoplasmic reticulum (ER) stress and promote activation of apoptotic regulators of the unfolded protein response (Liu et al., 2014; Park et al., 2008; Senkal et al., 2011; Swanton et al., 2007). Other studies have revealed that ceramides can form pores in planar membranes as well as in the outer membrane of isolated mitochondria that are large enough to allow passage of cytochrome *c* (Siskind et al., 2002, 2006). Interestingly, members of the anti-apoptotic Bcl-2 protein family prevent ceramide-induced permeabilization of isolated mitochondria, whereas a combination of pro-apoptotic Bax and ceramides enhances permeabilization (Ganesan et al., 2010; Siskind et al., 2008). This indicates that ceramides can act directly on mitochondria to promote MOMP and trigger apoptotic cell death. In line with this idea, mitochondrial targeting of a bacterial sphingomyelinase to generate ceramides in mitochondria induces cytochrome *c* release and apoptosis (Birbes et al., 2001). Moreover, ER-like membranes associated with isolated mitochondria appear to

[1]Molecular Cell Biology Division, Department of Biology/Chemistry, University of Osnabrück, Osnabrück D-49076, Germany. [2]Max-Planck-Institute for Molecular Cell Biology and Genetics, Dresden D-01307, Germany. [3]Membrane Biochemistry & Biophysics, Bijvoet Center and Institute of Biomembranes, Utrecht University, Utrecht 3584 CH, The Netherlands.

*Author for correspondence (holthuis@uos.de)

K.E., 0000-0001-9800-2781; J.C.M.H., 0000-0001-8912-1586

Received 23 June 2016; Accepted 14 November 2016

Journal of Cell Science (2017) 130, 360-371 doi:10.1242/jcs.194191

produce enough ceramides to allow transient penetration of the outer membrane by pro-apoptotic proteins (Stiban et al., 2008). However, the actual contribution of mitochondrial ceramides to the apoptotic response in living cells is a topic of controversy (Ségui et al., 2006; Wang et al., 2009; Chipuk et al., 2012). Resolving this issue is challenging because ceramides are readily metabolized into various other bioactive lipid species, which can influence the sensitivity of cells to apoptosis through multiple pathways (Hait et al., 2006; Hannun and Obeid, 2008). Moreover, apoptotic stimuli such as TNFα trigger ceramide accumulation in multiple organelles (Birbes et al., 2005; Dbaibo et al., 2001; Luberto et al., 2002).

Ceramides are synthesized *de novo* through N-acylation of sphingoid bases, a reaction that is catalyzed by ceramide synthases on the cytosolic surface of the ER (Tidhar and Futerman, 2013). In mammals, the bulk of newly synthesized ceramides is converted to sphingomyelin by sphingomyelin synthase in the lumen of the trans-Golgi (Tafesse et al., 2006). Delivery of ER ceramides to the site of sphingomyelin production requires the cytosolic ceramide transfer protein CERT (encoded by *COL4A3BP*) (Hanada et al., 2003). Besides a ceramide transfer or START domain, CERT contains a pleckstrin homology domain that binds to phosphatidylinositol 4-monophosphate (PI4P) at the trans-Golgi and a FFAT motif that is recognized by the ER-resident VAMP-associated proteins A and B (VAP-A and VAP-B, respectively) (Kawano et al., 2006). CERT might operate within the narrow cytoplasmic gap at contact sites between the ER and trans-Golgi to establish efficient ceramide transport for sphingomyelin production. Mammalian cells contain two sphingomyelin synthase isoforms, namely SMS1 in the trans-Golgi and SMS2 at the plasma membrane (also known as SGMS1 and SGMS2, respectively) (Huitema et al., 2004; Yamaoka et al., 2004). Together with SMS-related protein SMSr (also known as SAMD8), they form the SMS family. SMSr is not a conventional sphingomyelin synthase but instead synthesizes trace amounts of the sphingomyelin analog ceramide phosphoethanolamine in the lumen of the ER (Vacaru et al., 2009). SMSr is the best-conserved member of the SMS family, with homologs in organisms that lack sphingomyelin (Vacaru et al., 2013). Unexpectedly, disrupting SMSr catalytic activity in mammalian cells causes an accumulation of ER ceramides and their mislocalization to mitochondria, triggering a mitochondrial pathway of apoptosis (Tafesse et al., 2014; Vacaru et al., 2009). Apoptosis induction is prevented by blocking *de novo* ceramide synthesis, stimulating ceramide export from the ER or targeting a bacterial ceramidase to mitochondria (Tafesse et al., 2014). These results imply that ER ceramides are authentic transducers of apoptosis and that their arrival in mitochondria is a critical step in committing cells to death.

In the present study, we verified the above concept by diverting CERT-mediated ceramide transport to mitochondria. This was accomplished by targeting CERT to the OMM while retaining its ability to interact with VAP proteins in the ER. We found that expression of mitoCERT triggers a mitochondrial pathway of apoptosis, as evidenced by cytosolic translocation of cytochrome *c* and activation of caspase 9. Apoptosis induction was abolished through the removal of Bax, required ongoing *de novo* ceramide biosynthesis and critically relied on the ability of mitoCERT to transport ceramides at ER–mitochondria junctions. These results indicate that ceramide delivery to mitochondria specifically induces apoptotic cell death, and they highlight a novel approach for probing the compartment-specific functions of ceramides as key determinants of cell fate.

RESULTS

Mitochondrial targeting of CERT

CERT targets the Golgi by recognizing PI4P through its N-terminal plextrin homology domain (Hanada et al., 2003). To direct CERT-mediated ceramide transport to mitochondria, the plextrin homology domain of CERT was swapped against the OMM (OMM) anchor sequence of mouse A-kinase anchor protein 1 (AKAP1), generating mitoCERT (Fig. 1A). A FLAG-tag was added to the C-terminus of CERT and mitoCERT to facilitate their detection. Contrary to CERT, mitoCERT expressed in human HeLa cells colocalized with a mitochondrial marker and was fully recovered from a membrane-bound fraction, indicating that the protein was efficiently targeted to mitochondria (Fig. 1B,C).

CERT contains a short peptide sequence or FFAT motif (consensus sequence EFFDAxE, where x is any amino acid), which interacts with the ER-resident tail-anchored proteins VAP-A and VAP-B (Kawano et al., 2006; Loewen et al., 2003). The interaction between CERT and VAPs is crucial for efficient ER-to-Golgi transfer of ceramide. Indeed, CERT carrying a mutation in its FFAT motif (D324A) loses the ability to bind VAPs and cannot transfer ceramide to the Golgi efficiently (Kawano et al., 2006). Therefore, we next investigated the ability of mitoCERT to interact with VAPs. When expressed in HeLa cells, VAP-A that had been fused to GFP displayed a reticular cytosolic distribution that was reminiscent of the ER (Fig. 2A). Upon co-expression with CERT, GFP-tagged VAP-A accumulated in the perinuclear region. This perinuclear localization of VAP-A was lost when co-expressed with a CERT-D324A point mutant, as reported previously (Kawano et al., 2006) (Fig. 2A). When co-expressed with mitoCERT, VAP-A showed a tubular distribution that largely coincided with the mitoCERT- and Tom20-positive mitochondrial network (Fig. 2A,B). In cells expressing mitoCERT with the D324A point mutation, VAP-A retained a reticular distribution throughout the cytosol that showed little overlap with the mitochondrial network (Fig. 2A,B). This indicates that mitochondria-localized mitoCERT is able to bind to VAP receptors in the ER.

MitoCERT acts as a VAP-dependent ER–mitochondria tether

The ability of mitoCERT to interact with ER-resident VAP receptors suggests that the protein might influence the contact area between ER and mitochondria by acting as an inter-organellar tether. To address this possibility, we first monitored changes in ER–mitochondria contacts using rapamycin-inducible linkers based on the FKBP–FRB heterodimerization system (Csordás et al., 2010) (Fig. 3A). These linkers were tagged with photoconvertable fluorophores to allow visualization of ER–mitochondria contacts by super-resolution microscopy. Addition of rapamycin caused a rapid (within 10 min) expansion of ER–mitochondria contact sites in cells that expressed the linkers (Fig. 3B,F). Consistent with this finding, subcellular fractionation experiments revealed that ∼40% of the ER-resident protein calnexin was recovered from mitochondrial pellets prepared from rapamycin-treated cells, whereas no more than 5% of calnexin was recovered from mitochondrial pellets of control cells (Fig. 3C). In contrast, super-resolution fluorescence microscopy and subcellular fractionation experiments revealed that expression of mitoCERT did not lead to any obvious increase in the contact area between ER and mitochondria. However, in cells that overproduced VAP-A, mitoCERT expression caused a significant expansion of ER–mitochondria contact sites (Fig. 3D–F). Based on these results, we conclude that mitoCERT acts as a VAP-dependent ER–mitochondria tether.

Journal of Cell Science (2017) 130, 360-371 doi:10.1242/jcs.194191

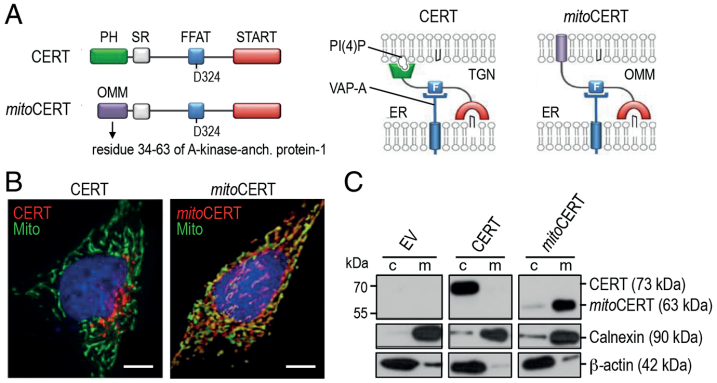

Fig. 1. Mitochondrial targeting of ceramide transfer protein CERT. (A) Schematic outline of CERT and mitoCERT. PH, pleckstrin homology domain; SR, serine-rich domain; FFAT, VAP-binding domain; START, ceramide-binding domain; PI(4)P, phosphatidylinositol-4-phosphate; TGN, trans-Golgi network; OMM, outer mitochondrial membrane. (B) MitoCERT localizes to mitochondria. HeLa cells that had been transfected with Flag-tagged CERT or mitoCERT were fixed, co-stained with antibodies against the Flag epitope (red) and mitochondrial protein p60 (Mito, green), and then visualized by fluorescence microscopy. (C) Contrary to CERT, mitoCERT co-fractionated with membranes. Immunoblots of cytosol (c) and total membranes (m) derived from HeLa cells that had been transfected as described in B were stained for the Flag epitope, calnexin and β-actin. EV, empty vector.

MitoCERT mediates ceramide delivery to mitochondria

We next examined whether mitoCERT can mediate ceramide transfer to mitochondria. First, we analyzed the ability of the protein to bind to ceramide. To this end, lysates of mitoCERT-expressing HeLa cells were photoaffinity-labeled with pacCer, a bifunctional ceramide analog containing a photoactivatable diazirine and clickable alkyne group in its 15-carbon-long N-linked fatty acyl chain (Fig. 4A). Ultraviolet (UV) irradiation of the diazirine group generates a highly-reactive pacCer intermediate that can form a covalent linkage with proteins in its direct vicinity (Svenja Bockelmann, John Mina, Per Haberkant and J.C.M.H., unpublished data). Click chemistry is then used to decorate the alkyne group with a fluorophore, allowing visualization of the crosslinked protein–lipid complex by in-gel fluorescence. As proof-of-principle, lysates of HeLa cells expressing FLAG-tagged CERT were incubated with pacCer-containing liposomes and then

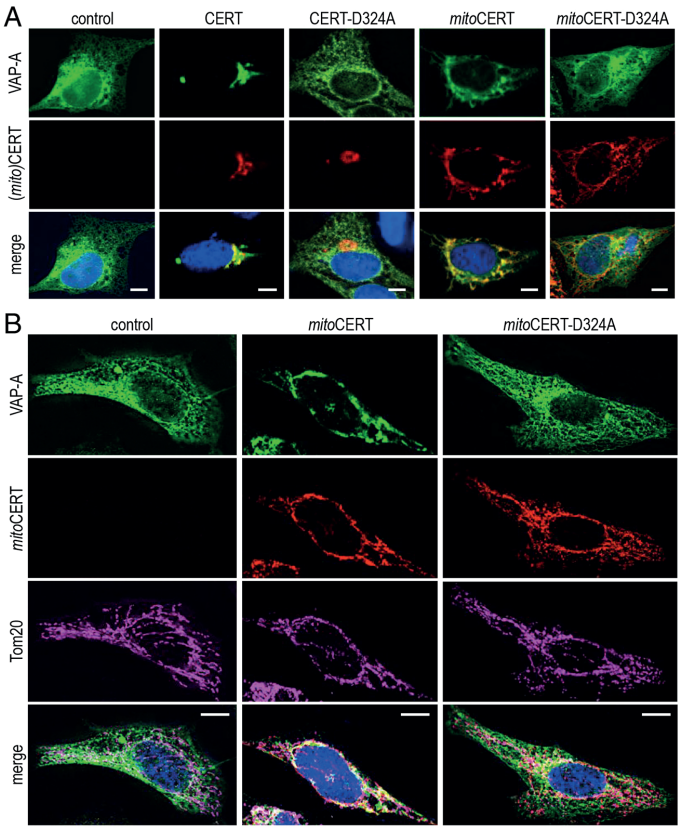

Fig. 2. Mitochondria-localized mitoCERT interacts with VAP-A in the ER. (A) HeLa cells that had been co-transfected with eGFP–VAP-A (green) and Flag-tagged CERT, mitoCERT or the VAP-A-binding mutants CERT-D324A and mitoCERT-D324A were fixed, stained with anti-Flag antibody (red) and then visualized by fluorescence microscopy. Scale bars: 10 µm. (B) HeLa cells that had been co-transfected with mCherry–VAP-A (green), Tom20–eGFP (magenta) and Flag-tagged mitoCERT or the VAP-A-binding mutant mitoCERT-D324A were fixed and stained with anti-Flag antibody (red) and then visualized by fluorescence microscopy. Scale bars: 10 µm.

Journal of Cell Science (2017) 130, 360-371 doi:10.1242/jcs.194191

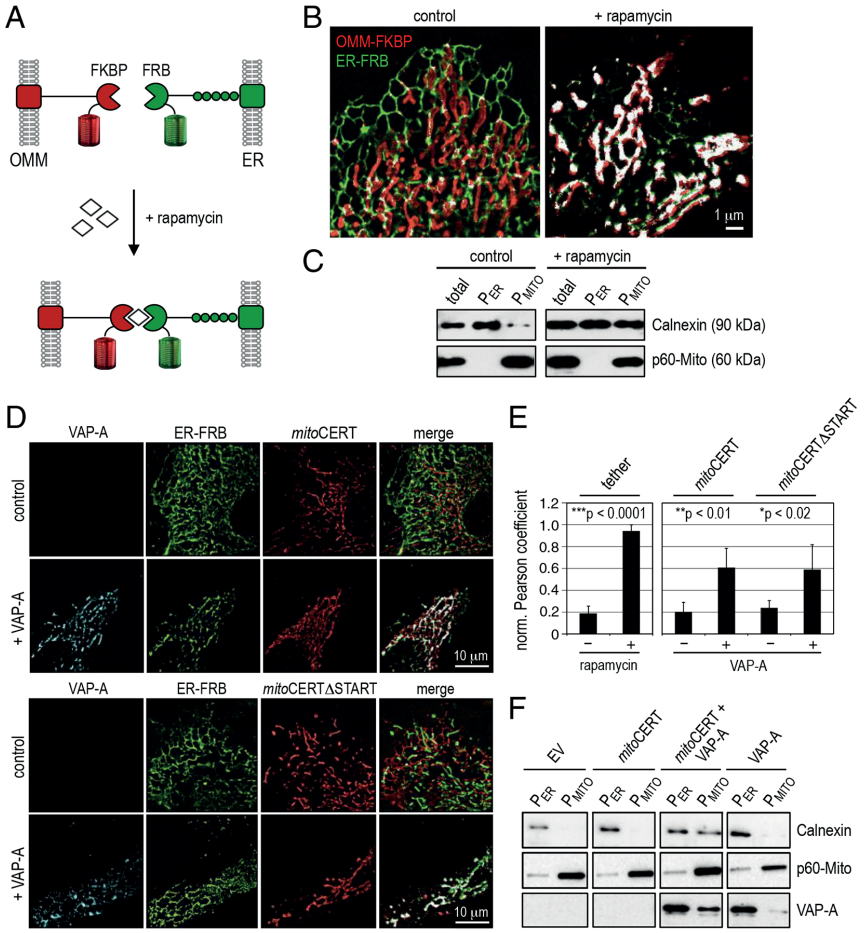

Fig. 3. Impact of mitoCERT expression on contact sites between ER and mitochondria. (A) Schematic of the rapamycin-inducible fluorescent ER–mitochondria linkers paGFP-ER-FRB and OMM-FKBP-HALO. (B) Fluorescence photoactivation localization microscopy (fPALM) and dStorm images showing ER (green) and mitochondrial networks (red) in HeLa cells that had been transfected with rapamycin-inducible ER–mitochondria linkers before (control) and after treatment with rapamycin (+rapamycin; 50 nM, 30 min). OMM-FKBP-HALO was conjugated to HTL-TMR. Note that contact areas between ER and mitochondria (white) expanded dramatically upon rapamycin treatment. (C) Subcellular fractionation analysis confirmed rapamycin-induced expansion of ER–mitochondria junctions. HeLa cells that had been transfected with rapamycin-inducible ER–mitochondria linkers were treated as described in B and then subjected to subcellular fractionation, yielding total membranes (total) and membrane fractions enriched for ER (P_{ER}) or mitochondria (P_{MITO}). Equal volumes of each fraction where analyzed by immunoblotting against markers for ER (calnexin) and mitochondria (P60-Mito). (D) MitoCERT acts as a VAP-dependent ER–mitochondria tether. fPALM and dStorm images of HeLa cells that had been co-transfected with the indicated combinations of HALO-ER-FRB (green), mitoCERT–Flag (red), mitoCERTΔSTART–Flag (red) and paGFP–VAP-A (cyan). Immunodetection of Flag-tagged proteins was with Cy5-conjugated rabbit polyclonal secondary antibody. Contact areas between ER and mitochondria (white) expanded substantially when mitoCERT or mitoCERTΔSTART were co-expressed with paGFP–VAP-A (+VAP-A). (E) Pearson correlation coefficients between ER and mitochondria determined in cells treated as described in B and D. The maximum correlation coefficient measured was set at 1. Data are mean±s.d. (n=3). ***P<0.0001; **P<0.01; *P<0.02, by two-tailed unpaired Student's t-test. (F) Subcellular fractionation analysis confirming mitoCERT-dependent expansion of ER–mitochondria junctions in VAP-A-overproducing cells. HeLa cells that had been transfected with Flag-tagged mitoCERT, mitoCERTΔSTART and/or paGFP–VAP-A were processed as described in C. Note that co-expression of paGFP–VAP-A and mitoCERT resulted in expanded ER–mitochondria contact sites, as evidenced by an enhanced recovery of ER-resident calnexin and paGFP–VAP-A (VAP-A) from mitochondrial membrane pellets. Immunoblots shown are representative of two independent experiments.

subjected to UV irradiation followed by a click reaction with Alexa-Fluor-647 azide. This approach yielded a fluorescent protein of 73 kDa that reacted with anti-FLAG antibodies and that was absent in pacCer-labeled lysates of control cells (Fig. 4B, left panel). Photoaffinity-labeled lysates of cells that expressed FLAG-tagged mitoCERT, by contrast, contained a fluorescent and immunoreactive protein of 63 kDa (Fig. 4B, right panel). Removal of the ceramide transfer or START domain yielded a 38-kDa protein, mitoCERTΔSTART, which failed to react with pacCer upon UV cross-linking. These data show that, analogous to CERT, mitoCERT is able to extract ceramide from a lipid bilayer through its START domain.

Journal of Cell Science (2017) 130, 360-371 doi:10.1242/jcs.194191

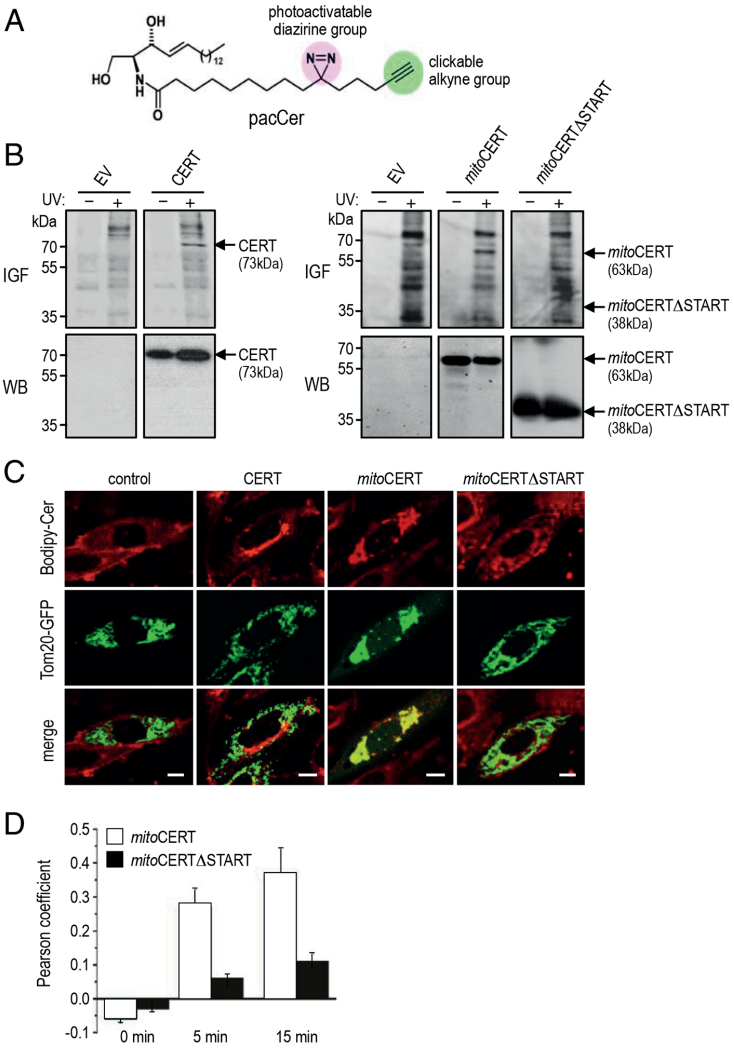

Fig. 4. MitoCERT binds to ceramides and catalyzes their transport to mitochondria. (A) Structure of the photoactivatable and clickable C15-ceramide analog, pacCer. (B) Photoaffinity labeling of mitoCERT with pacCer. Total lysates of HeLa cells expressing Flag-tagged CERT, mitoCERT or mitoCERTΔSTART were incubated with pacCer-containing liposomes for 30 min at 37°C, subjected to UV irradiation and then click-reacted with Alexa-Fluor-647 azide. Lysates were analyzed by in-gel fluorescence (top) or processed for immunoblotting using an anti-Flag antibody (bottom). (C) MitoCERT mediates delivery of C5-Bodipy–ceramide to mitochondria. CHO LY-A cells that had been co-transfected with the mitochondrial marker Tom20–GFP and empty vector (control), CERT, mitoCERT or mitoCERTΔSTART were incubated with 0.5 µM red fluorescent C5-Bodipy–ceramide at 4°C for 30 min, chased at 37°C for 15 min, and then visualized by confocal fluorescence microscopy. Scale bars: 10 µm. (D) Pearson correlation coefficients between C5-Bodipy–ceramide and mitochondria were determined in CHO LY-A cells that had been co-transfected with Tom20–GFP and mitoCERT or mitoCERTΔSTART. Cells were pulse-labeled with C5-Bodipy–ceramide at 4°C for 30 min and then chased for 0, 5 or 15 min at 37°C. Data are mean±s.d. (n=3).

We next addressed whether mitoCERT can mediate ceramide transport to mitochondria. To this end, the intracellular movement of a fluorescent analog of ceramide (C5-Bodipy–Cer) was monitored in Chinese hamster ovary (CHO) LY-A cells that had been transfected with GFP-tagged Tom20 as mitochondrial marker. In these cells, ER-to-Golgi transport of C5-Bodipy–Cer is disrupted owing to a loss-of-function mutation in the CERT-encoding gene (Hanada et al., 2003). In cells that expressed wild-type CERT, transport was restored and C5-Bodipy–Cer accumulated in the perinuclear Golgi region (Fig. 4C). However, in cells that expressed mitoCERT, C5-Bodipy–Cer was readily delivered to mitochondria. In contrast, cells expressing mitoCERTΔSTART failed to deliver C5-Bodipy–Cer to mitochondria (Fig. 4C,D). These results demonstrate that mitoCERT is able to bind to ceramides and can mediate their transport to mitochondria.

MitoCERT triggers ceramide-dependent mitochondrial apoptosis

A rise in mitochondrial ceramide levels has been implicated in the activation of mitochondrial apoptosis (Birbes et al., 2001; Lee et al., 2011; Tafesse et al., 2014). Therefore, we next analyzed the ability of mitoCERT to trigger mitochondria-mediated cell death. Within 24 h after transfection, mitoCERT-expressing HeLa cells released cytochrome *c* into the cytosol (Fig. 5A) and displayed proteolytic activation of caspase 9 (Fig. 5B,C), two hallmarks of mitochondrial apoptosis that are also observed in staurosporine-treated cells. Moreover, mitoCERT expression led to cleavage of the caspase substrate PARP, membrane blebbing and cell death (Fig. 5B; data not shown). Treatment with the pan-caspase inhibitor z-VAD-fmk blocked cleavage of caspase 9 and PARP (Fig. 5D), and prevented membrane blebbing and cell death (data not shown), indicating that mitoCERT activates a caspase-dependent pathway of

Journal of Cell Science (2017) 130, 360-371 doi:10.1242/jcs.194191

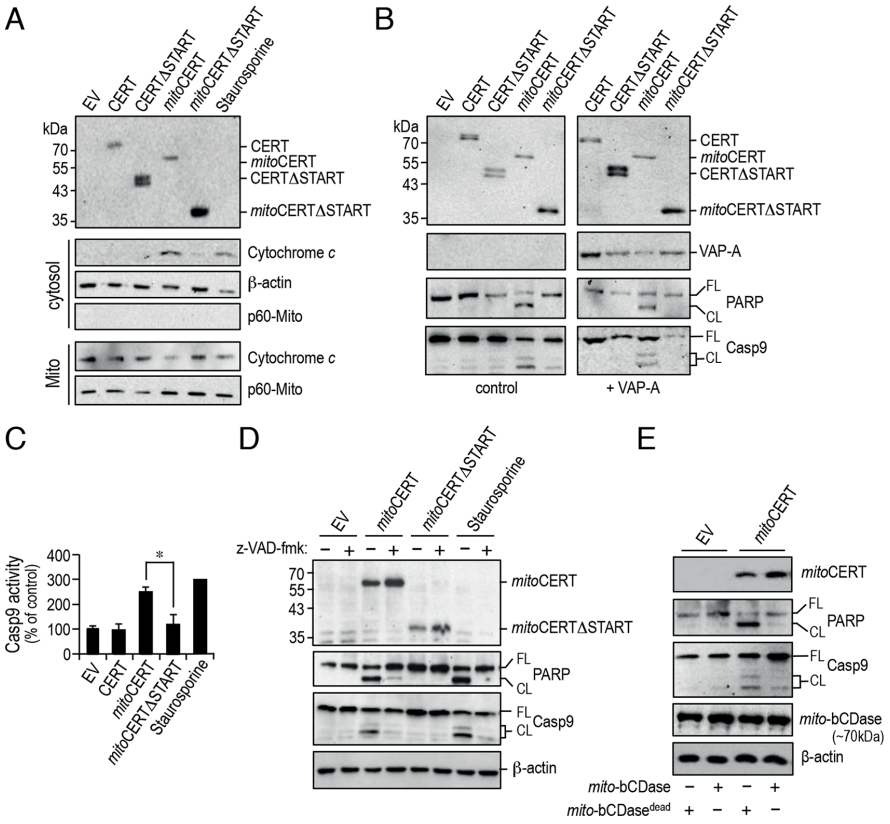

Fig. 5. MitoCERT activates a ceramide-dependent pathway of mitochondrial apoptosis. (A) MitoCERT expression triggers cytosolic release of cytochrome *c*. HeLa cells that had been treated with staurosporine (1 µM, 4 h) or transfected with empty vector (EV), Flag-tagged CERT, CERTΔSTART, mitoCERT or mitoCERTΔSTART (24 h) were lysed and subjected to subcellular fractionation. Total cell lysates, cytosol and mitochondrial pellets were processed for immunoblotting with antibodies against the Flag epitope (top), cytochrome *c*, β-actin and mitochondrial protein p60-Mito (bottom). Note that removal of the START domain abolished the ability of mitoCERT to induce translocation of cytochrome *c*. (B) MitoCERT expression induces cleavage of caspase 9 (Casp9) and PARP. HeLa cells that had been co-transfected with empty vector (control) or VAP-A–eGFP (+VAP-A) and Flag-tagged CERT, CERTΔSTART, mitoCERT or mitoCERTΔSTART were lysed and processed for immunoblotting with antibodies against the Flag epitope, eGFP (VAP-A), PARP and caspase 9. FL, full length; CL, cleaved. (C) Cells that had been treated as described in A were lysed and analyzed for caspase-9 activity using a colorimetric assay. Levels of caspase-9 activity were expressed relative to that in cells that had been transfected with empty vector (EV). Error bars indicate mean±s.d., n=3. *P<0.05 by two-tailed unpaired Student's t-test. (D) Pan-caspase inhibitor z-VAD-fmk blocks caspase-9 and PARP cleavage in mitoCERT-expressing cells. HeLa cells that had been treated as described in A were incubated in the absence (–) or presence (+) of z-VAD-fmk and then processed for immunoblotting. (E) Targeting a bacterial ceramidase to mitochondria abrogates apoptosis induction in mitoCERT-expressing cells. HeLa cells that had been co-transfected with empty vector (EV) or Flag-tagged mitoCERT and a catalytically active or dead bacterial ceramidase carrying a mitochondria-targeting signal and Myc tag (mito-bCDase, mito-bCDase^{dead}) were lysed and processed for immunoblotting with antibodies against PARP, caspase 9 and the Flag and Myc epitopes. Immunoblots shown are representative of two independent experiments.

apoptosis. In contrast, cells overproducing CERT or expressing mitoCERTΔSTART were devoid of any of the aforementioned apoptotic phenotypes (Fig. 5A–D). Although mitoCERTΔSTART was unable to bind to and transfer ceramides (Fig. 4), it retained the ability to act as a VAP-dependent ER–mitochondria tether (Fig. 3D,F). This implies that ER–mitochondria tethering is unlikely to represent the principal mechanism by which mitoCERT-expressing cells are committed to death. Indeed, expanding the contact area between ER and mitochondria through overproduction of VAP-A had no obvious impact on the fate of either mitoCERT- or mitoCERTΔSTART-expressing cells (Fig. 5B). Rather, the ability of mitoCERT to catalyze ceramide transport to mitochondria appeared to be important for its apoptogenic activity. To examine this further, we next used a *Mycobacterium*-derived ceramidase equipped with an N-terminal mitochondrial-targeting signal, mito-bCDase. We have previously demonstrated that heterologous expression of mito-bCDase effectively prevents ceramide accumulation in mitochondria of SMSr-depleted HeLa cells (Tafesse et al., 2014). When co-expressed with mito-bCDase, mitoCERT lost the ability to induce caspase-9 and PARP cleavage (Fig. 5E). This rescuing effect was abolished through mutation of two invariant histidine residues (His96 and His98) in the active site of mito-bCDase, indicating that a catalytically active form of the enzyme is required to prevent mitoCERT-mediated cell death. From

Journal of Cell Science (2017) 130, 360-371 doi:10.1242/jcs.194191

this, we conclude that the apoptogenic activity of mitoCERT crucially relies on its ability to deliver ceramides to mitochondria.

The apoptogenic activity of mitoCERT relies on its interaction with VAP and requires *de novo* ceramide synthesis

As mitoCERT interacts with ER-resident VAPs, a likely source of the ceramides responsible for committing mitoCERT-expressing cells to death is the ER. To test this directly, we initially set out to monitor mitochondrial delivery of *de novo* synthesized ceramides through metabolic labeling of control and mitoCERT-expressing cells with [2,3,3-d3] serine (D_3-serine) followed by mass spectrometry quantification of D_3-serine-labeled ceramides in purified mitochondria. However, this approach did not yield a conclusive answer as D_3-serine-labeled ceramides were hard to detect and it was difficult to exclude their partial turnover during the time-consuming preparation of mitochondria that were free of ER and other contaminating organelles. Therefore, we next investigated the impact of blocking *de novo* ceramide synthesis on mitoCERT-induced cell death. Treatment with long chain base synthase inhibitor myriocin or ceramide synthase inhibitor fumonisin B1 in each case fully suppressed cleavage of caspase 9 and PARP in mitoCERT-expressing cells (Fig. 6A). Addition of HPA12, a specific inhibitor of CERT-mediated ceramide transport (Kumagai et al., 2005), also blocked caspase-9 and PARP cleavage in these cells. Collectively, these data support the idea that mitoCERT triggers apoptosis by transferring ceramides from the ER to mitochondria. As efficient ceramide trafficking from the ER to the Golgi is crucially dependent on the ability of CERT to interact with ER-resident VAPs (Kawano et al., 2006), we next analyzed VAP-binding mutant mitoCERT-D324A for its ability to induce apoptosis. Unlike mitoCERT, expression of mitoCERT-D324A failed to trigger cleavage of caspase 3, caspase 9 and PARP in HeLa cells (Fig. 6B–D). These results indicate that the ceramides responsible for activating mitochondrial apoptosis in mitoCERT-expressing cells primarily originate from the ER.

MitoCERT-induced apoptosis is crucially dependent on Bax but not Bak

Besides HeLa cells, several other human cancer cell lines proved to be susceptible to mitoCERT-induced apoptosis. These included ovarium carcinoma OVCAR3 and SKOV1, non-small lung carcinoma A549, and colon carcinoma HCT116 cells. In all cases examined, removal of the START domain or substitution of Ala for Asp at position 324 in the FFAT motif abolished mitoCERT-mediated apoptogenic activity (Fig. 7A). These results indicate that diverting CERT-mediated ceramide trafficking to mitochondria is sufficient to commit cells to death and that this process is not restricted to one particular cell type. It has been proposed that ceramides can trigger apoptosis by forming channels in the OMM to allow passage of cytochrome *c* (Siskind et al., 2002, 2006). However, other models postulate that ceramide-mediated apoptosis relies on participation of the pro-apoptotic Bcl-2 proteins Bax and Bak (Beverly et al., 2013; Chipuk et al., 2012; von Haefen et al., 2002). This led us to examine the consequences of Bax and Bak removal on mitoCERT-induced apoptosis in HCT116 cells. Treatment with staurosporine served as control. Loss of Bak had no measurable impact on caspase-9 or PARP cleavage in either mitoCERT-expressing or staurosporine-treated cells (Fig. 7B). In contrast, removal of Bax essentially abolished caspase-9 and PARP cleavage in both mitoCERT-expressing and staurosporine-treated cells. MitoCERT expression caused, at best, only some residual PARP cleavage in Bax-deficient cells. The apoptogenic activity of mitoCERT was completely eliminated in Bak- and Bax-deficient

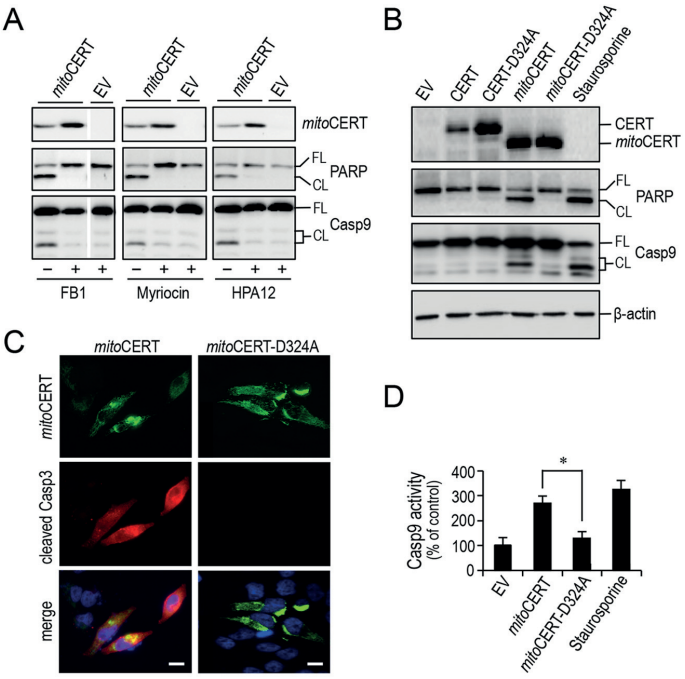

Fig. 6. Apoptogenic activity of mitoCERT relies on its interaction with VAP and is sensitive to inhibitors of *de novo* ceramide synthesis. (A) HeLa cells that had been transfected with empty vector (EV) or Flag-tagged mitoCERT were treated with inhibitors of long-chain base synthase (myriocin, 30 µM), ceramide synthase (fuminosin FB1, 25 µM) or CERT (HPA12, 10 µM), lysed and processed for immunoblotting with antibodies against the Flag epitope, PARP and caspase 9 (Casp9). (B) HeLa cells that had been transfected with empty vector (EV) or Flag-tagged CERT, mitoCERT or the VAP-binding mutants CERT-D324A or mitoCERT-D324A were lysed and processed for immunoblotting with antibodies against the Flag epitope, PARP, caspase 9 and β-actin. (C) HeLa cells that had been transfected with Flag-tagged mitoCERT or mitoCERT-D324A were fixed, co-stained with DAPI (blue) and antibodies against the Flag epitope (green) or cleaved caspase 3 (red; Casp3) and then visualized by fluorescence microscopy. Scale bars: 20 µm. (D) Cells that had been treated as described in B were lysed and analyzed for caspase-9 activity with a colorimetric assay. Levels of caspase-9 (Casp9) activity were expressed relative to those in cells that had been transfected with empty vector (EV). Error bars indicate mean±s.d., n=3. *P<0.05 by two-tailed unpaired Student's t-test. FL, full length; CL, cleaved.

Journal of Cell Science (2017) 130, 360-371 doi:10.1242/jcs.194191

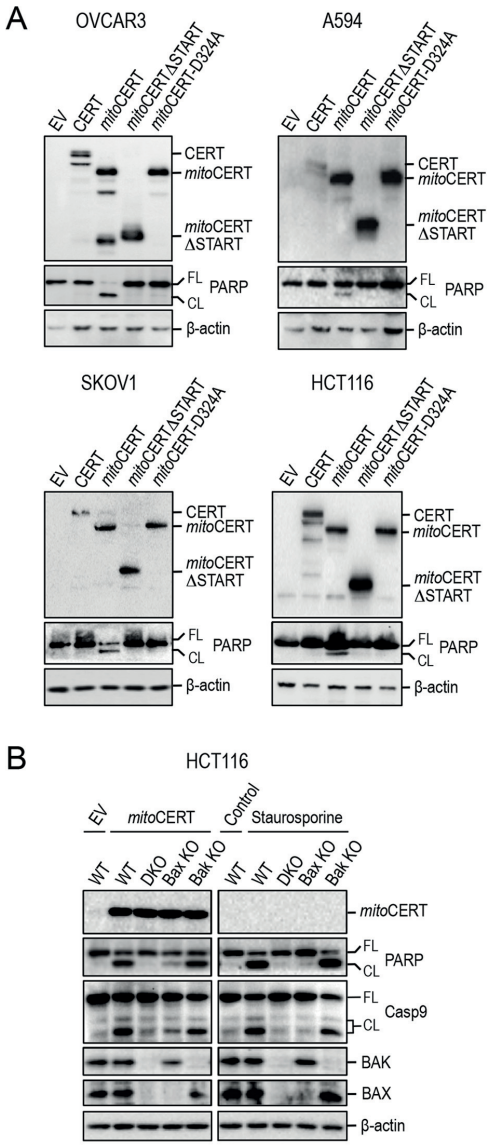

Fig. 7. MitoCERT-induced apoptosis is largely independent of cell type and crucially relies on the pro-apoptotic Bcl-2 protein Bax. (A) Human ovarium carcinoma OVCAR3 cells, ovarium carcinoma SKOV1 cells, non-small lung carcinoma A549 cells and colon carcinoma HCT116 cells were transfected with empty vector (EV) or Flag-tagged versions of CERT, mitoCERT, mitoCERTΔSTART or mitoCERT-D324A. At 24 h post-transfection, cells were processed for immunoblotting with antibodies against the Flag epitope, PARP and β-actin. FL, full length; CL, cleaved. (B) Wild-type (WT), $Bax^{-/-}$ (Bax KO), $Bak^{-/-}$ (Bak KO) and $Bax^{-/-}Bak^{-/-}$ (DKO) HCT116 cells were treated with staurosporine (1 µM, 4 h) or transfected with empty vector (EV) or Flag-tagged mitoCERT. At 24 h post transfection, cells were processed for immunoblotting with antibodies against the Flag epitope, PARP, caspase 9 (Casp9), Bak, Bax and β-actin. Note that removal of Bax virtually abolished mitoCERT-induced PARP and caspase-9 cleavage. Immunoblots shown are representative of three independent experiments.

cells. From this, we conclude that activation of mitochondrial apoptosis by mitoCERT primarily relies on Bax, analogous to the apoptotic pathway activated in staurosporine-treated HCT116 cells (Wang and Youle, 2012).

DISCUSSION

Ceramides are widely believed to be authentic transducers of apoptosis, but how these biomolecules help commit cells to death is not well understood. A deregulation of ceramide levels in the ER has frequently been linked to induction of mitochondrial apoptosis. Although some reports indicate that ceramides influence this process by sensitizing cells to ER stress and activating apoptotic regulators of the unfolded protein response, experiments with isolated mitochondria suggest that ceramides are able to initiate the execution phase of apoptosis by directly promoting MOMP. To better define where and how ceramides exert their apoptogenic activity in cells, we here analyzed the consequences of targeting the biosynthetic ceramide flow to mitochondria using a ceramide transfer protein equipped with an OMM anchor, mitoCERT. We show that mitoCERT expression activates a ceramide-mediated mitochondrial pathway of apoptosis that requires the pro-apoptotic Bcl-2 protein Bax. Our findings provide a direct demonstration that translocation of ER ceramides to mitochondria suffices to commit cells to death, hence highlighting subcellular topology as a key determinant in ceramide-induced apoptosis.

Complementary lines of evidence indicate that apoptosis induction in mitoCERT-expressing cells is due to the arrival of ER ceramides in the mitochondria. To begin with, the apoptogenic activity of mitoCERT required an intact ceramide transfer or START domain and was crucially dependent on the ability of the mitochondria-anchored protein to bind to VAP receptors in the ER. The latter observation raised the possibility that mitoCERT triggers apoptosis by tightening the contact area between the ER and mitochondria, which has previously been reported to make mitochondria prone to Ca^{2+} overloading, resulting in MOMP and apoptotic cell death (Csordás et al., 2010, 2006). However, mitoCERT-mediated tethering between ER and mitochondria, although required, was not sufficient to initiate mitochondrial apoptosis given that removal of the START domain abolished the apoptogenic activity of mitoCERT without compromising its ER–mitochondria tethering activity. In addition, overproduction of VAP-A in either mitoCERT- or mitoCERTΔSTART-expressing cells greatly expanded the contact area between ER and mitochondria without having any impact on cell fate. Moreover, mitoCERT-induced apoptosis was effectively blocked by HPA12, an antagonistic inhibitor of CERT-mediated ceramide trafficking (Kudo et al., 2010; Kumagai et al., 2005). Thus, a ceramide transfer-competent form of mitoCERT capable of bridging the cytoplasmic gap between mitochondria and ER proved critical for apoptosis induction. Blocking *de novo* ceramide production by pharmacological inhibitors of ceramide or long chain base synthases abrogated apoptosis induction in mitoCERT-expressing cells, indicating that mitochondrial delivery of ER ceramides by mitoCERT is responsible for triggering cell death. Indeed, targeting a catalytically active bacterial ceramidase to mitochondria fully suppressed mitoCERT-induced cell death.

Our current work complements and extends previous *in vitro* studies indicating that ceramides can act directly on mitochondria to promote MOMP and trigger apoptotic cell death. So how do ceramides help accomplish the release of pro-apoptotic proteins from the mitochondrial intermembrane space? Recent biochemical experiments with purified mitochondria have revealed that ceramides can influence mitochondrial integrity indirectly,

namely as precursors of two other molecules, sphingosine-1-PO_4 (S1P) and hexadecenal, which co-operate specifically with Bak and Bax to promote MOMP (Chipuk et al., 2012). Activation of these functionally related proteins involves a displacement of helix α1, leading to distal exposure of their BH3 domains. Binding of S1P to Bak and hexadecenal to Bax might lower the thermodynamic constraints on these conformational changes, thus facilitating their assembly into proteolipid pores that mediate the release of cytochrome *c*. This implies that ceramides, upon arrival in mitochondria, are metabolically converted into S1P and hexadecenal through the consecutive actions of three distinct enzymes: ceramidase, sphingosine kinase and S1P lyase (Chipuk et al., 2012). However, we here show that mitochondrial targeting of a bacterial ceramidase prevents apoptosis in mitoCERT-expressing cells, arguing that apoptogenic activity relies on intact ceramides rather than the downstream metabolic intermediates of ceramide turnover. Other studies have revealed that Bak can influence ceramide-induced apoptosis by acting as a positive regulator of *de novo* ceramide synthesis, a function unrelated to its pore-forming activity (Siskind et al., 2010). Thus, ceramides arriving in mitochondria might dissociate Bak from anti-apoptotic Bcl-2 proteins, thereby increasing the concentration of Bak available to activate ceramide synthases and establishing a feed-forward loop to promote apoptosis (Beverly et al., 2013). As removal of Bak had no influence on mitoCERT-induced apoptosis, it appears unlikely that an upregulation of *de novo* ceramide synthesis is part of the mechanism by which mitoCERT commits cells to death.

Another model is based on the observation that ceramides can form stable channels in planar lipid bilayers as well as in the outer membrane of purified mitochondria that are large enough to allow passage of cytochrome *c* (Siskind et al., 2002, 2006). Formation of ceramide channels does not require any auxiliary proteins but is disrupted by anti-apoptotic Bcl2 proteins (Chang et al., 2015; Siskind et al., 2008). Thus, the pore-forming activity of ceramides has been put forward as a potential mechanism for releasing pro-apoptotic proteins during the induction phase of apoptosis (Colombini, 2016). However, our finding that mitoCERT-induced apoptosis requires Bax is hard to reconcile with the idea that MOMP in mitoCERT-expressing cells relies exclusively on self-assembly of ceramides into channels. One possibility compatible with our data is that the pore-forming activity of ceramides synergizes with that of Bax to induce MOMP and initiate end-stage apoptosis. Indeed, experiments performed on mitochondria that had been isolated from rat liver or yeast indicated that, at concentrations at which externally added ceramides and Bax have little effect on their own, the combination induces substantial MOMP (Ganesan et al., 2010). Other studies have revealed that ceramides accumulating in the mitochondrial membrane of mammalian cells upon irradiation might form platforms into which Bax inserts, oligomerizes and functions as a pore (Lee et al., 2011). Interestingly, ceramides have a profound impact on membrane curvature (Trajkovic et al., 2008), and mitochondrial shape has been shown to govern Bax-mediated MOMP and apoptosis (Renault et al., 2015). Thus, rather than acting as autonomous apoptotic factors per se, ceramides might primarily serve to enhance mitochondrial Bax insertion and its functionalization into a proteolipid pore. Whether this process relies on direct and specific interactions between Bax and ceramides, mitochondria-associated ceramide effector proteins and/or ceramide-induced alterations in membrane curvature remains to be established.

So far, most studies addressing ceramide-activated cell death pathways rely on the application of cell-permeable (truncated) ceramides or the treatment of cells with apoptotic stimuli that influence ceramide pools in multiple organelles. Because lipid-mediated pathways typically operate at the level of individual organelles, such approaches make it hard to de-convolute the sequence of events through which ceramides commit cells to death. Experiments with isolated organelles, by contrast, require validation in intact cells. Application of mitoCERT bypasses a number of drawbacks associated with the above methods, thus providing a novel opportunity to unravel compartment-specific mechanisms that govern ceramide-mediated apoptotic cell death.

MATERIALS AND METHODS

Reagents

Staurosporine, myriocin, rapamycin and glucose oxidase were purchased from Sigma-Aldrich and catalase from Roche Applied Science. z-VAD-fmk was from Calbiochem and fumonisin B1 was obtained from Cayman Chemicals. Bodipy-TR-labeled C5-ceramide (Bodipy–Cer) and Alexa-Fluor-647 azide were from Thermo Fischer Scientific. 1,2-dioleoyl-sn-glycero-3-phosphocholine (DOPC) and 1,2-dioleoyl-sn-glycero-3-phosphoethanolamine (DOPE) were from Avanti Polar Lipids. D-erythro-sphingosine was purchased from Enzo Biochem.

Synthesis of pacCer and HPA12

A 15-carbon (C15)-long fatty acid containing a photoactivatable diazerine and clickable alkyne group, pacFA, was synthesized in three steps from commercially available educts as described previously (Haberkant et al., 2013). Next, pacFA was coupled to D-erythro-sphingosine using a combination of 1-ethyl-3-(3-dimethylaminopropyl)carbodiimide (EDCI) and hydroxybenzotriazole (HOBT) as condensing reagents, yielding the photoactivatable and clickable C15-ceramide analog, pacCer (Svenja Bockelmann, John Mina, Per Haberkant and J.C.M.H., unpublished data). CERT inhibitor HPA12 was generated in nine steps from available educts with a total yield of 13% as described previously (Ďuriš et al., 2011), with the following modifications. We found that catalytic hydrogenative de-protection of the amino-function in the intermediate (1-phenylethylamino) diole caused removal of the benzylic hydroxyl group. Complementary protection of all hydroxyl groups in the form of tert-butyldimethylsilyl (TBDMS) ethers enabled us to avoid this undesirable reduction during the hydrogenation step. Further acylation of the free amine with lauric acid (DCC/DMAP) followed by hydrolytic desilylation (TBAF) resulted in the formation of HPA12 with satisfactory total yield. All synthetic compounds were purified to a high degree (>99%), and their structures were confirmed by ^{1}H and ^{13}C nuclear magnetic resonance and electrospray-ionization mass spectrometry (ESI MS) analyses.

Antibodies

The following antibodies were used: mouse monoclonal anti-β-actin (cat. no. A1978, 1:10.000; Sigma-Aldrich), rabbit polyclonal anti-FLAG (cat. no. 2368, 1:1000; Cell Signaling), rabbit monoclonal anti-Bak (cat. no. 12105, 1:1000; Cell Signaling), rabbit monoclonal anti-Bax (cat. no. 5023, 1:1000; Cell Signaling), rabbit polyclonal anti-cleaved caspase-3 (cat. no. 9661, 1:200; Cell Signaling) and rabbit polyclonal anti-caspase-9 (cat. no. 9502, 1:700; Cell Signaling), mouse monoclonal anti-cytochrome *c* (sc13156, 1:500; Santa Cruz), mouse monoclonal anti-PARP-1 (sc8007, 1:1000; Santa Cruz), rabbit polyclonal anti-Myc (sc789, 1:700; Santa Cruz) and rabbit polyclonal anti-calnexin (sc11397, 1:1000; Santa Cruz), mouse monoclonal anti-mitochondrial surface protein p60 (cat. no. MAB1273, 1:1000; Millipore) and rabbit polyclonal anti-GFP (cat. no. NB600-303, 1:5000; Novus Biologicals) antibodies. Goat anti-mouse (cat. no. 31430, 1:10.000) and goat anti-rabbit IgG conjugated to horseradish peroxidase (cat. no. 31460, 1:10.000) were from Thermo Fischer Scientific. Cy™-dye-conjugated donkey anti-mouse and donkey anti-rabbit antibodies (cat. no. 715-225-150, 715-225-152, 715-165-150, 715-165-152, 715-175-150 and 715-175-152, 1:400 each) were from Jackson ImmunoResearch Laboratories.

DNA constructs

A DNA insert encoding human CERT with a C-terminal FLAG tag (DYKDDDDK) was created by PCR and inserted into *Not*I and *Xba*I

restriction sites of mammalian expression vector pcDNA3.1 (+). MitoCERT was created by substituting the first 117 N-terminal residues of CERT for the OMM anchor sequence of mouse AKAP1 (V84389, residues 34–63: MAIQLRSLFPLALPGLLALLGWWWFFSRKK). Deletion of their START domains (residues 346–597) yielded CERTΔSTART and mitoCERTΔSTART. VAP-binding-deficient mutants CERT-D324A and mitoCERT-D324A were created using site-directed mutagenesis. Ectopic expression of fluorescent proteins was performed using mammalian expression vector pSEMS (Covalys Biosciences) containing monomeric eGFP (meGFP), photoactivatable GFP (paGFP) or HaloTag (HALO) (Wilmes et al., 2015). A cDNA encoding human VAP-A (kindly provided by Neale Ridgway, Dalhousie University, Halifax, Canada) was PCR amplified and inserted into pSEMS-mCherry, pSEMS-meGFP or pSEMS-paGFP in *Xho*I and *Sac*I restriction sites, creating mCherry–VAP-A, meGFP–VAP-A and paGFP–VAP-A, respectively. Constructs encoding the rapamycin-inducible fluorescent ER-mitochondria linkers paGFP-FRB-ER (Sac1), HALO-FRB-ER(Sac1) and OMM(Akap1)-FKBP-HALO were created by inserting the relevant domains from constructs CFP-FRB-ER (Sac1) and OMM(Akap1)-FKBP-RFP (Csordás et al., 2010) (kindly provided by György Hajnóczky, Thomas Jefferson University, Philadelphia) into pSEMS-paGFP and pSEMS-HALO expression vectors into *Xho*I and *Sac*II or *Eco*RV and *Eco*RI restriction sites. Constructs encoding mitochondrially targeted and catalytically active or dead bacterial ceramidase (mito-bCDase and mito-bCDaseH96A-H98A, respectively) have been described previously (Tafesse et al., 2014). Tom20–eGFP was a kind gift from Karin Busch, University of Osnabrück, Germany.

Cell culture and transfection

Unless indicated otherwise, all cell lines used in this study were obtained from the American Type Culture Collection (ATCC) and routinely tested for mycoplasma contamination. HeLa (ATCC-CCL2), SKOV1 (kindly provided by Toon de Kroon, University of Utrecht, the Netherlands) and A594 cells (ATCC-CCL185) were cultured in high-glucose Dulbecco's modified Eagle's medium (DMEM) supplemented with 2 mM L-glutamine and 10% FBS. OVCAR3 cells (ATCC-HTB161) were cultured in RPMI with 10% FBS and CHO-LYA cells in Ham's F12 minimal essential medium with 10% FBS. HCT116 (ATCC-CCL247), HCT116-Bax$^{-/-}$, HCT116-Bak$^{-/-}$ and HCT116-Bax$^{-/-}$Bak$^{-/-}$ cells (kindly provided by Richard Youle, National Institute of Health, Bethesda, MD) were cultured in McCoy's medium with 10% FBS. Cells were transfected with DNA constructs using Effectene (Qiagen) according to the manufacturer's protocol. Fuminosin B1 (25 µM), myriocin (30 µM) and HPA12 (10 µM) were added immediately after transfection. Staurosporine (1 µM) was added 4–5 h before cell harvest. Both adherent and non-adherent cells were harvested 24 h post-transfection, washed twice in ice-cold 0.25 M sucrose and homogenized in ice-cold IM buffer (5 mM Hepes-KOH, pH 7.0, 250 mM mannitol, 0.5 mM EGTA, 1 mM protease inhibitor cocktail, 0.1 mM phenylmethanesulfonyl fluoride) by flushing through a Balch homogenizer 20–30 times using a 2-ml syringe as described previously (Tafesse et al., 2014). Cell homogenates were centrifuged twice at 600 g_{max} for 5 min at 4°C to remove nuclei. The protein concentration of post-nuclear supernatants was determined by using a Bradford assay (Bio-Rad). Post-nuclear supernatants were normalized for total protein content before immunoblot analysis. Caspase-9 enzyme activity levels were determined using a colorometric assay kit (Biovision) following the manufacturer's protocol.

Subcellular fractionation

Post-nuclear supernatants were centrifuged at 9000 g_{max} for 10 min at 4°C to pellet mitochondria. Mitochondrial pellets were washed in ice-cold IM buffer and centrifuged twice (9000 g_{max} for 10 min, 4°C) to remove contaminating ER. The post-mitochondrial supernatant was centrifuged again at 9000 g_{max} for 10 min at 4°C to remove contaminating mitochondria and at 100,000 g_{max} for 1 h at 4°C to pellet microsomal membranes. The post-microsomal supernatant (cytosolic fraction) was collected, and the microsomal pellet was washed once in IM buffer and centrifuged again (100,000 g_{max} for 60 min, 4°C) to remove contaminating cytosol. Mitochondrial and microsomal pellets were resuspended in Buffer R (10 mM Tris-HCl, pH 7.4, 0.25 M sucrose, 1 mM protease inhibitor cocktail, 0.1 mM PMSF) before immunoblot analysis using organelle-specific antibodies.

Photoaffinity labeling

Unilamellar liposomes containing pacCer were prepared from a defined lipid mixture (DOPC:DOPE:pacCer, 80:20:1 mol%) in $CHCl_3$:MeOH (9:1, v:v) using a mini-extruder (Avanti Polar Lipids). In brief, 10 µmol of total lipid was dried in a Rotavap, and the resulting lipid film was resuspended in 1 ml Buffer L (50 mM Tris-HCl, pH 7.4, 50 mM NaCl) by vigorous vortexing and sonication, yielding a 10 mM lipid suspension. Liposomes with an average diameter of ∼100 nm were obtained by sequential extrusion of the lipid suspension through 0.4-µm, 0.2-µm and 0.1-µm track-etched polycarbonate membranes (Whatman-Nuclepore) and stored under N_2 at 4°C until use. Post-nuclear supernatants that had been prepared from HeLa cells transfected with FLAG-tagged CERT, mitoCERT or mitoCERTΔSTART were centrifuged at 100,000 g_{max} for 1 h at 4°C to generate a cytosolic and total membrane fraction. The cytosolic fraction was concentrated using an Amicon Ultra filter unit (nominal molecular mass limit, 10 kDa; MilliPore). Protein concentrations in both fractions were determined by Bradford assay and adjusted to 1 mg/ml in IM Buffer. Cytosolic and membrane fractions were mixed with pacCer-containing liposomes at 1:1 (v:v). Cytosolic fractions were incubated for 30 min at 37°C, and membrane fractions were incubated in the presence of 1 mM β-cyclodextrin for 90 min at 37°C in a thermomixer before UV irradiation for 90 s on ice. UV irradiation was performed using a 1000 W high-pressure mercury lamp (Oriel Photomax) equipped with a Pyrex glass filter to remove wavelengths below 350 nm at a distance of 30 cm from the light source. Samples were subjected to $CHCl_3$:MeOH precipitation, and the resulting protein pellets were resuspended in PBS with 1% SDS for 10 min at 37°C in a thermomixer. Click reactions were performed by incubating ∼20 µg of total protein per sample in 25 µl PBS with 1% SDS containing 1 mM Tris(2-carboxyethyl)phosphin (TCEP), 0.1 mM Tris[(1-benzyl-1H-1,2,3-triazol-4-yl)methyl]amin (TBTA), 1 mM $CuSO_4$ and 80 µM Alexa-Fluor-647 azide for 1 h at 37°C. Next, 5× sample buffer [300 mM Tris, pH 6.8, 10% (w/v) SDS, 50% (v/v) glycerol, 10% (v/v) β-mercaptoethanol and 0.025% (w/v) bromophenol blue] was added, and samples were heated to 95°C for 5 min before SDS-PAGE separation. The gel was washed in milliQ H_2O for 1 h at room temperature, subjected to in-gel fluorescence analysis using a FLA-9500 Biomolecular Imager (GE Healthcare Life Sciences) and then processed for immunoblotting using an anti-FLAG antibody.

Immunofluorescence microscopy

HeLa cells that had been grown on glass coverslips and transfected as above were fixed in 4% paraformaldehyde in PBS for 10 min, washed in PBS and then quenched in 50 mM NH_4Cl in PBS for 10 min at room temperature. Cells were permeabilized in PM buffer (0.1% saponin and 0.2% BSA in PBS), immuno-labeled with primary antibodies and Cy3- or Cy5-conjugated secondary antibodies, counter stained with DAPI (300 nM in PBS) and mounted in Prolong Gold Antifade Mountant (Thermo Fischer Scientific). Images presented in Figs 2A and 6C were captured at room temperature with a Leica DM5500 B microscope using a 63×1.40 NA Plan Apo oil objective and a SPOT Pursuit camera. Fluorochromes used were DAPI, $\lambda_{excitation}$=360 nm and $\lambda_{emission}$=460 nm; FITC and Alexa-Fluor-488, $\lambda_{excitation}$=488 nm and $\lambda_{emission}$=515 nm; Texas Red and Alexa-Fluor-568, $\lambda_{excitation}$=568 nm and $\lambda_{emission}$=585 nm. Images presented in Fig. 2B were captured at room temperature with an Olympus IX-71 inverted microscope using a 60×1.42 NA Plan ApoN U1S2 objective, a sCMOS camera (PCO, Kelheim, Germany), an InsightSSI illumination system and SoftWoRx 6.0, beta27 software (Applied Precision, Issaquah, WA). Fluorochromes used were DAPI, $\lambda_{excitation}$=390 nm and $\lambda_{emission}$=435 nm; FITC/GFP, $\lambda_{excitation}$=475 nm and $\lambda_{emission}$=523 nm; mCherry/TRITC, $\lambda_{excitation}$=542 nm and $\lambda_{emission}$=594/45 nm; Cy5, $\lambda_{excitation}$=632 nm, $\lambda_{excitation}$=676 nm. Images were processed using Fiji software (NIH, Bethesda, MD).

In vivo ceramide transfer assay

CHO-LYA cells that had been grown on glass cover slips were co-transfected with FLAG-tagged CERT, mitoCERT or mitoCERTΔSTART

and Tom20–GFP. At 24 h post transfection, cells were labeled with 0.5 µM Bodipy–Cer complexed to BSA at 4°C for 20 min and then washed twice in ice-cold Hanks' buffered saline solution (HBSS). After shifting the cells to fresh culture medium, the temperature was raised to 37°C, and fluorescent images were captured at various time points with an Olympus LSM FV1000 confocal microscope using an UPLSAPO 60×1.35 NA oil objective. Fluorochromes used were eGFP, $\lambda_{excitation}$=488 nm and $\lambda_{emission}$=515 nm; Bodipy–Texas-Red, $\lambda_{excitation}$=589 nm and $\lambda_{emission}$=617 nm. Images were processed using Fiji software.

Super-resolution microscopy

Cells that had been transfected with various DNA constructs were seeded onto glass cover slips coated with poly-L-lysine-polyethylenglucol-arginine-glycine-aspartate (PLL-PEG-RGD) (VandeVondele et al., 2003) 24 h post-transfection and cultured in medium without Phenol Red and with 10 mM HEPES [4-(2-hydroxyethyl)-1-piperazine ethanesulfonic acid]. Cells expressing Halo-tagged proteins were labeled with 30 nM HTL-tetramethylrhodamine (HTL-TMR) (Los and Wood, 2007), washed three times with PBS and then incubated for 1 h in Phenol-Red-free medium with 10 mM HEPES. Cells were processed for immunofluorescence microscopy as described above, but DAPI staining was omitted. Super-resolution microscopy was performed at room temperature using PBS complemented with an oxygen scavenger (0.5 mg/ml glucose oxidase, 40 mg/ml catalase, 5% w/v glucose, 50 mM β-mercaptoethanolamine) to switch the synthetic fluorophores between the on and off states (van de Linde et al., 2012). Imaging was performed with an inverted Olympus IX71 microscope equipped with a Quad-line TIR-illumination condenser, a back-illuminated electron multiplied CCD camera (iXon DU897D, 512×512 pixels from Andor Technology) and a UAPON 150×1.45 NA total internal reflection fluorescence microscope objective. Solid 488-nm (LuxX Omicron), 561-nm (Colbolt Jive) and 647-nm (LuxX Omicron) lasers were coupled into the microscope through a polarization-maintaining monomode fiber (KineFlex, Pointsource). The excitation beam was reflected into the objective by a quad-line dichroic beam splitter for reflection at 405 nm, 488 nm, 568 nm and 647 nm (Di01 R405, 488, 561 and 647, respectively, Semrock). Fluorescence was detected through a quadruple bandpass filter (FF01446, 523, 600 and 677–25, respectively, Semrock).

Images were split by a quadview filter to separate Cy5 and TMR. Fluorescence imaging was performed by excitation at 561 and 647 nm with a typical power density of 1–10 kW/mm^2 at the objective. The camera was operated at −80°C with a typical electron-multiplying gain of 300 and a frame rate of 32 Hz. The laser was pulse-synchronized to the camera read-out using the acousto-optic tunable filter and the modulation input of the laser. Localization of each single molecule was achieved using MATLAB based on a modified multiple target algorithm (Sergé et al., 2008). Overlaying the images from different channels with sub-pixel precision was achieved by employing calibration with multicolor fluorescence beads (TetraSpeck microspheres 0.1 µm from Invitrogen) and calculation of a spatial transformation matrix in MATLAB using the function cp2tform and the parameter 'nonreflective similarity'. Pearson colocalization coefficients for ER- and mitochondria-resident fluorescent proteins were determined using the Fiji plugin Coloc 2 (Dunn et al., 2011). The maximum colocalization coefficient, which was observed in rapamycin-treated cells co-expressing HALO-FRB-ER and OMM-FKBP-paGFP, was set at 1. Pearson coefficients were calculated based on duplicate measurements in three independent experiments, using six cells per experimental condition. A two-tailed unpaired Student's *t*-test was performed to determine differences between two groups. Significance was judged when $P<0.05$.

Acknowledgements

We thank Karin Busch (University of Osnabrück, Osnabrück, Germany), György Hajnóczky (Thomas Jefferson University, Philadelphia), Toon de Kroon (University of Utrecht, Utrecht, The Netherlands), Neale Ridgway (Dalhousie University, Halifax, Canada) and Richard Youle (National Institute of Health, Bethesda, MD) for sharing DNA constructs and cell lines.

Competing interests

The authors declare no competing or financial interests.

Author contributions

J.C.M.H. conceived and managed the project. A.J. designed and performed most experiments with crucial input from O.B. and K.E. S.K. synthesized chemical reagents. A.J. and J.C.M.H. wrote the manuscript with hypothesis development, experimental design and data interpretation contributed by all authors.

Funding

This work was supported by the European Union Seventh Framework Programme Marie-Curie Innovative Training Networks (ITN) 'Sphingonet' (289278); and the Deutsche Forschungsgemeinschaft Sonderforschungsbereich (SFB944-P14 to J.C.M.H.).

References

Alphonse, G., Bionda, C., Aloy, M.-T., Ardail, D., Rousson, R. and Rodriguez-Lafrasse, C. (2004). Overcoming resistance to gamma-rays in squamous carcinoma cells by poly-drug elevation of ceramide levels. *Oncogene* **23**, 2703-2715.

Beverly, L. J., Howell, L. A., Hernandez-Corbacho, M., Casson, L., Chipuk, J. E. and Siskind, L. J. (2013). BAK activation is necessary and sufficient to drive ceramide synthase-dependent ceramide accumulation following inhibition of BCL2-like proteins. *Biochem. J.* **452**, 111-119.

Birbes, H., El Bawab, S., Hannun, Y. A. and Obeid, L. M. (2001). Selective hydrolysis of a mitochondrial pool of sphingomyelin induces apoptosis. *FASEB J.* **15**, 2669-2679.

Birbes, H., Luberto, C., Hsu, Y.-T., El Bawab, S., Hannun, Y. A. and Obeid, L. M. (2005). A mitochondrial pool of sphingomyelin is involved in TNFalpha-induced Bax translocation to mitochondria. *Biochem. J.* **386**, 445-451.

Bose, R., Verheij, M., Haimovitz-Friedman, A., Scotto, K., Fuks, Z. and Kolesnick, R. (1995). Ceramide synthase mediates daunorubicin-induced apoptosis: an alternative mechanism for generating death signals. *Cell* **82**, 405-414.

Bourbon, N. A., Sandirasegarane, L. and Kester, M. (2002). Ceramide-induced inhibition of Akt is mediated through protein kinase Czeta: implications for growth arrest. *J. Biol. Chem.* **277**, 3286-3292.

Chang, K.-T., Anishkin, A., Patwardhan, G. A., Beverly, L. J., Siskind, L. J. and Colombini, M. (2015). Ceramide channels: destabilization by Bcl-xL and role in apoptosis. *Biochim. Biophys. Acta* **1848**, 2374-2384.

Chipuk, J. E., McStay, G. P., Bharti, A., Kuwana, T., Clarke, C. J., Siskind, L. J., Obeid, L. M. and Green, D. R. (2012). Sphingolipid metabolism cooperates with BAK and BAX to promote the mitochondrial pathway of apoptosis. *Cell* **148**, 988-1000.

Colombini, M. (2016). Ceramide channels and mitochondrial outer membrane permeability. *J. Bioenerg. Biomembr.* [Epub ahead of print] doi: 0.1007/s10863-016-9646-z.

Csordás, G., Renken, C., Várnai, P., Walter, L., Weaver, D., Buttle, K. F., Balla, T., Mannella, C. A. and Hajnóczky, G. (2006). Structural and functional features and significance of the physical linkage between ER and mitochondria. *J. Cell Biol.* **174**, 915-921.

Csordás, G., Várnai, P., Golenár, T., Roy, S., Purkins, G., Schneider, T. G., Balla, T. and Hajnóczky, G. (2010). Imaging interorganelle contacts and local calcium dynamics at the ER-mitochondrial interface. *Mol. Cell* **39**, 121-132.

Czabotar, P. E., Lessene, G., Strasser, A. and Adams, J. M. (2014). Control of apoptosis by the BCL-2 protein family: implications for physiology and therapy. *Nat. Rev. Mol. Cell Biol.* **15**, 49-63.

Dbaibo, G. S., El-Assaad, W., Krikorian, A., Liu, B., Diab, K., Idriss, N. Z., El-Sabban, M., Driscoll, T. A., Perry, D. K. and Hannun, Y. A. (2001). Ceramide generation by two distinct pathways in tumor necrosis factor alpha-induced cell death. *FEBS Lett.* **503**, 7-12.

Deng, X., Yin, X., Allan, R., Lu, D. D., Maurer, C. W., Haimovitz-Friedman, A., Fuks, Z., Shaham, S. and Kolesnick, R. (2008). Ceramide biogenesis is required for radiation-induced apoptosis in the germ line of C. elegans. *Science* **322**, 110-115.

Dobrowsky, R. T., Kamibayashi, C., Mumby, M. C. and Hannun, Y. A. (1993). Ceramide activates heterotrimeric protein phosphatase 2A. *J. Biol. Chem.* **268**, 15523-15530.

Dunn, K. W., Kamocka, M. M. and McDonald, J. H. (2011). A practical guide to evaluating colocalization in biological microscopy. *Am. J. Physiol. Cell Physiol.* **300**, C723-C742.

Ďuriš, A., Wiesenganger, T., Moravčíková, D., Baran, P., Kožíšek, J., Daïch, A. and Berkeš, D. (2011). Expedient and practical synthesis of CERT-dependent ceramide trafficking inhibitor HPA-12 and its analogues. *Org. Lett.* **13**, 1642-1645.

Ganesan, V., Perera, M. N., Colombini, D., Datskovskiy, D., Chadha, K. and Colombini, M. (2010). Ceramide and activated Bax act synergistically to permeabilize the mitochondrial outer membrane. *Apoptosis* **15**, 553-562.

García-Ruiz, C., Colell, A., Marí, M., Morales, A., Calvo, M., Enrich, C. and Fernández-Checa, J. C. (2003). Defective TNF-alpha–mediated hepatocellular apoptosis and liver damage in acidic sphingomyelinase knockout mice. *J. Clin. Invest.* **111**, 197-208.

Haberkant, P., Raijmakers, R., Wildwater, M., Sachsenheimer, T., Brügger, B., Maeda, K., Houweling, M., Gavin, A.-C., Schultz, C., van Meer, G. et al. (2013). In vivo profiling and visualization of cellular protein-lipid interactions using bifunctional fatty acids. *Angew. Chem. Int. Ed. Engl.* **52**, 4033-4038.

Hait, N. C., Oskeritzian, C. A., Paugh, S. W., Milstien, S. and Spiegel, S. (2006). Sphingosine kinases, sphingosine 1-phosphate, apoptosis and diseases. *Biochim. Biophys. Acta* **1758**, 2016-2026.

Hanada, K., Kumagai, K., Yasuda, S., Miura, Y., Kawano, M., Fukasawa, M. and Nishijima, M. (2003). Molecular machinery for non-vesicular trafficking of ceramide. *Nature* **426**, 803-809.

Hannun, Y. A. and Obeid, L. M. (2008). Principles of bioactive lipid signalling: lessons from sphingolipids. *Nat. Rev. Mol. Cell Biol.* **9**, 139-150.

Huitema, K., van den Dikkenberg, J., Brouwers, J. F. H. M. and Holthuis, J. C. M. (2004). Identification of a family of animal sphingomyelin synthases. *EMBO J.* **23**, 33-44.

Kawano, M., Kumagai, K., Nishijima, M. and Hanada, K. (2006). Efficient trafficking of ceramide from the endoplasmic reticulum to the Golgi apparatus requires a VAMP-associated protein-interacting FFAT motif of CERT. *J. Biol. Chem.* **281**, 30279-30288.

Kudo, N., Kumagai, K., Matsubara, R., Kobayashi, S., Hanada, K., Wakatsuki, S. and Kato, R. (2010). Crystal structures of the CERT START domain with inhibitors provide insights into the mechanism of ceramide transfer. *J. Mol. Biol.* **396**, 245-251.

Kumagai, K., Yasuda, S., Okemoto, K., Nishijima, M., Kobayashi, S. and Hanada, K. (2005). CERT mediates intermembrane transfer of various molecular species of ceramides. *J. Biol. Chem.* **280**, 6488-6495.

Kuwana, T., Mackey, M. R., Perkins, G., Ellisman, M. H., Latterich, M., Schneiter, R., Green, D. R. and Newmeyer, D. D. (2002). Bid, Bax, and lipids cooperate to form supramolecular openings in the outer mitochondrial membrane. *Cell* **111**, 331-342.

Lee, H., Rotolo, J. A., Mesicek, J., Penate-Medina, T., Rimner, A., Liao, W.-C., Yin, X., Ragupathi, G., Ehleiter, D., Gulbins, E. et al. (2011). Mitochondrial ceramide-rich macrodomains functionalize Bax upon irradiation. *PLoS ONE* **6**, e19783.

Liu, Z., Xia, Y., Li, B., Xu, H., Wang, C., Liu, Y., Li, Y., Li, C., Gao, N. and Li, L. (2014). Induction of ER stress-mediated apoptosis by ceramide via disruption of ER Ca(2+) homeostasis in human adenoid cystic carcinoma cells. *Cell Biosci.* **4**, 71.

Loewen, C. J. R., Roy, A. and Levine, T. P. (2003). A conserved ER targeting motif in three families of lipid binding proteins and in Opi1p binds VAP. *EMBO J.* **22**, 2025-2035.

Los, G. V. and Wood, K. (2007). The HaloTag: a novel technology for cell imaging and protein analysis. *Methods Mol. Biol.* **356**, 195-208.

Luberto, C., Hassler, D. F., Signorelli, P., Okamoto, Y., Sawai, H., Boros, E., Hazen-Martin, D. J., Obeid, L. M., Hannun, Y. A. and Smith, G. K. (2002). Inhibition of tumor necrosis factor-induced cell death in MCF7 by a novel inhibitor of neutral sphingomyelinase. *J. Biol. Chem.* **277**, 41128-41139.

Luna-Vargas, M. P. A. and Chipuk, J. E. (2016). The deadly landscape of pro-apoptotic BCL-2 proteins in the outer mitochondrial membrane. *FEBS J.* **283**, 2676-2689.

Mesicek, J., Lee, H., Feldman, T., Jiang, X., Skobeleva, A., Berdyshev, E. V., Haimovitz-Friedman, A., Fuks, Z. and Kolesnick, R. (2010). Ceramide synthases 2, 5, and 6 confer distinct roles in radiation-induced apoptosis in HeLa cells. *Cell. Signal.* **22**, 1300-1307.

Moldoveanu, T., Follis, A. V., Kriwacki, R. W. and Green, D. R. (2014). Many players in BCL-2 family affairs. *Trends Biochem. Sci.* **39**, 101-111.

Mukhopadhyay, A., Saddoughi, S. A., Song, P., Sultan, I., Ponnusamy, S., Senkal, C. E., Snook, C. F., Arnold, H. K., Sears, R. C., Hannun, Y. A. et al. (2009). Direct interaction between the inhibitor 2 and ceramide via sphingolipid-protein binding is involved in the regulation of protein phosphatase 2A activity and signaling. *FASEB J.* **23**, 751-763.

Park, M. A., Zhang, G., Martin, A. P., Hamed, H., Mitchell, C., Hylemon, P. B., Graf, M., Rahmani, M., Ryan, K., Liu, X. et al. (2008). Vorinostat and sorafenib increase ER stress, autophagy and apoptosis via ceramide-dependent CD95 and PERK activation. *Cancer Biol. Ther.* **7**, 1648-1662.

Patwardhan, G. A., Beverly, L. J. and Siskind, L. J. (2016). Sphingolipids and mitochondrial apoptosis. *J. Bioenerg. Biomembr.* **48**, 153-168.

Renault, T. T., Floros, K. V., Elkholi, R., Corrigan, K.-A., Kushnareva, Y., Wieder, S. Y., Lindtner, C., Serasinghe, M. N., Asciolla, J. J., Buettner, C. et al. (2015). Mitochondrial shape governs BAX-induced membrane permeabilization and apoptosis. *Mol. Cell* **57**, 69-82.

Salvador-Gallego, R., Mund, M., Cosentino, K., Schneider, J., Unsay, J., Schraermeyer, U., Engelhardt, J., Ries, J. and García-Sáez, A. J. (2016). Bax assembly into rings and arcs in apoptotic mitochondria is linked to membrane pores. *EMBO J.* **35**, 389-401.

Ségui, B., Andrieu-Abadie, N., Jaffrézou, J.-P., Benoist, H. and Levade, T. (2006). Sphingolipids as modulators of cancer cell death: potential therapeutic targets. *Biochim. Biophys. Acta* **1758**, 2104-2120.

Senkal, C. E., Ponnusamy, S., Manevich, Y., Meyers-Needham, M., Saddoughi, S. A., Mukhopadyay, A., Dent, P., Bielawski, J. and Ogretmen, B. (2011). Alteration of ceramide synthase 6/C16-ceramide induces activating transcription factor 6-mediated Endoplasmic Reticulum (ER) stress and apoptosis via perturbation of cellular Ca2+ and ER/golgi membrane network. *J. Biol. Chem.* **286**, 42446-42458.

Sergé, A., Bertaux, N., Rigneault, H. and Marguet, D. (2008). Dynamic multiple-target tracing to probe spatiotemporal cartography of cell membranes. *Nat. Methods* **5**, 687-694.

Siskind, L. J., Kolesnick, R. N. and Colombini, M. (2002). Ceramide channels increase the permeability of the mitochondrial outer membrane to small proteins. *J. Biol. Chem.* **277**, 26796-26803.

Siskind, L. J., Kolesnick, R. N. and Colombini, M. (2006). Ceramide forms channels in mitochondrial outer membranes at physiologically relevant concentrations. *Mitochondrion* **6**, 118-125.

Siskind, L. J., Feinstein, L., Yu, T., Davis, J. S., Jones, D., Choi, J., Zuckerman, J. E., Tan, W., Hill, R. B., Hardwick, J. M. et al. (2008). Anti-apoptotic Bcl-2 Family Proteins Disassemble Ceramide Channels. *J. Biol. Chem.* **283**, 6622-6630.

Siskind, L. J., Mullen, T. D., Romero Rosales, K., Clarke, C. J., Hernandez-Corbacho, M. J., Edinger, A. L. and Obeid, L. M. (2010). The BCL-2 protein BAK is required for long-chain ceramide generation during apoptosis. *J. Biol. Chem.* **285**, 11818-11826.

Stiban, J., Caputo, L. and Colombini, M. (2008). Ceramide synthesis in the endoplasmic reticulum can permeabilize mitochondria to proapoptotic proteins. *J. Lipid Res.* **49**, 625-634.

Swanton, C., Marani, M., Pardo, O., Warne, P. H., Kelly, G., Sahai, E., Elustondo, F., Chang, J., Temple, J., Ahmed, A. A. et al. (2007). Regulators of mitotic arrest and ceramide metabolism are determinants of sensitivity to paclitaxel and other chemotherapeutic drugs. *Cancer Cell* **11**, 498-512.

Tafesse, F. G., Ternes, P. and Holthuis, J. C. M. (2006). The multigenic sphingomyelin synthase family. *J. Biol. Chem.* **281**, 29421-29425.

Tafesse, F. G., Vacaru, A. M., Bosma, E. F., Hermansson, M., Jain, A., Hilderink, A., Somerharju, P. and Holthuis, J. C. M. (2014). Sphingomyelin synthase-related protein SMSr is a suppressor of ceramide-induced mitochondrial apoptosis. *J. Cell Sci.* **127**, 445-454.

Tait, S. W. G. and Green, D. R. (2013). Mitochondrial regulation of cell death. *Cold Spring Harb. Perspect. Biol.* **5**, a008706.

Tidhar, R. and Futerman, A. H. (2013). The complexity of sphingolipid biosynthesis in the endoplasmic reticulum. *Biochim. Biophys. Acta* **1833**, 2511-2518.

Trajkovic, K., Hsu, C., Chiantia, S., Rajendran, L., Wenzel, D., Wieland, F., Schwille, P., Brügger, B. and Simons, M. (2008). Ceramide triggers budding of exosome vesicles into multivesicular endosomes. *Science* **319**, 1244-1247.

Vacaru, A. M., Tafesse, F. G., Ternes, P., Kondylis, V., Hermansson, M., Brouwers, J. F. H. M., Somerharju, P., Rabouille, C. and Holthuis, J. C. M. (2009). Sphingomyelin synthase-related protein SMSr controls ceramide homeostasis in the ER. *J. Cell Biol.* **185**, 1013-1027.

Vacaru, A. M., van den Dikkenberg, J., Ternes, P. and Holthuis, J. C. M. (2013). Ceramide phosphoethanolamine biosynthesis in Drosophila is mediated by a unique ethanolamine phosphotransferase in the Golgi lumen. *J. Biol. Chem.* **288**, 11520-11530.

van de Linde, S., Heilemann, M. and Sauer, M. (2012). Live-cell super-resolution imaging with synthetic fluorophores. *Annu. Rev. Phys. Chem.* **63**, 519-540.

VandeVondele, S., Vörös, J. and Hubbell, J. A. (2003). RGD-grafted poly-L-lysine-graft-(polyethylene glycol) copolymers block non-specific protein adsorption while promoting cell adhesion. *Biotechnol. Bioeng.* **82**, 784-790.

von Haefen, C., Wieder, T., Gillissen, B., Stärck, L., Graupner, V., Dörken, B. and Daniel, P. T. (2002). Ceramide induces mitochondrial activation and apoptosis via a Bax-dependent pathway in human carcinoma cells. *Oncogene* **21**, 4009-4019.

Wang, C. and Youle, R. J. (2012). Predominant requirement of Bax for apoptosis in HCT116 cells is determined by Mcl-1's inhibitory effect on Bak. *Oncogene* **31**, 3177-3189.

Wang, X., Rao, R. P., Kosakowska-Cholody, T., Masood, M. A., Southon, E., Zhang, H., Berthet, C., Nagashim, K., Veenstra, T. K., Tessarollo, L. et al. (2009). Mitochondrial degeneration and not apoptosis is the primary cause of embryonic lethality in ceramide transfer protein mutant mice. *J. Cell Biol.* **184**, 143-158.

Wei, M. C., Zong, W.-X., Cheng, E. H.-Y., Lindsten, T., Panoutsakopoulou, V., Ross, A. J., Roth, K. A., MacGregor, G. R., Thompson, C. B. and Korsmeyer, S. J. (2001). Proapoptotic BAX and BAK: a requisite gateway to mitochondrial dysfunction and death. *Science* **292**, 727-730.

Wilmes, S., Beutel, O., Li, Z., Francois-Newton, V., Richter, C. P., Janning, D., Kroll, C., Hanhart, P., Hötte, K., You, C. et al. (2015). Receptor dimerization dynamics as a regulatory valve for plasticity of type I interferon signaling. *J. Cell Biol.* **209**, 579-593.

Yamaoka, S., Miyaji, M., Kitano, T., Umehara, H. and Okazaki, T. (2004). Expression cloning of a human cDNA restoring sphingomyelin synthesis and cell growth in sphingomyelin synthase-defective lymphoid cells. *J. Biol. Chem.* **279**, 18688-18693.

Zhu, Q.-Y., Wang, Z., Ji, C., Cheng, L., Yang, Y.-L., Ren, J., Jin, Y.-H., Wang, Q.-J., Gu, X.-J., Bi, Z.-G. et al. (2011). C6-ceramide synergistically potentiates the anti-tumor effects of histone deacetylase inhibitors via AKT dephosphorylation and α-tubulin hyperacetylation both in vitro and in vivo. *Cell Death Dis.* **2**, e117.

Chapter 3

Resolving the sequence of events in ceramide-induced apoptosis using switchable ceramide transfer proteins

Amrita Jain[1], Shashank Dadsena[1], Joost C.M. Holthuis[1,2]

[1]Molecular Cell Biology Division, Department of Biology/Chemistry, University of Osnabrück, D-49076 Osnabrück, Germany [2]Membrane Biochemistry & Biophysics, Bijvoet Center and Institute of Biomembranes, Utrecht University, 3584 CH Utrecht, The Netherlands

Manuscript in preparation

Resolving the sequence of events in ceramide-induced apoptosis using switchable ceramide transfer proteins

Amrita Jain[1], Shashank Dadsena[1], Joost C.M. Holthuis[1,2]

[1]Molecular Cell Biology Division, Department of Biology/Chemistry, University of Osnabrück, D-49076 Osnabrück, Germany [2]Membrane Biochemistry & Biophysics, Bijvoet Center and Institute of Biomembranes, Utrecht University, 3584 CH Utrecht, The Netherlands

ABSTRACT

We recently reported that mitochondrial translocation of ER ceramides triggers a Bax-dependent pathway of apoptosis. To further elucidate the mechanism by which ceramides activate Bax and commit cells to death, we here developed a switchable version of the ceramide transfer protein CERT, sCERT, using FKB-FRBP chemical dimerization technology. We demonstrate that sCERT can be readily targeted to mitochondria in response to rapamycin. Upon its drug-induced recruitment to mitochondria, sCERT retains the ability to bind VAP protein receptors in the ER and catalyzes mitochondrial import of an externally added fluorescent ceramide analogue. We also show that mitochondrial recruitment of sCERT is accompanied by a major shift in the subcellular distribution of Bax from the cytosol to mitochondria. Importantly, the ability of mitochondria-bound sCERT to catalyze ceramide import and induce mitochondrial translocation of Bax is critically dependent on its ceramide transfer or START domain. Collectively, these results substantiate our previous finding that mistargeting of ER ceramides to mitochondria specifically activates Bax-mediated apoptosis and establish sCERT as a new tool to dissect the underlying mechanism in a time-resolved manner.

INTRODUCTION

During mitochondrial apoptosis, the most common form of programmed cell death, multiple pathways converge on mitochondria to induce mitochondrial outer membrane permeabilization (MOMP) and subsequent release of intermembrane space proteins like cytochrome *c* (Cyto *c*) into the cytosol. Release of Cyto *c* damages the bioenergetics function of mitochondria and initiates the caspase cascade that eventually dismantles the cell (Bratton and Cohen, 2001; Green and Kroemer, 2004). MOMP is controlled by members of the B-cell lymphoma-2 (Bcl-2) family of proteins, which have been classified in pro-survival and pro-apoptotic family members (Czabotar et al., 2013). The principal pro-apoptotic Bcl-2 protein in mammals is Bax, which is a soluble monomeric protein that constitutively shuttles between the cytosol and mitochondria of healthy cells. In response to DNA damage and other types of cellular stress, Bax is activated and accumulates on the mitochondrial surface, where it undergoes major conformational changes to form oligomers in the outer mitochondrial membrane (OMM; (Luna-Vargas and Chipuk, 2016; Moldoveanu et al., 2014). A widely supported model of

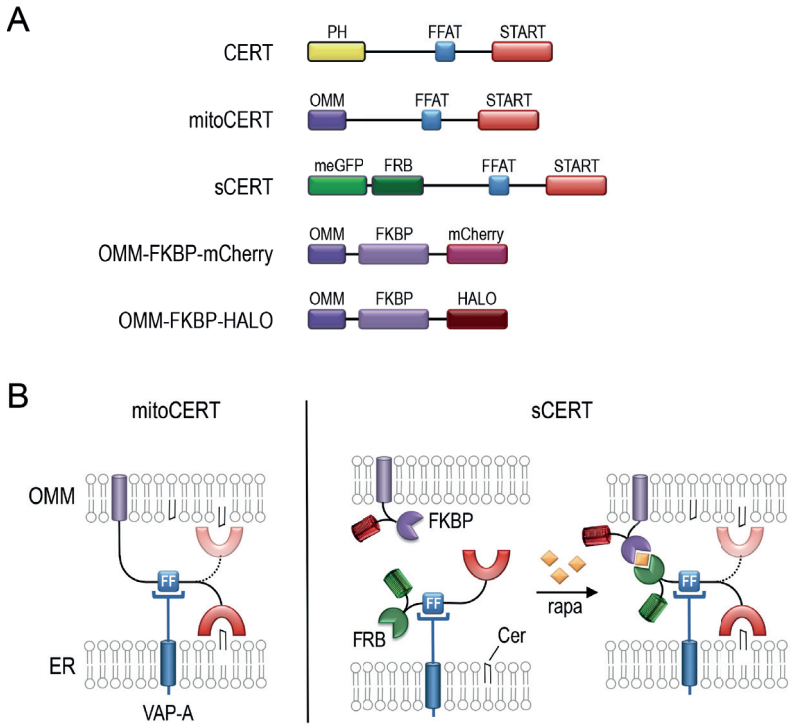

Figure 1. Design principle of sCERT. (**A**) Schematic outline of expression constructs used in this study. PH, pleckstrin homology domain; FFAT, VAP-A binding motif; START, ceramide transfer domain; OMM, outer mitochondrial membrane anchor; sCERT, rapamycin-inducible (switchable) CERT; meGFP, monomeric enhanced green fluorescent protein; FRB, FKBP-rapamycin-binding domain; FKBP, FK506 binding protein; mCherry, monomeric cherry fluorescent protein; HALO, haloalkane dehalogenase domain for covalent binding to synthetic fluorophore. (**B**) Schematic outline of working mechanism of mitoCERT and rapamycin-inducible sCERT. ER, endoplasmic reticulum; FF, FFAT motif; Cer, ceramide; rapa, rapamycin. See text for further details.

MOMP is that Bax oligomerization creates pores that allow Cyto *c* and other apoptotic factors to escape to the cytosol. Indeed, recent studies revealed ring-like Bax structures on apoptotic mitochondria by super-resolution microscopy (Große et al., 2016; Salvador-Gallego et al., 2016). Pro-survival Bcl-2 proteins inhibit Bax via direct interactions or by sequestering Bax-activating proteins (Czabotar et al., 2013). Such regulatory interactions are only observed in the presence of mitochondria or liposomes, suggesting that mitochondrial apoptosis signaling involves membrane-embedded proteins (García-Sáez et al., 2009).

Several reports have indicated that ceramides, the essential building blocks of sphingolipids, actively participate in mitochondrial apoptosis. For example, a rise in mitochondrial ceramide levels has been observed to precede MOMP for a variety of distinct stresses (Ardail et al.,

2009; BIRBES et al., 2005; Dai et al., 2004). In experiments with isolated mitochondria, exogenously added ceramides and recombinant Bax were found to act coordinately to induce the release of Cyto *c* (Ganesan et al., 2010). Moreover, ceramides have been reported to induce an activating conformational change in Bax in mitochondrial membranes (Kashkar et al., 2005). Other work revealed that ceramides can form stable channels in planar lipid bilayers as well as in the outer membrane of isolated mitochondria that allow passage of Cyto *c* (Perera et al., 2016; Siskind et al., 2006). The pore-forming activity of ceramides does not seem to require any auxiliary proteins but can be blocked by anti-apoptotic Bcl-2 proteins (Chang et al., 2015). Yet other studies indicated that ceramides influence mitochondrial integrity indirectly, namely as precursors of two other signaling molecules, sphingosine-1-phosphate and hexadecenal, which co-operate specifically with Bak and Bax to promote MOMP (Chipuk et al., 2012). Hence, although *in vitro* studies indicate that ceramides initiate cell death by acting directly on mitochondria, their actual contribution to the apoptotic response in living cells is not well understood.

Ceramides are produced *de novo* by *N*-acylation of sphingoid long-chain bases on the cytosolic surface of the ER. In mammals, the bulk of newly synthesized ceramides is converted to sphingomyelin (SM) by SM synthase SMS1 in the lumen of the *trans*-Golgi (Halter et al., 2007; Huitema et al., 2004; Yamaoka et al., 2004). Efficient delivery of ER ceramides to the site of SM production requires the cytosolic ceramide transfer protein CERT (Hanada, 2006). CERT contains an *N*-terminal pleckstrin homology (PH) domain that binds phosphatidylinositol-4-phosphate, a lipid enriched on the cytosolic surface of the *trans*-Golgi. Additionally, CERT possesses a central diphenylalanine-in-an-acidic tract (FFAT) motif that binds the ER-resident membrane proteins VAP-A and VAP-B, and a START domain that binds and transfers ceramides (Kawano et al., 2006; Kudo et al., 2008). Because of its dual targeting motifs, CERT has been proposed to shuttle ceramides across the narrow cytosolic gap at membrane contact sites between the ER and *trans*-Golgi (Levine, 2004). Directional transport is achieved by ongoing SM production in the *trans*-Golgi, which serves as a metabolic trap for newly synthesized ceramides. Cloning of the responsible enzyme, SMS1, led to identification of an SMS1-related protein, SMSr (also known as sterile a-motif domain-containing protein SAMD8; (Huitema et al., 2004). SMSr catalyzes production of the SM analogue ceramide phosphoethanolamine in the lumen of the ER. Acute disruption of SMSr catalytic activity in mammalian cells causes an accumulation of ER ceramides and their mislocalization to mitochondria, triggering a mitochondrial pathway of apoptosis (Tafesse et al., 2014; Vacaru et al., 2009). Apoptosis induction was prevented by blocking *de novo* ceramide synthesis or targeting a bacterial ceramidase to mitochondria, suggesting that the arrival of ER ceramides in mitochondria is a critical step in committing cells to death (Tafesse et al., 2014). We recently confirmed this concept by analyzing the consequences of targeting the biosynthetic flow of ceramides to mitochondria using a ceramide transfer protein equipped with an OMM anchor, mitoCERT. Cells expressing mitoCERT underwent mitochondrial apoptosis, as evidenced by cytosolic release of Cyto *c*

and activation of caspase 9 (Jain et al., 2016). Apoptosis induction was blocked upon removal of Bax, required ongoing *de novo* ceramide synthesis and critically relied on the ability of mitoCERT to transport ceramides at ER-mitochondria junctions. These results provided first demonstration that ceramide delivery to mitochondria is sufficient to commit cells to death.

To further resolve the mechanism by which ceramides activate Bax and trigger apoptotic cell death in real time, we here developed and applied a drug-inducible version of mitoCERT. We demonstrate that an acute mislocalization of ceramides to mitochondria triggers mitochondrial translocation of Bax, hence substantiating our previous finding that subcellular topology is a key determinant in ceramide-induced cell death.

RESULTS

Design of switchable ceramide transfer protein sCERT

We previously demonstrated that translocation of ER ceramides to mitochondria triggers a Bax-dependent pathway of apoptosis (Jain et al., 2016). This was accomplished by expressing a ceramide transfer protein equipped with an outer mitochondrial membrane (OMM) anchor, mitoCERT. To help resolve the mechanism by which ceramides commit cells to death, we designed a switchable version of mitoCERT using the rapamycin-inducible FKBP/FRB heterodimerization system (Putyrski and Schultz, 2012). To this end, the *N*-terminal Golgi-targeting PH domain of CERT was replaced by meGFP and a FRB domain, yielding meGFP-FRB-CERT or switchable CERT (sCERT; Fig. 1). A version of sCERT lacking the ceramide transfer or START domain, sCERTΔSTART, served as control. To allow rapamycin-induced recruitment of sCERT to mitochondria, the OMM anchor sequence of A-kinase anchor protein 1 (mAKAP1) was fused to a FKBP domain and mCherry or HALO-tag as fluorescent marker, yielding OMM-FKBP-mCherry and OMM-FKBP-HALO, respectively. To direct sCERT to the plasma membrane, we created two additional constructs, PM-FKBP-mCherry and PM-FKBP-HALO, in which the OMM anchor sequence was replaced by the *N*-terminal palmitoylation/myristoylation signal of the Lyn protein, which serves as plasma membrane targeting sequence. Next, these multi-domain constructs were subjected to a detailed functional analysis.

sCERT undergoes drug-induced recruitment to specific organelles

To check whether sCERT can be recruited to mitochondria in response to rapamycin, HeLa cells were co-transfected with sCERT and OMM-FKBP-mCherry, treated with 50 nM rapamycin for 30 min and then analyzed by fluorescence microscopy. In untreated cells, sCERT was distributed throughout the cytosol while OMM-FKBP-mCherry localized to mitochondria. However, upon addition of rapamycin, the bulk of cytosolic sCERT was translocated to mitochondria, as evidenced by extensive co-localization of the protein with OMM-FKBP-mCherry (Fig. 2A). Likewise, in cells co-expressing sCERT and PM-FKBP-mCherry, addition of rapamycin led to a rapid redistribution of sCERT from cytosol to the plasma membrane (Fig. 2B). Similar results were obtained when analyzing the

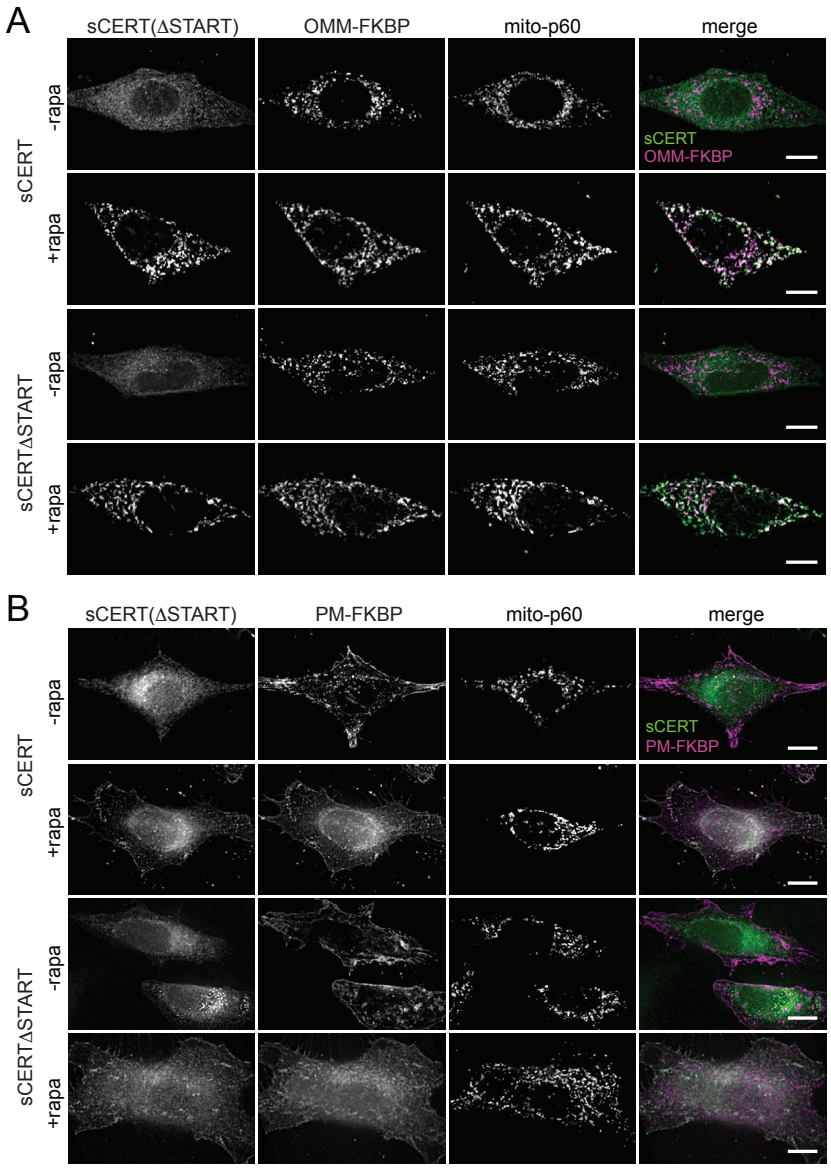

Figure 2. Rapamycin-induced translocation of sCERT to distinct organelles. (**A**) HeLa cells were co-transfected with sCERT or sCERTΔSTART and OMM-FKBP-mCherry (OMM-FKBP) and then incubated for 30 min in the absence (-rapa) or presence of 50 nM rapamycin (+rapa). Next, cells were fixed, immuno-stained against mitochondrial marker mito-p60 and then visualized by fluorescence microscopy. Confocal sections of cells are shown. Note that rapamycin treatment caused a marked increase in overlap between sCERT/sCERTΔSTART (green) and OMM-FKBP-associated fluorescence (magenta). (**B**) HeLa cells were co-transfected with sCERT or sCERTΔSTART and PM-FKBP-mCherry (PM-FKBP) and then treated as in (A). Note that rapamycin treatment caused a marked increase in overlap between sCERT/sCERTDSTART (green) and PM-FKBP-associated fluorescence (magenta). Bar, 10 μM.

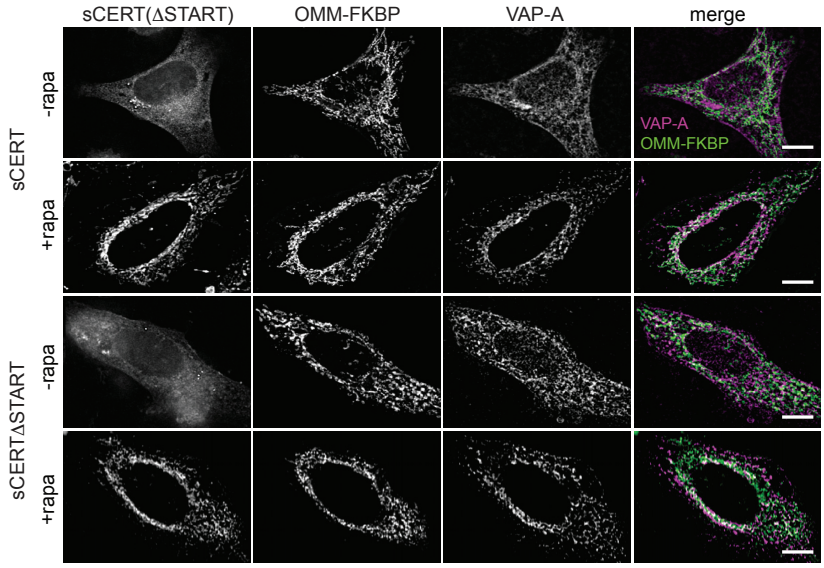

Figure 3. Mitochondria-associated sCERT retains the ability to bind ER-resident VAP-A. HeLa cells were co-transfected with sCERT or sCERTΔSTART, OMM-FKBP-HALO (OMM-FKBP) and mCherry-VAP-A (VAP-A), and then incubated for 30 min in the absence (-rapa) or presence of 50 nM rapamycin (+rapa). Next, cells were fixed and visualized by fluorescence microscopy. Confocal sections of cells are shown. Note that rapamycin treatment caused a marked increase in overlap between VAP-A (magenta) and OMM-FKBP-associated fluorescence (green). Bar, 10 μM.

impact of rapamycin on the subcellular distribution of sCERTΔSTART in cells expressing OMM-FKBP-mCherry or PM-FKBP-mCherry (Fig. 2A,B). Importantly, sCERT and sCERTΔSTART remained largely associated with their target organelle when rapamycin-treated cells were washed and incubated for an additional 24 h in the absence of the drug (data not shown). From this we conclude that a short and transient exposure of cells to rapamycin suffices to induce efficient recruitment of sCERT and sCERTΔSTART to their target organelle.

sCERT interacts with ER-resident VAP-A

CERT contains a short peptide sequence or FFAT motif, which is recognized by the ER-resident tail-anchored proteins VAP-A and VAP-B. The interaction between CERT and VAPs is crucial for efficient ER-to-Golgi transfer of ceramide (Kawano et al., 2006). Moreover, the apoptogenic activity of mitoCERT critically relies on an intact FFAT motif and the ability of the protein to function as a VAP-dependent ER-mitochondrial tether (Jain et al., 2016). This led us to investigate whether sCERT is able to interact with VAPs upon its rapamycin-induced recruitment to mitochondria. To this end, HeLa cells were co-transfected with sCERT, OMM-FKBP-HALO and mCherry-tagged VAP-A (VAP-A-mCherry). In the absence of rapamycin, sCERT was distributed throughout the cytosol whereas VAP-A-mCherry displayed a reticular staining reminiscent of the ER

that showed little overlap with the tubular mitochondrial network marked by OMM-FKBP-HALO (Fig. 3). By contrast, upon 30 min exposure to 50 nM rapamycin, the bulk of sCERT redistributed to mitochondria. Importantly, mitochondrial translocation of sCERT was accompanied by an increased overlap between VAP-A-mCherry and OMM-FKBP-HALO-positive networks. Similar drug-mediated changes were observed in cells co-expressing sCERTΔSTART, OMM-FKBP-HALO and VAP-A-mCherry (Fig. 3). These results indicate that the rapamycin-induced translocation of sCERT and sCERTΔSTART to mitochondria does not interfere with the ability of these proteins to interact with VAP receptors in the ER.

sCERT mediates ceramide delivery to mitochondria in drug-treated cells

We next addressed whether sCERT can mediate ceramide transport to mitochondria when translocated to these organelles in rapamycin-treated cells. To this end, we monitored the intracellular movement of a fluorescent analogue of ceramide (C5-Bodipy-Cer) in Chinese hamster ovary (CHO) LY-A cells. In these cells, ER-to-Golgi transport of C5-Bodipy-Cer is disrupted by a loss-of-function mutation in the CERT-encoding gene (Hanada et al., 2003). As shown in Fig. 4, LY-A cells co-transfected with sCERT and OMM-FKBP-HALO readily internalized externally added C5-Bodipy-Cer, distributing the analogue throughout the cytosol. However, when cells were pre-treated with rapamycin prior to addition of C5-Bodipy-Cer, the analogue accumulated in sCERT-positive mitochondria. By contrast, when added to rapamycin-treated cells co-expressing sCERTΔSTART and OMM-FKBP-HALO, C5-Bodipy-Cer remained largely associated with the plasma membrane (Fig. 4). These results indicate that sCERT is able to bind to ceramides and can mediate their transport to mitochondria upon its rapamycin-induced recruitment to these organelles.

mitoCERT expression triggers mitochondrial translocation of Bax

Our previous work revealed that cells expressing mitoCERT import ceramides to mitochondria and undergo Bax-dependent apoptosis (Jain et al., 2016). Bax is a pro-apoptotic member of the Bcl2 protein family that actively participates in the release of Cyto *c* from mitochondria, which results in caspase activation (Green and Kroemer, 2004). In healthy cells, Bax is a soluble monomer that primarily resides in the cytosol. Upon exposure to pro-apoptotic stimuli, Bax undergoes a conformational change that frees up a *C*-terminal membrane anchor, which eventually inserts in the OMM to tether the protein to mitochondria (Moldoveanu et al., 2014). Subsequent oligomerization of the OMM-associated protein marks a crucial step in the creation of the proteolipid pores responsible for Cyto *c* release (Salvador-Gallego et al., 2016).

To further unravel the mechanism by which ceramides commit cells to death, we monitored mitochondrial translocation of Bax in HeLa cells transfected with mitoCERT by immuno-fluorescence microscopy. To uncouple this step from downstream processes mediated by caspases, cells were incubated with the broad-spectrum caspase inhibitor z-VAD-fmk during the onset apoptosis. We first analyzed the subcellular distribution of Bax

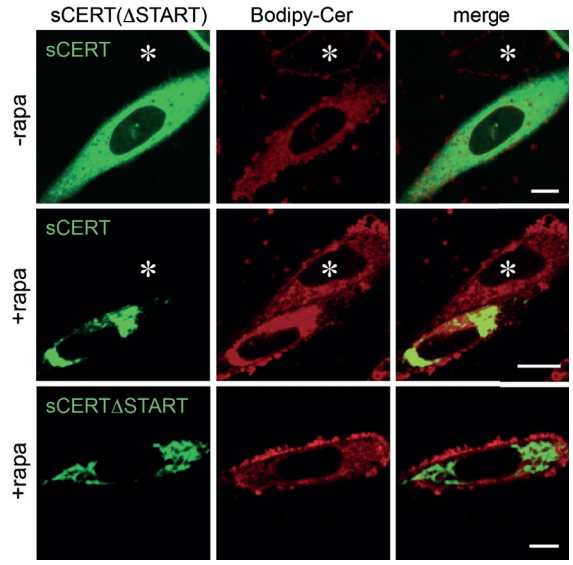

Figure 4. sCERT mediates ceramide delivery to mitochondria when recruited to these organelles. CHO-LYA cells co-transfected with sCERT or CERTΔSTART and OMM-FKBP-HALO were incubated with 0.5 μM red fluorescent C5-Bodipy-ceramide (Bodipy-Cer) at 4°C for 20 min. Next, cells were chased at 37°C for 10 min and then incubated at 37°C in the absence (-rapa) or presence of 50 nm rapamycin (+rapa) for another 25 min before visualization by confocal fluorescence microscopy. Note that, while sCERT-expressing cells readily internalize Bodipy-Cer, untransfected cells (marked with asterisks) or cells expressing CERTΔSTART primarily accumulate Bodipy-Cer at the plasma membrane. Bar, 10 μM.

in control and staurosporin-treated cells expressing GFP-tagged Tom20 as mitochondrial marker. Immuno-staining of control cells with a monoclonal anti-Bax antibody yielded a grainy staining pattern throughout the cytosol and nucleus that showed little overlap with mitochondria. By contrast, in cells treated with staurosporin for 90 min, the bulk of immuno-stained Bax concentrated in small dots that displayed extensive co-localization with mitochondria (Fig. 5A,B). We then addressed the impact of mitoCERT on Bax localization. As shown in Fig. 6A, expression of mitoCERT caused a marked redistribution of Bax from the cytosol to mitochondria, similar to that observed in staurosporin-treated cells. Interestingly, mitochondrial translocation of Bax was abolished when mitoCERT-expressing cells were treated with myriocin, a specific inhibitor of long chain base synthase (Fig. 6A,B). Furthermore, contrary to mitoCERT, expression of mitoCERTΔSTART failed to trigger mitochondrial recruitment of Bax. These results indicate that mitoCERT-induced Bax recruitment to mitochondria requires *de novo* ceramide biosynthesis as well as a ceramide transfer-competent form of mitoCERT. This is in line with our previous finding that apoptosis in mitoCERT-expressing cells is triggered by the translocation of ER ceramides to mitochondria and dependent on Bax (Jain et al., 2016).

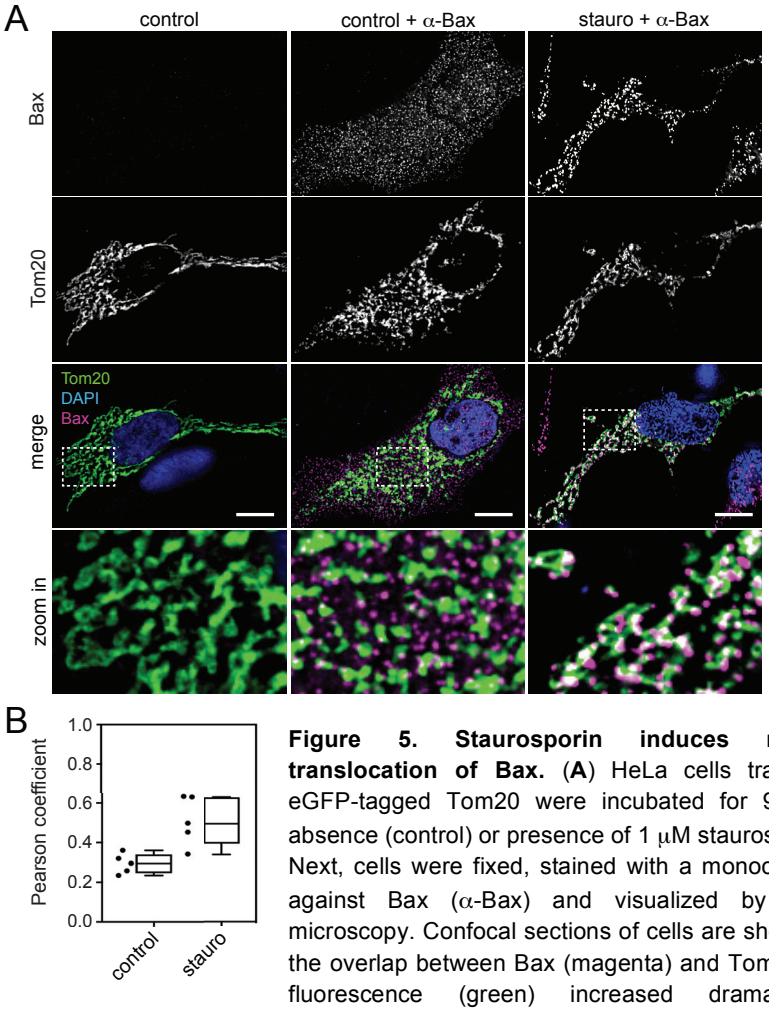

Figure 5. Staurosporin induces mitochondrial translocation of Bax. (**A**) HeLa cells transfected with eGFP-tagged Tom20 were incubated for 90 min in the absence (control) or presence of 1 μM staurosporin (stauro). Next, cells were fixed, stained with a monoclonal antibody against Bax (α-Bax) and visualized by fluorescence microscopy. Confocal sections of cells are shown. Note that the overlap between Bax (magenta) and Tom20-associated fluorescence (green) increased dramatically upon staurosporin treatment. Bar, 10 μM. (**B**) Pearson correlation coefficients between Bax and Tom20 determined in cells treated as in (A). Five cells were analyzed per condition. For each boxplot, the middle line denotes the median while the top and bottom of the box indicate the 75th and 25th percentile. Whiskers denote the minimum and maximum values.

Recruitment of sCERT to mitochondria triggers mitochondrial translocation of Bax

We next set out to exploit sCERT to analyze the impact of mitochondrial translocation of ER ceramides on the subcellular distribution of Bax in a time-resolved manner. When immuno-stained with a monoclonal anti-Bax antibody, cells co-expressing sCERT and OMM-FKBP-mCherry displayed a grainy staining pattern

throughout the cytosol and nucleus that showed little overlap with mitochondria. However, when cells were exposed to rapamycin for 30 min, washed and then incubated for 8 h in the absence of the drug, Bax immuno-staining was primarily found in small dots that co-localized extensively with mitochondria (Fig. 7A), analogous to the subcellular distribution of Bax in staurosporin-treated or mitoCERT-expressing cells (Figs. 5,6). Thus, rapamycin-induced recruitment of sCERT to mitochondria triggers mitochondrial translocation of Bax. Importantly, this was not observed when the experiment was repeated with cells expressing a ceramide transfer-defective form of sCERT, sCERTΔSTART (Fig. 7A,B), hence ruling out that rapamycin is directly responsible for triggering mitochondrial translocation of Bax. From this we conclude that mitochondrial translocation of Bax is due to sCERT-mediated delivery of ceramides, and that this process is initiated within 8 h after diverting the biosynthetic ceramide flow to mitochondria.

DISCUSSION

Mitochondrial translocation of ER ceramides activates a Bax-mediated pathway of apoptosis, but the molecular principles by which this occurs remain to be established. To further elucidate the mechanism by which ceramides commit cells to death, we here developed a rapamycin-inducible version of the ceramide transfer protein CERT, sCERT, using FKB-FRBP chemical dimerization technology. We demonstrate that a short and transient exposure of cells to rapamycin suffices to induce efficient recruitment of sCERT to its target organelle. Upon its drug-induced recruitment to mitochondria, sCERT retains the ability to bind VAP protein receptors in the ER and catalyzes mitochondrial delivery of an externally added fluorescent ceramide analogue. Additionally, we show that mitochondrial recruitment of sCERT is accompanied by a major shift in the steady state distribution of Bax from the cytosol to mitochondria, analogous to what is observed when cells are exposed to the mitochondrial apoptosis-inducing agent, staurosporin. Importantly, the ability of mitochondria-bound sCERT to catalyze mitochondrial ceramide import and trigger mitochondrial translocation of Bax is abolished upon removal of its ceramide transfer or START domain. Together, these data corroborate our previous finding that mistargeting of ER ceramides to mitochondria specifically activates Bax-dependent apoptosis (Jain et al., 2016) and establish sCERT as a suitable novel tool to dissect the underlying mechanism in a time-resolved manner.

Bax and Bak are pro-apoptotic members of the Bcl-2 protein family that, upon activation, commit cells to death by forming oligomeric pores in the OMM (Große et al., 2016; Salvador-Gallego et al., 2016). Both proteins are regulated by a constant translocation to mitochondria and retro-translocation back into the cytosol, with pro-survival Bcl-2 proteins promoting retro-translocation (Edlich et al., 2011; Todt et al., 2015). In healthy cells, a fast retro-translocation of Bax leads to its steady state accumulation in the cytosol. While Bak is also present in the cytosol, its low retro-translocation rate causes its predominant mitochondrial localization. Swapping the *C*-terminal OMM anchors of Bax and Bak reverses their subcellular distribution. Interestingly, reducing Bax retro-translocation to the level of Bak shuttling

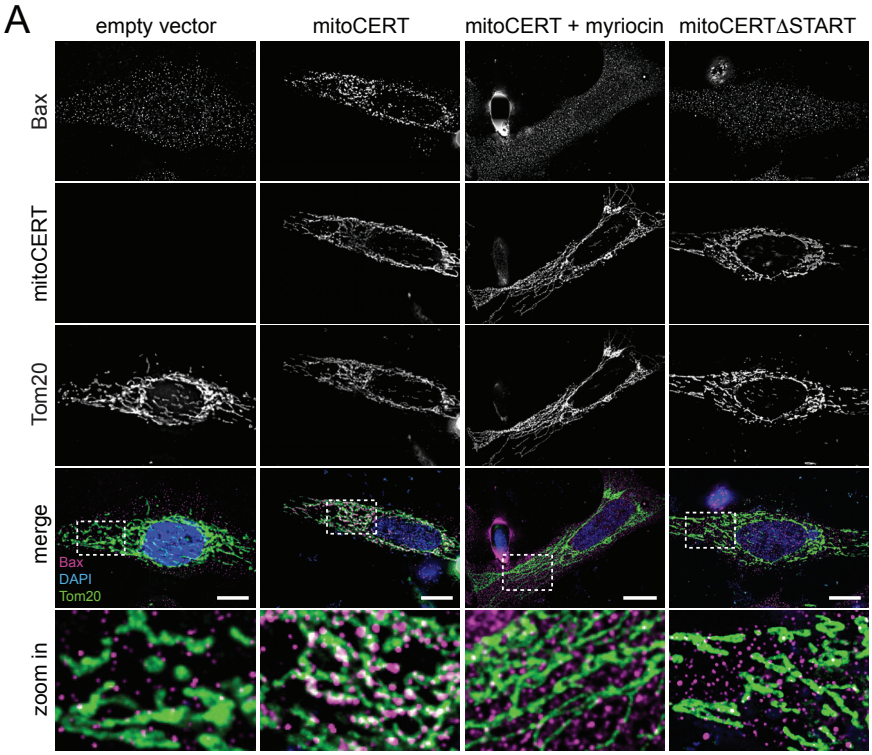

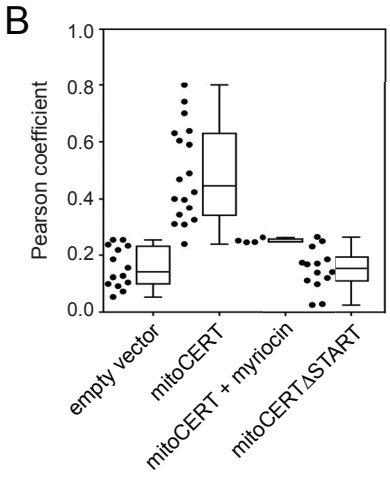

Figure 6. MitoCERT triggers a ceramide-dependent translocation of Bax to mitochondria. (**A**) HeLa cells co-transfected with eGFP-tagged Tom20 and empty vector, Flag-tagged mitoCERT or Flag-tagged mitoCERTDSTART were incubated in the absence or presence of 30 mM myriocin. At 24 h post-transfection, cells were fixed, double-stained with a monoclonal anti-Bax antibody and polyclonal anti-Flag antibody, counterstained with DAPI (blue), and then visualized by fluorescence microscopy. Confocal sections of cells are shown. Note that expression of mitoCERT greatly enhanced the overlap between Tom20 (green) and Bax-associated fluorescence (magenta), an effect abolished by myriocin or removal of the ceramide transfer or START domain. Bar, 10 μM. (**B**) Pearson correlation coefficients between Tom20 and Bax determined in cells treated as described in (A). At least 18 cells were analyzed per condition. For each boxplot, the middle line denotes the median while the top and bottom of the box indicate the 75th and 25th percentile. Whiskers denote the minimum and maximum values.

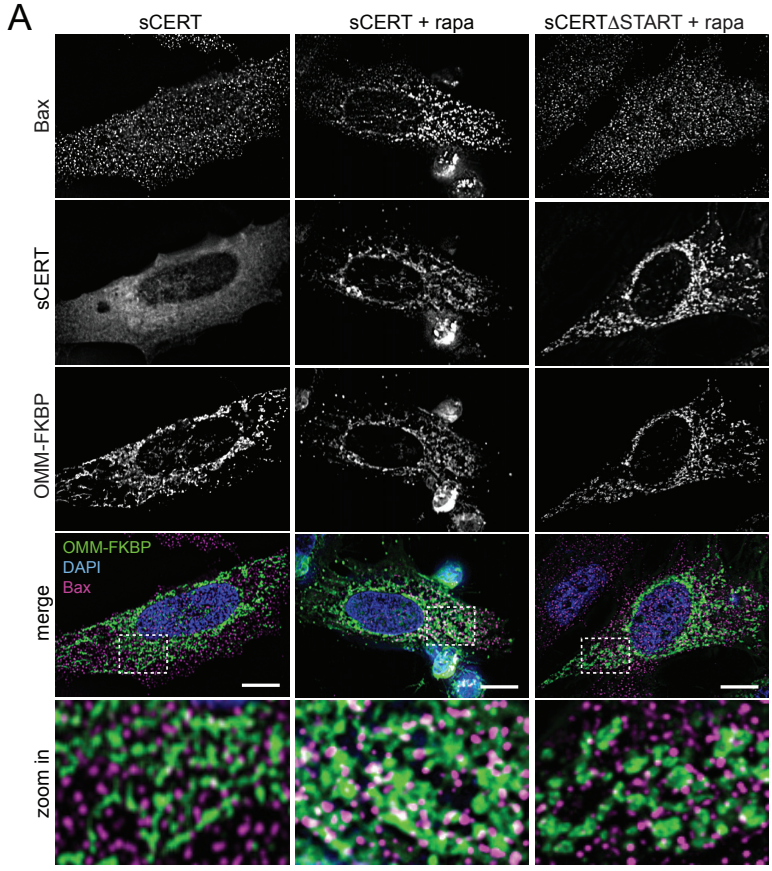

Figure 7. Mitochondrial recruitment of sCERT triggers mitochondrial translocation of Bax. (**A**) HeLa cells co-transfected with sCERT or sCERTDSTART and OMM-FKBP-mCherry (OMM-FKBP) were incubated in the absence (-rapa) or presence of 50 nM rapamycin for 30 min (+rapa), washed and then cultured for another 8 h. Next, cells were fixed, stained with a monoclonal antibody against Bax (magenta), counter-stained with DAPI (blue) and visualized by fluorescence microscopy. Confocal sections of cells are shown. Note that the overlap between OMM-FKBP-positive mitochondria (green) and Bax (magenta) increased dramatically upon rapamycin treatment of sCERT-expressing cells. Bar, 10 μM. (**B**) Pearson correlation coefficients between OMM-FKBP and Bax determined in cells treated as described in (A). At least 18 cells were analyzed per condition. For each boxplot, the middle line denotes the median while the top and bottom of the box indicate the 75th and 25th percentile. Whiskers denote the minimum and maximum values.

renders Bax cytotoxic, resulting in apoptosis induction in the absence of any stress signal (Todt et al., 2015). Thus, ceramides may exert their pro-apoptotic activity on mitochondria by interfering with efficient Bax retro-translocation from mitochondria into the cytosol. Recent studies with isolated mitochondria revealed that retro-translocation of endogenous Bax also occurs *in vitro* (Lauterwasser et al., 2016) and that the pore-forming activity of externally added Bax is enhanced significantly in the presence of ceramides (Ganesan et al., 2010). Whether ceramides enhance mitochondrial insertion of Bax and its functionalization into an apoptotic pore through direct and specific interactions, or whether this process requires mitochondria-resident ceramide effector proteins remains to be seen. In any case, direct experimental validation of the idea that the apoptogenic activity of mitochondrial ceramides relies on their ability to block Bax retro-translocation warrants a detailed spatiotemporal analysis of Bax dynamics in live cells upon induction of ceramide-mediated apoptosis. To this end, our ongoing efforts are aimed at the development of assays for real-time imaging of Bax and other core components of the mitochondrial apoptotic machinery in conjunction with the application of sCERT.

EXPERIMENTAL PROCEDURES

DNA constructs

A DNA insert encoding human CERT with a *C*-terminal FLAG tag (DYKDDDDK) was created by PCR and inserted in the NotI and XbaI restriction sites of mammaliam expression vector pcDNA3.1(+). The first 117 *N*-terminal residues of CERT were substituted for an FKBP-rapamycin-binding (FRB) domain-encoding sequence with monomeric eGFP fused to its *N*-terminus to create GFP-FRB-CERT or switchable CERT (sCERT). Deletion of the START domain (residues 346-597) yielded sCERTΔSTART. The FK506 binding protein (FKBP) domain with a *N*-terminal outer mitochondrial membrane (OMM) anchor (corresponding to residues 34-63 of mouse AKAP1) was PCR amplified from DNA construct OMM-FKBP-RFP (Csordás et al., 2010**,** kindly provided by G. Hajnóczky, Thomas Jefferson University, Philadelphia) and inserted into the EcoRI and EcoRV restriction sites of pSEMS-mCherry and pSEMS-HALO expression vectors (Covalys Biosciences), yielding OMM-FKBP-mCherry and OMM-FKBP-HALO. The OMM anchor sequence in these constructs was swapped for the *N*-terminal palmitoylation/myristolation signal of the Lyn protein (MGCIKSKGKDSAGA)(Inoue et al, 2005) by PCR, yielding PM-FKBP-mCherry and PM-FKBP-HALO. A cDNA encoding human VAP-A (kindly provided by Neale Ridgway, Dalhousie University, Halifax, Canada) was PCR amplified and inserted into the XhoI and SacI restrictions sites of pSEMS-mCherry to generate mCherry-VAP-A.

Cell culture and transfection

HeLa cells (ATCC-CCL2) were grown in high glucose DMEM supplemented with 2 mM L-glutamine and 10%FBS. Chinese hamster ovary CHO-LYA cells (a kind gift from Kentaro Hanada, University of Tokyo, Japan) were cultured in Ham's F12 MEM with 10% FBS. 24 h prior to transfection, cells were seeded on glass coverslips coated with poly-L-lysin-polyethylenglucol-arginine-glycine-aspartate (PLL-PEG-RGD) (VandeVondele et al., 2003). Transfection was performed using Effectene transfection reagent (Qiagen) according to instructions of the manufacturer. Z-VAD-fmk (10 µM; Calbiochem) and myriocin (30 µM; Sigma-Aldrich) were added to cells at the time of

transfection. 16 h post-transfection, cells were treated with 50 nM rapamycin (Sigma-Aldrich) for 30 min, washed, and then incubated for another 8 h before immunofluorescence analysis, unless indicated otherwise. Staurosporin (1 µM; Sigma-Aldrich) was added 1.5 h before immunofluorescence analysis.

Immunofluorescence microscopy

Transfected cells were fixed with 3% paraformaldehyde in PBS for 10 min, washed in PBS, and then quenched in 50 mM NH_4Cl in PBS for 10 min at RT. Cells were permeabilized in PM buffer (0.1% saponin and 0.2% BSA in PBS), immuno-labeled with the following primary antibodies: rabbit polyclonal anti-FLAG (cat. no. 2368, 1:1000, Cell Signaling); rabbit monoclonal anti-Bax (cat. no. 5023, 1:1000, Cell Signaling); mouse monoclonal anti-mitochondrial surface protein p60 (cat. no. MAB1273, 1:1000, Millipore). Next, cells were incubated with Cy5/Cy3-conjugated donkey anti-rabbit or donkey anti-mouse secondary antibodies (cat. no.711-175-152/150, 711-165-152/150, 1:400 each; Jackson ImmunoResearch Laboratories). Cells expressing HALO-tagged proteins were labeled with 50 nM HTL-tetramethylrhodamine (HTL-TMR) (Los and Wood, 2007). After counter staining with DAPI (300 nM in PBS), cells were mounted in Prolong Gold Antifade Mountant (Thermo Fischer Scientific) and sealed with nail varnish. Images were captured at RT with a DeltaVision Elite Imaging System (GE healthcare) built on an inverted Olympus IX-71 microscope, a 60x1.42 NA Plan ApoN UIS2 objective, a sCMOS camera (PCO, Kelheim, Germany), an InsightSSI illumination system and SoftWoRx, 6.0, beta27 software (Applied precision, Issaquah, WA). Fluorochromes used were DAPI, λex=390 nm and λem=435 nm; FITC/GFP, λex=475 nm and λem=523 nm; mCherry/TRITC, λex=542 nm and λem=594/45 nm; Cy5, λex=632 nm and λex=676 nm. Z-stacks of 0.2 µm in 20 optical slices to cover a total of 4 µm were acquired, followed by deconvolution using SoftWoRx software. Images were further processed using Fiji software (National Institute of Health, Bethesda, MD). Individual cells were analyzed for co-localization studies using the JACoP plugin in Fiji. Box and whisker graphs were created using GraphPad Prism Version 7 (Graph pad software, La Jolla California USA).

***In vivo* ceramide tranfer assay**

CHO-LYA cells grown on glass coverslips were co-transfected with sCERT or sCERTΔSTART and OMM-FKBP-HALO. 24 h post-transfection, cells were incubated with 0.5 µM Bodipy-TR-labeled C5-ceramide (Bodipy-Cer; Thermo-Fischer Scientific) complexed to bovine serum albumin at 4°C for 20 min and then washed twice in ice-cold Hanks' buffered saline solution (HBSS). After addition of fresh culture medium, cells were chased at 37°C for 10 min and then incubated in the absence or presence of 50 nm rapamycin for another 25 min before visualization by confocal fluorescence microscopy. Fluorescent images were captured using an Olympus LSM FV1000 confocal microscope equipped with an UPLSAPO 60X NA 1.35 oil immersion objective (Olympus). Fluorochromes used were eGFP, λex=488 nm and λem=515 nm; Bodipy-TR, λex=589 nm and λem=617 nm. Images were processed using Fiji software (National Institute of Health, Bethesda, MD).

REFERENCES

Ardail, D., Maalouf, M., Boivin, A., Chapet, O., Bodennec, J., Rousson, R. and Rodriguez-Lafrasse, C. (2009). Diversity and complexity of ceramide generation after exposure of jurkat leukemia cells to irradiation. *Int. J. Radiat. Oncol. Biol. Phys.* **73**, 1211–8.

Birbes, H., Luberto, C., Hsu, Y.-T., EL bawab, S., Hannun, Y. A. and Obeid, L. M. (2005). A mitochondrial pool of sphingomyelin is involved in TNFα-induced Bax translocation to mitochondria. *Biochem. J.* **386**, 445–451.

Bratton, S. B. and Cohen, G. M. (2001). Caspase Cascades in Chemically-Induced Apoptosis.pp. 407–420. Springer US.

Chang, K.-T., Anishkin, A., Patwardhan, G. A., Beverly, L. J., Siskind, L. J. and Colombini, M. (2015). Ceramide channels: destabilization by Bcl-xL and role in apoptosis. *Biochim. Biophys. Acta* **1848**, 2374–84.

Chipuk, J. E., McStay, G. P., Bharti, A., Kuwana, T., Clarke, C. J., Siskind, L. J., Obeid, L. M. and Green, D. R. (2012). Sphingolipid metabolism cooperates with BAK and BAX to promote the mitochondrial pathway of apoptosis. *Cell* **148**, 988–1000.

Czabotar, P. E., Lessene, G., Strasser, A. and Adams, J. M. (2013). Control of apoptosis by the BCL-2 protein family: implications for physiology and therapy. *Nat. Rev. Mol. Cell Biol.* **15**, 49–63.

Dai, Q., Liu, J., Chen, J., Durrant, D., McIntyre, T. M. and Lee, R. M. (2004). Mitochondrial ceramide increases in UV-irradiated HeLa cells and is mainly derived from hydrolysis of sphingomyelin. *Oncogene* **23**, 3650–3658.

Edlich, F., Banerjee, S., Suzuki, M., Cleland, M. M., Arnoult, D., Wang, C., Neutzner, A., Tjandra, N. and Youle, R. J. (2011). Bcl-xL Retrotranslocates Bax from the Mitochondria into the Cytosol. *Cell* **145**, 104–116.

Ganesan, V., Perera, M. N., Colombini, D., Datskovskiy, D., Chadha, K. and Colombini, M. (2010). Ceramide and activated Bax act synergistically to permeabilize the mitochondrial outer membrane. *Apoptosis* **15**, 553–562.

García-Sáez, A. J., Ries, J., Orzáez, M., Pérez-Payà, E. and Schwille, P. (2009). Membrane promotes tBID interaction with BCLXL. *Nat. Struct. Mol. Biol.* **16**, 1178–1185.

Green, D. R. and Kroemer, G. (2004). The Pathophysiology of Mitochondrial Cell Death. *Science (80-.).* **305**, 626–629.

Große, L., Wurm, C. A., Brüser, C., Neumann, D., Jans, D. C. and Jakobs, S. (2016). Bax assembles into large ring-like structures remodeling the mitochondrial outer membrane in apoptosis. *EMBO J.* **35**, 402–413.

Halter, D., Neumann, S., van Dijk, S. M., Wolthoorn, J., de Mazière, A. M., Vieira, O. V., Mattjus, P., Klumperman, J., van Meer, G. and Sprong, H. (2007). Pre- and post-Golgi translocation of glucosylceramide in glycosphingolipid synthesis. *J. Cell Biol.* **179**, 101–115.

Hanada, K. (2006). Discovery of the molecular machinery CERT for endoplasmic reticulum-to-Golgi trafficking of ceramide. *Mol. Cell. Biochem.* **286**, 23–31.

Hanada, K., Kumagai, K., Yasuda, S., Miura, Y., Kawano, M., Fukasawa, M. and Nishijima, M. (2003). Molecular machinery for non-vesicular trafficking of ceramide. *Nature* **426**, 803–9.

Huitema, K., van den Dikkenberg, J., Brouwers, J. F. H. M. and Holthuis, J. C. M. (2004). Identification of a family of animal sphingomyelin synthases. *EMBO J.* **23**, 33–44.

Jain, A., Beutel, O., Ebell, K., Korneev, S. and Holthuis, J. C. M. (2016). Diverting CERT-mediated ceramide transport to mitochondria triggers Bax-dependent apoptosis. *J. Cell Sci.*

Kashkar, H., Wiegmann, K., Yazdanpanah, B., Haubert, D. and Krönke, M. (2005). Acid sphingomyelinase is indispensable for UV light-induced Bax conformational

change at the mitochondrial membrane. *J. Biol. Chem.* **280**, 20804–13.

Kawano, M., Kumagai, K., Nishijima, M. and Hanada, K. (2006). Efficient trafficking of ceramide from the endoplasmic reticulum to the Golgi apparatus requires a VAMP-associated protein-interacting FFAT motif of CERT. *J. Biol. Chem.* **281**, 30279–88.

Kudo, N., Kumagai, K., Tomishige, N., Yamaji, T., Wakatsuki, S., Nishijima, M., Hanada, K. and Kato, R. (2008). Structural basis for specific lipid recognition by CERT responsible for nonvesicular trafficking of ceramide. *Proc. Natl. Acad. Sci.* **105**, 488–493.

Lauterwasser, J., Todt, F., Zerbes, R. M., Nguyen, T. N., Craigen, W., Lazarou, M., van der Laan, M. and Edlich, F. (2016). The porin VDAC2 is the mitochondrial platform for Bax retrotranslocation. *Sci. Rep.* **6**, 32994.

Levine, T. (2004). Short-range intracellular trafficking of small molecules across endoplasmic reticulum junctions. *Trends Cell Biol.* **14**, 483–90.

Los, G. V and Wood, K. (2007). The HaloTag: a novel technology for cell imaging and protein analysis. *Methods Mol. Biol.* **356**, 195–208.

Luna-Vargas, M. P. A. and Chipuk, J. E. (2016). The deadly landscape of pro-apoptotic BCL-2 proteins in the outer mitochondrial membrane. *FEBS J.* **283**, 2676–2689.

Moldoveanu, T., Follis, A. V., Kriwacki, R. W. and Green, D. R. (2014). Many players in BCL-2 family affairs. *Trends Biochem. Sci.* **39**, 101–11.

Perera, M. N., Ganesan, V., Siskind, L. J., Szulc, Z. M., Bielawska, A., Bittman, R. and Colombini, M. (2016). Ceramide channel: Structural basis for selective membrane targeting. *Chem. Phys. Lipids* **194**, 110–116.

Putyrski, M. and Schultz, C. (2012). Protein translocation as a tool: The current rapamycin story. *FEBS Lett.* **586**, 2097–2105.

Salvador-Gallego, R., Mund, M., Cosentino, K., Schneider, J., Unsay, J., Schraermeyer, U., Engelhardt, J., Ries, J. and Garcia-Saez, A. J. (2016). Bax assembly into rings and arcs in apoptotic mitochondria is linked to membrane pores. *EMBO J.* **35**, 389–401.

Siskind, L. J., Kolesnick, R. N. and Colombini, M. (2006). Ceramide forms channels in mitochondrial outer membranes at physiologically relevant concentrations. *Mitochondrion* **6**, 118–125.

Tafesse, F. G., Vacaru, A. M., Bosma, E. F., Hermansson, M., Jain, A., Hilderink, A., Somerharju, P. and Holthuis, J. C. M. (2014). Sphingomyelin synthase-related protein SMSr is a suppressor of ceramide-induced mitochondrial apoptosis. *J. Cell Sci.* **127**,.

Todt, F., Cakir, Z., Reichenbach, F., Emschermann, F., Lauterwasser, J., Kaiser, A., Ichim, G., Tait, S. W., Frank, S., Langer, H. F., et al. (2015). Differential retrotranslocation of mitochondrial Bax and Bak. *EMBO J.* **34**, 67–80.

Vacaru, A. M., Tafesse, F. G., Ternes, P., Kondylis, V., Hermansson, M., Brouwers, J. F. H. M., Somerharju, P., Rabouille, C. and Holthuis, J. C. M. (2009). Sphingomyelin synthase-related protein SMSr controls ceramide homeostasis in the ER. *J. Cell Biol.* **185**,.

VandeVondele, S., Vörös, J. and Hubbell, J. A. (2003). RGD-grafted poly-l-lysine-graft-(polyethylene glycol) copolymers block non-specific protein adsorption while promoting cell adhesion. *Biotechnol. Bioeng.* **82**, 784–790.

Yamaoka, S., Miyaji, M., Kitano, T., Umehara, H. and Okazaki, T. (2004). Expression Cloning of a Human cDNA Restoring Sphingomyelin Synthesis and Cell Growth in Sphingomyelin Synthase-defective Lymphoid Cells. *J. Biol. Chem.* **279**, 18688–18693.

Chapter 4

Development of split-GFP-based assays for real-time imaging of mitochondrial apoptosis

Amrita Jain[1], Jannis Schoppe[2], J.C.M. Holthuis[1, 3]

[1]Molecular Cell Biology Division, Department of Biology/Chemistry, University of Osnabrück, D-49076 Osnabrück, Germany; [2]Biochemistry Division, Department of Biology/Chemistry, University of Osnabrück, D-49076 Osnabrück, Germany; [3]Membrane Biochemistry & Biophysics, Bijvoet Center and Institute of Biomembranes, Utrecht University, 3584 CH Utrecht, The Netherlands

Manuscript in preparation

Development of split-GFP-based assays for real-time imaging of mitochondrial apoptosis

Amrita Jain[1], Jannis Schoppe[2], J.C.M. Holthuis[1, 3]

[1]Molecular Cell Biology Division, Department of Biology/Chemistry, University of Osnabrück, D-49076 Osnabrück, Germany; [2]Biochemistry Division, Department of Biology/Chemistry, University of Osnabrück, D-49076 Osnabrück, Germany; [3]Membrane Biochemistry & Biophysics, Bijvoet Center and Institute of Biomembranes, Utrecht University, 3584 CH Utrecht, The Netherlands

ABSTRACT

Our previous work revealed that mitochondrial translocation of ER ceramides triggers accumulation of pro-apoptotic Bcl-2 protein Bax on mitochondria, initiating the release of cytochrome *c*, caspase activation and cell death. However, the molecular principles by which ceramides induce these events are poorly understood. To allow a detailed spatiotemporal analysis of Bax and other participants in ceramide-induced cell death, we here took advantage of a split-GFP-based Cas9/sgRNA-mediated knockin strategy for GFP tagging of endogenous proteins. Through insertion of a small fragment of GFP at genomic loci of target proteins in cells constitutively producing the complementary GFP fragment, functional GFP tagging of proteins is achieved with minimal genomic disruption and without potential artifacts introduced by overexpression. We demonstrate functional GFP tagging of Bax and other components of the mitochondrial apoptotic machinery, hence paving the way to dissect the mechanism of ceramide-induced cell death in real time.

INTRODUCTION

Apoptosis is a tightly controlled cellular suicide program required for normal embryonic development and for the removal of damaged or diseased cells that undermine healthy tissue homeostasis (Jacobson et al., 1997; MacFarlane and Williams, 2004). Mitochondrial outer membrane permeabilization (MOMP) is a key event in the intrinsic pathway of apoptosis, enabling the release of cytochrome *c* (Cyto *c*) and other apoptotic intermembrane space proteins to activate caspases and commit cells to death (Budihardjo et al., 1999; Ott et al., 2002). MOMP is regulated by members of the Bcl-2 protein family (Czabotar et al., 2013; Lindsten et al., 2000; Wei et al., 2001). The pro-apoptotic Bcl2 proteins Bax (Bcl2-associated X protein) and Bak (Bcl2-antagonistic killer) are essential for mitochondrial apoptosis and actively participate in MOMP.

In healthy cells, Bax and Bak constantly shuttle between mitochondria and the cytosol. Due to different rates in retro-translocation to the cytosol, Bak primarily resides in the outer mitochondrial membrane whereas the bulk of Bax molecules localizes in the cytosol (Edlich, 2015; Schellenberg et al., 2013; Todt et al., 2015). In response to DNA damage or cytotoxic stress, retro-translocation of Bax

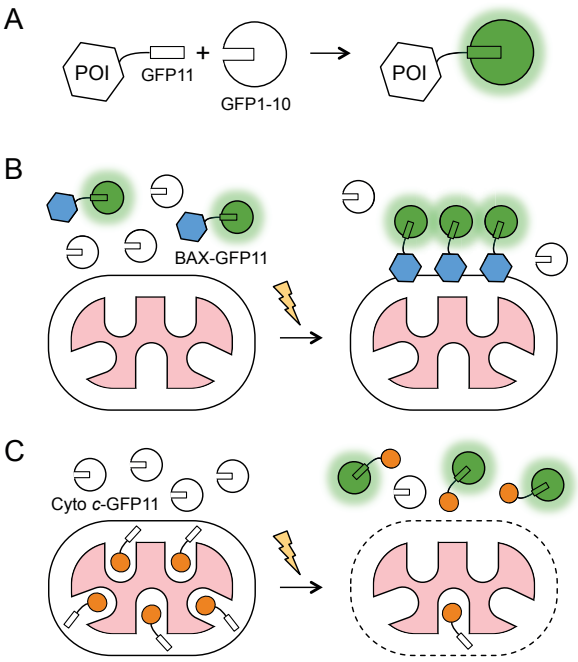

Figure 1. Design of split-GFP-based assays for imaging mitochondrial apoptosis *in vivo*. (**A**) Principle of split-GFP system. A protein of interest (POI) is tagged with the 11th β-strand of superfolder GFP, GFP11 (residues 215-230). The complementary GFP1-10 fragment (i.e. GFP without the 11th β-strand) contains an immature GFP chromophore and is non-fluorescent by itself. When co-expressed in the same cell, the GFP11 tag on the POI recruits its GFP1-10 partner to reconstitute functional GFP, rendering the tagged protein fluorescent. (**B**) Principle of a split-GFP-based assay to monitor mitochondrial translocation of Bax in apoptotic cells. (**C**) Principle of a split-GFP-based assay to monitor cytosolic translocation of Cyto *c* in apoptotic cells.

is blocked, causing an accumulation of the protein on the mitochondrial surface where it undergoes conformational changes, membrane insertion and assembly into apoptotic pores that mediate MOMP (Ferrer et al., 2012; Große et al., 2016; Hollville and Martin, 2012; Nechushtan et al., 1999b; Salvador-Gallego et al., 2016).

Ceramides are essential precursors of sphingolipid biosynthesis with a dual role as tumor suppressor lipids. Besides potentiating signaling events leading to cell cycle arrest, converging lines of evidence indicate that ceramides can initiate mitochondrial apoptosis (Hannun and Obeid, 2008). Defects in ceramide generation and turnover contribute to cancer cell survival and resistance to chemotherapy (Morad and Cabot, 2012). Consequently, the potential of ceramide-metabolizing enzymes as therapeutic targets in the treatment of cancer has become a major focus of interest. However, the molecular mechanisms whereby ceramides trigger mitochondria-mediated cell death

are not well understood. Previous *in vitro* studies indicate that ceramides or ceramide-derived metabolites can act directly on isolated mitochondria to promote MOMP (Chipuk et al., 2012; Perera et al., 2016; Siskind et al., 2006). We recently extended these observations by showing that an acute mislocalization of newly synthesized ceramides to mitochondria triggers mitochondrial translocation of Bax, culminating in Cyto *c* release, caspase activation and cell death (Jain et al., 2016; Chapter 3). In addition, we found that apoptogenic activity relies on intact ceramides rather than the downstream metabolic intermediates of ceramide turnover.

To facilitate further elucidation of the mechanisms underlying ceramide-induced cell death, we in here took advantage of a new split-GFP-based Cas9/sgRNA-mediated knockin strategy for GFP tagging of Bax and other core components of the mitochondrial apoptotic machinery at their genomic loci. Contrary to previous methods, this approach requires no cloning, involves minimal genomic disruption, and circumvents the potential cytotoxicity associated with heterologous expression of GFP-tagged pro-apoptotic proteins. Our findings pave the way to image, in real time, discrete steps by which ceramides commit cells to death.

RESULTS

Design of split-GFP-based assays for real-time imaging of mitochondrial apoptosis

During mitochondrial apoptosis, Bax undergoes mitochondrial translocation and subsequent oligomerization to permeabilize the outer mitochondrial membrane for intermembrane space proteins such as Cyto *c*. By initiating a major caspase activation pathway, the release of Cyto *c* to the cytosol marks a point of no-return in apoptotic cell death (Ott et al., 2002; Tait and Green, 2010). To study the dynamics of these key mediators of mitochondrial apoptosis in live cells, we set out to combine the advantages of a split-GFP system with CRISPR technology (Kamiyama et al., 2016; Leonetti et al., 2016). In this approach, a 16-residue fragment corresponding to the 11^{th} β-strand of superfolder GFP, GFP11, is fused to a protein of interest by CRISPR/Cas9-mediated kockin at its endogenous genomic locus. When expressed in cells producing the complementary GFP fragment (GFP1-10), the GFP11 tag on the protein of interest assembles noncovalently with its GFP1-10 partner to enable fluorescent tagging by GFP complementation (Fig. 1A). A key advantage of the approach is that GFP11-tagged proteins are produced at physiological levels with minimal disruption of their genomic loci. This is particularly relevant for pro-apoptotic proteins such as Bax and its close homologue Bak, which are known to induce apoptosis when overproduced (Pastorino et al., 1998). In cells expressing GFP11-tagged Cyto *c*, complementation with cytosolic GFP1-10 and creation of GFP fluorescence is expected to occur only upon induction of apoptosis. Thus, we next addressed whether the split-GFP approach can be used to monitor mitochondrial translocation of Bax and cytosolic release of Cyto *c* in real time (Fig. 1B,C).

Complementation of GFP11-tagged Bax does not interfere with its mitochondrial translocation upon apoptosis induction

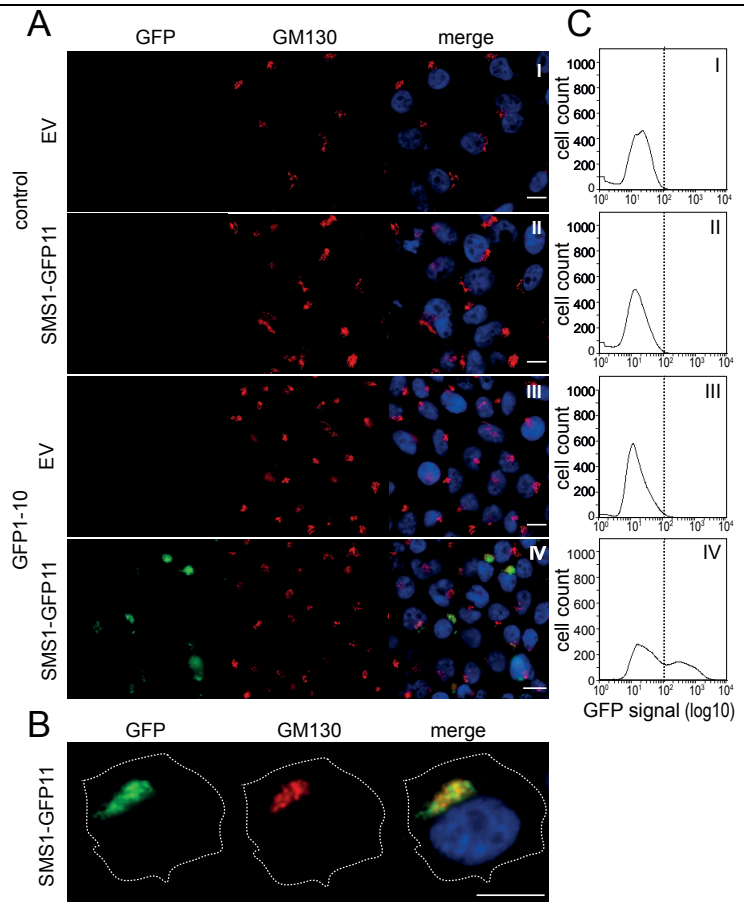

Figure 2. Functional complementation of GFP11-tagged SMS1. (**A**) 293T and 293T-GFP1-10 cells were transfected with empty vector or GFP11-tagged SMS1, immunostained with an antibody against the *cis*-Golgi marker GM130, and then visualized by florescence microscopy. (**B**) Zoom-in of cells co-expressing SMS1-GFP11 and GFP1-10 and processed as described in (A). Scale bars, 10 µM. (**C**) Flow cytometric analysis of the cells treated as in (A). The dashed line marks the threshold of background GFP fluorescence.

As a first proof-of-concept experiment, we fused a GFP11 tag to the *N*-terminus of the *trans*-Golgi-resident sphingomyelin synthase SMS1 and transfected the corresponding DNA construct into human embryonic kidney 293T cells stably expressing GFP1-10. Fluorescence microscopy of 293T-GFP1-10 cells transfected with SMS1-GFP11 yielded a GFP signal in the perinuclear region that displayed significant overlap with the *cis*-Golgi marker GM130 (Fig. 2A,B). In contrast, no GFP signal was detectable in untransfected 293T-GFP1-10 cells or when SMS1-GFP11 was transfected in 293T cells that do not express GFP1-10. Indeed, flow cytometry gave rise to a clear population of GFP+ cells only when SMS1-GFP11 was co-expressed with GFP1-10 (Fig. 2C). From this we conclude that GFP11-tagged

SMS1 is functionally complemented with GFP1-10 at a site that matches the predicted subcellular localization of the protein.

Next, we fused a GFP11 tag to the *N*-termini of Bax and Bak, two key mediators of mitochondrial apoptosis. Upon transfection in 293T-GFP1-10 cells, GFP11-Bax produced a GFP signal throughout the cytosol and nucleus. When the transfected cells were treated for 1 h with the apoptosis inducer staurosporin, the bulk of GFP signal coalesced into discrete clusters that were found on or near Tom20-positive mitochondria (Fig. 3A). Importantly, these clusters immuno-reacted with a monoclonal anti-Bax antibody, confirming that they correspond to GFP11-Bax that is complemented with GFP1-10 (Fig. 3B). Transfection of 293T-GFP1-10 cells with GFP11-Bak, on the other hand, produced a GFP signal that co-localized extensively with Tom20-positive mitochondria (Fig. 3C). However, upon staurosporin treatment, the GFP11-Bak associated fluorescence partially segregated from mitochondria and formed large clusters adjacent to mitochondria, consistent with previous work showing that Bak leaves mitochondria to form apoptotic microclusters during cell death progression (Nechushtan et al., 2001). Collectively, these results indicate that addition of an *N*-terminal GFP11 tag and its functional complementation with GFP1-10 do not interfere with the biological activities of Bax and Bak.

Complementation of GFP11-tagged cytochrome *c* occurs independently of apoptosis induction

To monitor cytochrome *c* translocation in live cells undergoing apoptosis, we next fused GFP11 to the *C*-terminus of Cyto *c*. Fluorescence microscopy of 293T-GFP1-10 cells transfected with Cyto-*c*-GFP11 yielded a GFP signal that distributed throughout the cytosol and nuclear compartment. In some transfected cells, GFP fluorescence was found concentrated in mitochondria (Figs. 4A, 5A), and areas of GFP fluorescence also immuno-reacted extensively with an anti-Cyto *c* antibody (Fig. 5B). Subcellular fractionation studies confirmed that part of Cyto *c*-GFP11 is imported into mitochondria (Fig. 5C). No GFP signal was detectable when Cyto *c*-GFP11 was transfected in 293T cells that do not express GFP1-10 (Fig. 4A,B). Together, these data indicate that already in the absence of an apoptotic stimulus, a portion of Cyto-*c*-GFP11 is complemented with GFP1-10 in the cytosol and then translocated into mitochondria as a functional complex. What fraction of mitochondrial Cyto *c*-GFP11 is associated with GFP1-10 is hard to judge as we did not find significant differences in GFP1-10 protein levels between mitochondrial pellets of control and Cyto *c*-GFP11-transfected cells (Fig. 5C). In any case, the amount of free Cyto *c*-GFP11 in mitochondria of transfected cells appears limited, as staurosporin treatment did not lead to any significant increase in GFP fluorescence (data not shown).

To reduce the apoptosis-independent complementation of Cyto *c*-GFP11 by GFP1-10, we put expression of the cytosolic GFP1-10 fragment under control of a doxycyclin-inducable promotor and co-transfected the construct with Cyto *c*-GFP11 into human HeLa Tet-on cells. 24 h post-transfection, cells were incubated in the absence or presence of 1 µg/ml doxycycline for 6 h to induce expression of

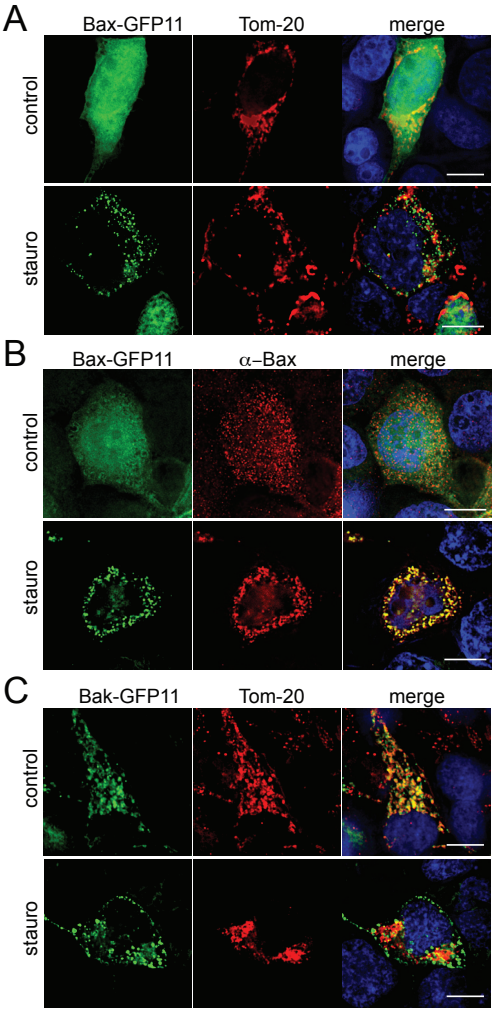

Figure 3. Functional complementation of GFP11-tagged Bax and Bak in control and apoptotic cells. (**A**) 293T-GFP1-10 cells were co-transfected with GFP11-tagged Bax and mCherry-tagged Tom20, incubated in the absence or presence of 1 μM staurosporin for 1 h, and then visualized by fluorescence microscopy. (**B**) 293T-GFP1-10 cells were transfected with GFP11-tagged Bax, incubated in the absence or presence of 1 μM staurosporin for 1 h, immuno-stained with an anti-Bax antibody and then visualized by fluorescence microscopy. (**C**) 293T-GFP1-10 cells were co-transfected with GFP11-tagged Bak and mCherry-tagged Tom20, incubated in the absence or presence of 1 μM staurosporin for 1 h, and then visualized by fluorescence microscopy.

GFP1-10. Next, the cells were stained with the mitochondrial membrane potential dye TMRE and incubated for 1 h in the absence or presence of the mitochondrial oxidative phosphorylation uncoupler FCCP to induce apoptosis and analyzed for GFP and TMRE fluorescence using flow cytometry. Treatment with doxycycline yielded a population of GFP+ cells (Fig. 6A,B). However, subsequent treatment with FCCP

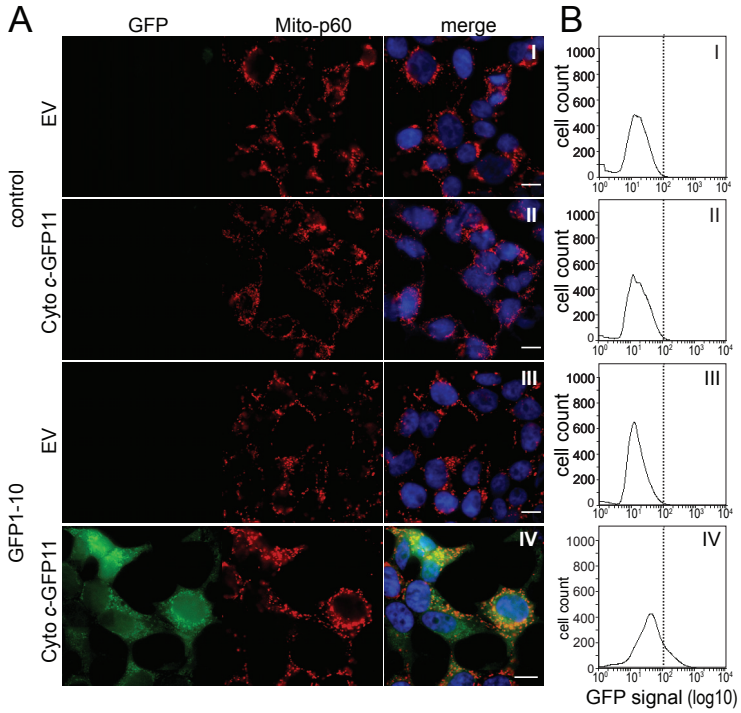

Figure 4. Functional complementation of GFP11-tagged Cyto *c*. (**A**) 293T and 293T-GFP1-10 cells were transfected with empty vector (EV) or GFP11-tagged Cyto *c*, immunostained with an antibody against the mitchondrial marker Mito-p60, and then visualized by fluorescence microscopy. Scale bars, 10 µM. (**B**) Flow cytometric analysis of GFP fluorescence in cells treated as in (A). The dashed line marks the threshold of background GFP fluorescence.

had no impact on the total number of GFP+ cells or on the overall GFP fluorescence levels measured, even though the drug caused a strong reduction in TMRE fluorescence. From this we conclude that in doxycycline-treated cells, the bulk of Cyto *c*-GFP11 is already complemented with GFP1-10 even before induction of apoptosis. It is conceivable that plasmid-mediated expression of Cyto *c*-GFP11 results in overproduction of the protein and saturates the mechanism responsible for its import into mitochondria. Therefore, we next engineered cell lines in which the GFP11-tagged proteins are expressed from their endogenous genomic loci.

Endogenous GFP11-tagging of apoptotic machinery using Cas9-RNP

For endogenous GFP11-tagging of proteins, we used the CRISPR/Cas9-based genomic knockin approach described by Leonetti et al (Leonetti et al., 2016). In this approach, Cas9/single guide RNA (sgRNA) ribonucleoprotein complexes (RNPs) are prepared *in vitro*, mixed with a single-stranded DNA (ssDNA) homologous-directed repair (HDR) donor and then electroporated into 293T-GFP1-10 cells (Fig. 7). sgRNAs were transcribed *in vitro* following PCR assembly of a template

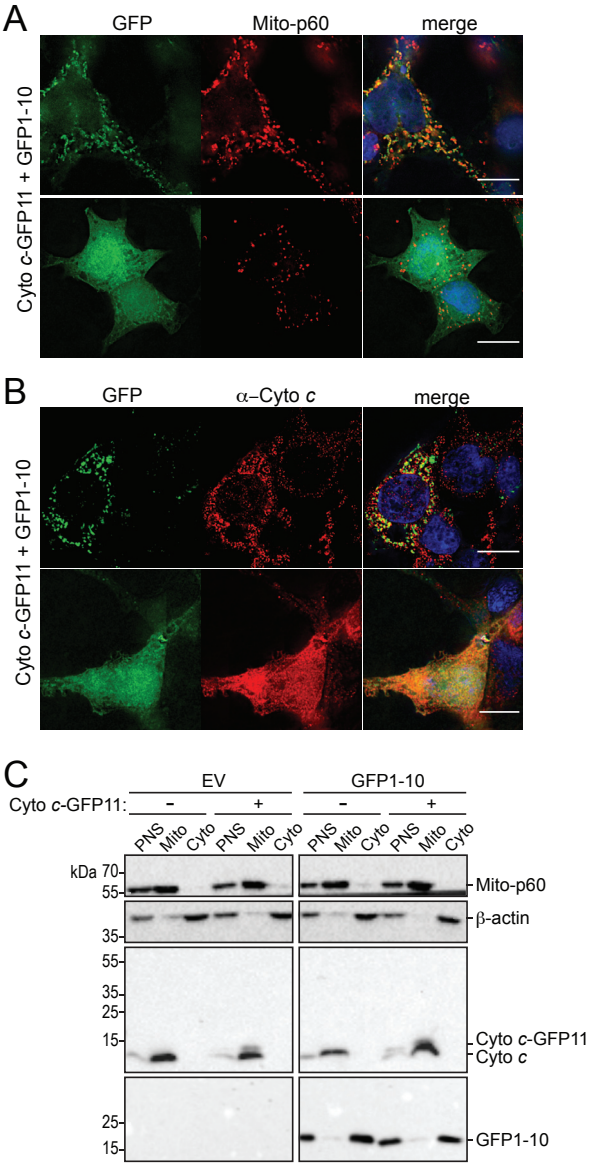

Figure 5. Subcellular distribution of GFP11-tagged Cyto *c*. (**A**) 293T-GFP1-10 cells were transfected with GFP11-tagged Cyto *c*, immuno-stained with an antibody against the mitchondrial marker Mito-p60, and then visualized by fluorescence microscopy. (**B**) 293T-GFP1-10 cells were transfected with GFP11-tagged Cyto *c*, immuno-stained with an antibody against Cyto *c*, and then visualized by fluorescence microscopy. Scale bars, 10 μM. (**C**) 293T and 293T-GFP1-10 cells were transfected with empty vector (EV) or GFP11-tagged Cyto *c*, lysed and then subjected to subcellular fractionation. Post-nuclear supernatants (PNS), mitochondrial pellets (Mito) and cytosolic fractions (Cyto) were collected and analyzed by immunoblotting using antibodies against Mito-p60, β-actin, Cyto *c* and GFP.

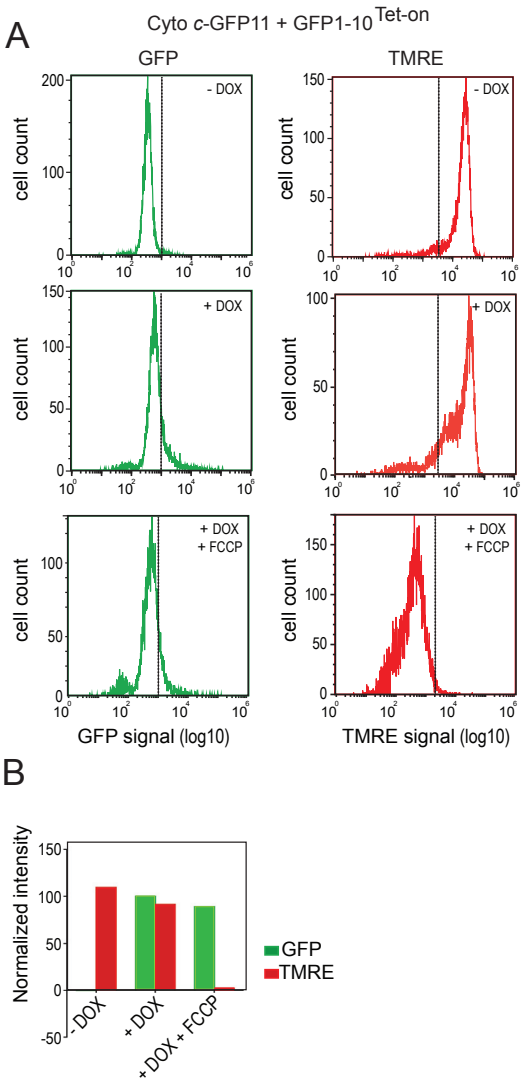

Figure 6. Functional complementation of GFP11-tagged Cyto *c* is independent of apoptosis induction. (**A**) HeLa cells constitutively expressing the Tetracyclin-controlled transcriptional *trans*-activator rTetR were transfected with GFP1-10:pTRE-Tight2 and Cyto *c*-GFP11, incubated in the absence or presence 1 µg/ml doxycycline for 6 h, and then treated with 50 µM tetramethylrhodamine ethyl-ester (TMRE) for 30 min. Cells were washed, incubated in the absence or presence of 10 µM carbonilcyanide p-trifluoromethoxyphenylhydrazone (FCCP) for 1 h and analyzed for GFP and TMRE fluororescence by flow cytometry. The dashed lines mark the threshold of background GFP and TMRE fluorescence. (**B**) Levels of GFP and TMRE fluorescence measured by flow cytometry of cells treated as in (A).

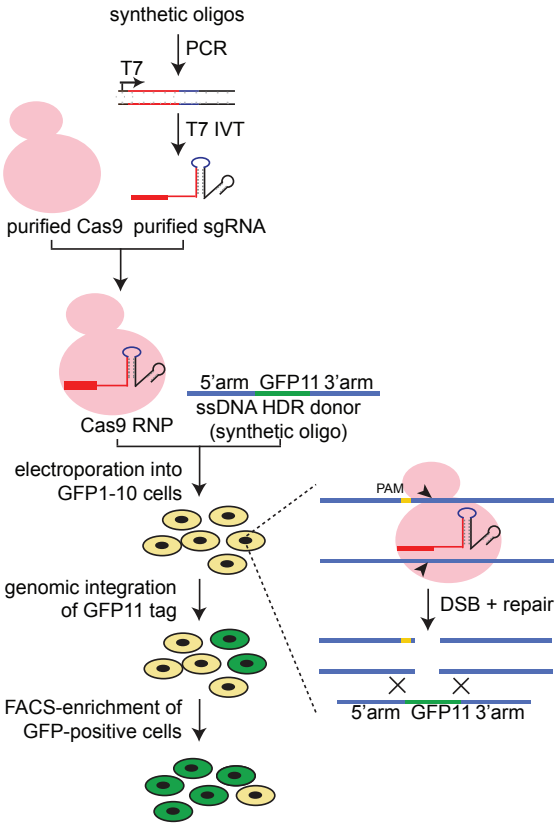

Figure 7. Workflow for endogenous GFP11-tagging using electroporation of Cas9-RNPs. T7 ITV, in vitro transcription using T7 polymerase; sgRNA, Cas9/single-guide RNA; RNP, ribonucleoprotein complex; HDR, homologous-directed repair; FACS, fluorescence-activated cell sorting; PAM, proto-spacer adjacent motif; DSB, double stranded break. See text for further details.

including a T7 promotor (Suppl. Fig. 1; Table1). RNPs were obtained by mixing sgRNAs with purified *S. pyogenes* Cas9 protein produced in *E. coli* (Kim et al., 2014). An *in vitro* plasmid cleavage assay was performed to verify the ability of the purified Cas9 protein to cleave double stranded DNA at site-specific location (Suppl. Fig.2). ssDNA HDR donors were obtained commercially and comprised the GFP11-encoding sequence (57 nt, including a 3-residue linker) flanked by two ~70-nt homology arms for HDR (Table 2). 293T-GFP1-10 cells were treated with nocodazole for 15 h before electroporation to increase HDR efficiency, as shown by Lin et al. (Lin et al., 2014; Suppl. Fig. 3).

To test our approach, we first targeted the inner nuclear membrane protein lamin A/C in 293T-GFP1-10 cells using an *N*-terminal GFP11-tag. Fluorescence microscopy demonstrated a high efficiency of functional GFP tagging, with 30% of cells showing GFP fluorescence in the immediate perinuclear region (Fig. 8A,B).

We next targeted SMS1, Bak and Bax using *N*-terminal GFP11 tags. Electroporation of 293T-GFP1-10 cells in each case yielded a subpopulation of GFP+ cells that showed fluorescence signals at the predicted subcellular localization, i.e. perinuclear region (SMS1), tubular network (Bak) and the nuclear and cytosolic compartment (Bax; Fig. 8A,B). However, the efficiency of functional GFP tagging of these proteins was considerably lower than that of lamin A/C and ranged between 2 and 5%. Sorting of GFP+ cell populations by flow cytometry allowed us to establish 293T-GFP1-10 cell lines in which nearly 100% of the cells displayed GFP tagging of the target protein for lamin A/C and SMS1 (Fig. 8C). Attempts to establish such cell lines for Bak and Bax were not successful, presumably because the endogenous expression levels of these proteins is too low to generate GFP signals necessary for an adequate sorting of GFP+ cells. Endogenous GFP11 tagging of Cyto *c* and the establishment of cell lines in which the efficiency of GFP tagging of Bak and Bax reaches 100% is currently in progress. Collectively, our results demonstrate that combined application of split-GFP technology and electroporation of Cas9/sgRNA RNPs is a suitable approach to specifically tag endogenous components of the cellular apoptotic machinery with GFP.

DISCUSSION

Mitochondrial translocation of ER ceramides triggers Bax-dependent apoptosis, but the mechanism by which these putative tumor suppressor lipids commit cells to death is poorly understood. In here, we successfully implemented a split-GFP-based Cas9/sgRNA-mediated knockin strategy for specific GFP tagging of endogenous Bax and other components of the mitochondrial apoptotic machinery. Together with the recent establishment of switchable ceramide transfer proteins for acute manipulation of mitochondrial ceramide levels (Chapter 3), this approach opens up important opportunities to resolve the spatio-temporal dynamics of core apoptotic machinery during ceramide-induced cell death. One major advantage of the present approach is that the function of GFP-tagged proteins can be analyzed at physiological expression levels, thus without perturbing the stoichiometry with their endogenous binding partners (Leonetti et al., 2016). This criterion is particularly relevant for Bax and Bak, two central regulators of apoptosis whose over- or underproduction directly influences cellular life-death decision-making (Pastorino et al., 1998). Another key advantage is that the small size of the GFP11 tag combined with Cas9 RNP electroporation enables a high knockin efficiency with minimal genomic disruption (Leonetti et al., 2016).

All endogenously GFP11-tagged proteins analyzed herein retained their normal subcellular distribution upon functional complementation with GFP1-10. We also found that GFP11-tagging and functional complementation of Bax do not interfere with its apoptosis-induced translocation to mitochondria. Even though the efficiency of endogenous GFP-tagging of proteins by the current approach greatly exceeds that of former methods (Lackner et al., 2015), sorting of GFP+ cells by flow cytometry is a necessary step to remove residual non-fluorescent cells. However, GFP-tagged proteins with low endogenous expression levels may score negative by flow cytometry. The abundance of a protein is

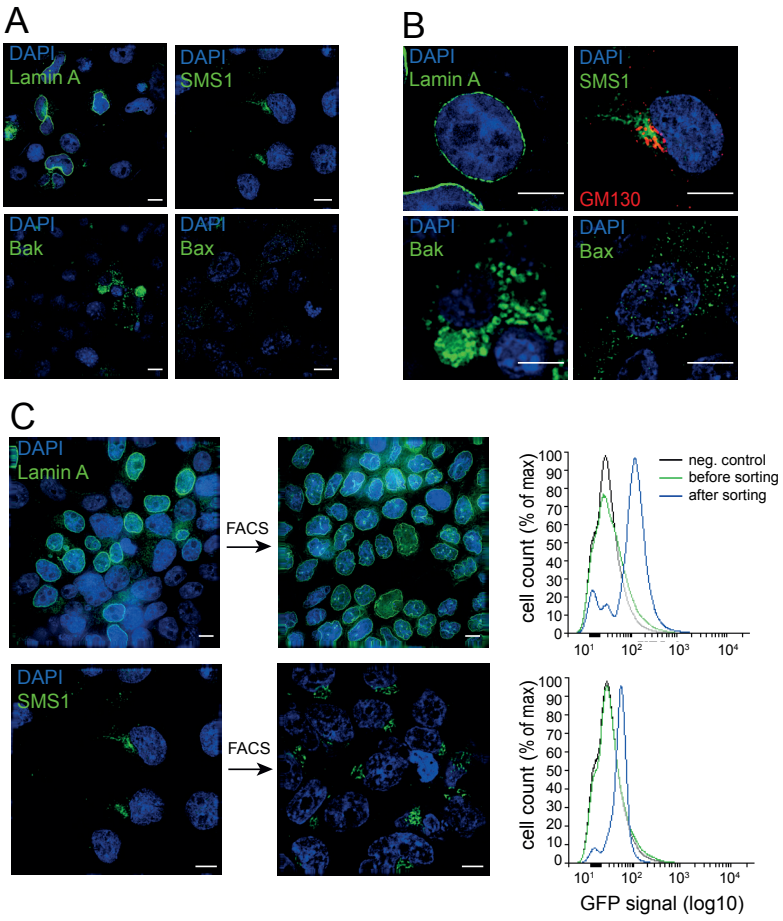

Figure 8. Endogenous GFP11-tagging of Lamin A/C, SMS1, Bax and Bak. (**A**) Fluorescence microscopy analysis of 293T-GFP1-10 cells after Cas9-RNP-mediated knockin of GFP11 at genomic loci of Lamin A/C, SMS1, Bax and Bak. Cells were stained with DAPI. (**B**) Zoom-in of cells treated as in (A). (**C**) GFP+ cells created as in (A) were isolated by FACS, stained with DAPI and analyzed by fluorescence microscopy. Scale bars, 10 µM.

closely associated with its rate of synthesis and can be estimated by ribosome profiling, a sequence-based method measuring the density of ribosomes present on cellular mRNAs and yielding a RPKM value (Li et al., 2014). The RPKM values for Lamin A/C and Bak in 293T cells are 61.2 and 17.18, respectively, whereas the threshold for GFP detection by flow cytometry lies at approximately 27 RPKM (Leonetti et al., 2016). This may explain why our attempts to sort GFP+ cells were successful for some protein targets (i.e. Lamin A/C, SMS1) but failed for others (i.e. Bak, Bax). Fluorescent detection of low abundant proteins can be achieved by knocking in multiple copies of the GFP11 tag, allowing recruitment of multiple GFP1-10 fragments per target

protein (Kamiyama et al., 2016; Leonetti et al., 2016).However, this approach requires longer ssDNA HDR donors than can be obtained commercially. Isolation of ssDNA from a PCR reaction in which one of the primers is coupled to biotin may provide a suitable approach to create long HDR donors (Wakimoto et al., 2014; Wilson, 2011). Upon denaturation of the dsDNA, streptavidin beads are then used to retain the biotinylated strand, allowing specific elution of the non-biotinylated strand for use as HDR donor.

We also explored the application of split-GFP technology to establish an assay for monitoring Cyto *c* translocation *in vivo* during ceramide-induced cell death (Fig. 1C). Unfortunately, we found that a large portion of GFP11-tagged Cyto *c* produced in cells transfected with the corresponding expression construct already formed a fluorescent complex with GFP1-10 prior to apoptosis induction. Whereas part of the GFP-labeled Cyto *c* distributed in the cytosolic and nuclear compartments, a portion was also found in mitochondria, indicating that recruitment of GFP1-10 by Cyto *c*-GFP11 does not interfere with mitochondrial import. Our efforts to reduce the apoptosis-independent complementation of Cyto *c*-GFP11 by using a doxycycline-inducible GFP1-10 construct were unsuccessful. Covalent attachment of a heme group in the intermembrane space is required to retain newly synthesized Cyto *c* in mitochondria as apo-Cyto c has been shown to freely equilibrate out of mitochondria (Allen, 2011). As overproduction of heterologously expressed Cyto *c*-GFP11 may saturate the enzymes responsible for heme attachment, our current efforts are aimed at tagging the endogenous protein with GFP11. However, due to the G-rich PAM preference of the Cas9 protein used in this study, the options for designing sgRNA sequences with the desired efficiency for introducing a C-terminal GFP11 tag at the genomic locus of Cyto *c* were limited. Recent characterization of CRISPR/Cas systems from a variety of prokaryotes yielded a functional homolog of Cas9, Cpf1, which recognizes 5'-TTN-3' as PAM sequence (Makarova et al., 2015; Zetsche et al., 2015). To extend options for GFP11-tagging of small A/T-rich genes such as Cyto *c*, our current efforts are aimed at implementing a CRISPR/Cpf1-based system.

MATERIALS AND METHODS

Antibodies

The following antibodies were used: mouse monoclonal anti-β-actin (cat. no. A1978, 1:10.000; Sigma-Aldrich), rabbit monoclonal anti-Bax (cat. no. 5023, 1:1000; Cell Signaling), mouse monoclonal anti-cytochrome c (sc13156, 1:500; Santa Cruz), mouse monoclonal anti-mitochondrial surface protein p60 (cat. no. MAB1273, 1:1000; Millipore) and rabbit polyclonal anti-GFP (cat. no. NB600-303,1:5000; Novus Biologicals) antibodies. Goat anti-mouse (cat. no. 31430, 1:10.000) and goat anti-rabbit IgG conjugated to horseradish peroxidase (cat. no. 31460, 1:10.000) were from Thermo Fischer Scientific. Cy™-dye-conjugated donkey anti-mouse and donkey anti-rabbit antibodies (cat. no. 715-225-150, 715-225-152, 715-165-150, 715-165-152, 715-175-150 and 715-175-152, 1:400 each) were from Jackson ImmunoResearch Laboratories.

DNA constructs

The following plasmids were used to create GFP11-tagged expression constructs: SMS1-V5-pcDNA3.1 (+) (Tafesse et al.,

2014), pEGFP-C3-Bax, pEGFP-C3-Bak (kind gift from Frank Edlich, Institute for Biochemistry and Microbiology, ZBMZ, University of Freiburg, Germany), and pBabe (LTR)-Cyto-c-GFP (Addgene plasmid #41183). DNA inserts encoding human SMS1, Bax and Bak with an *N*-terminal GFP11 tag were created by PCR using a forward primer containing the sequences for GFP11 (underlined), a short linker (italics) and the target protein (XXX), i.e. 5' TACGGATCCCGCCACCATGCGTGACCACATGGTCCTTCATGAGTATGTAAATGCTGCTGGGATTACA*GGTGGCGGCAAATTC* XXXX-3'. Inserts were cloned into the XhoI and EcoRI restriction sites of mammalian expression vector pcDNA3.1(+). A DNA insert encoding human cytochrome *c* with a *C*-terminal GFP11 tag was created by PCR using a reverse primer containing the sequences for GFP11 (underlined) and a short linker (italics), i.e. 5'TAGACTCGAGTCATGTAATCCCAGCAGCATTTACATACTCATGAAGGACCATGTGGTCAC*GGAATTTGCCGCCACC*CTCATTAGTAGCCTT-3', and the forward primer 5'TGGTGGAATTCGCCACCATGGGTGATGTTGAA-3'. For doxycycline-induced expression of GFP1-10, the corresponding ORF was PCR amplified from pcDNA3.1-GFP1-10 (a kind gift from Manual Leonetti, Dept. Cellular and Molecular Pharmacology, University of California, San Fransisco, USA) and subcloned into the BamHI and NheI restriction sites of pTRE-Tight2 (Addgene plasmid #19407). pSEMS-mCherry-Tom-20 was a kind gift from Karen Busch (Institute for Molecular Cell Biology, Westfälische Wilhelms-Universität, Münster, Germany). Bacterial expression of *Streptococcus pyogenes* Cas9 protein was achieved using construct pMJ915 (Addgene #69090).

Cell culture

HeLa (ATCC-CCL2), HeLa-tetR:Hygro/TevP-Neo (kind gift from Charles W. Morgan, Chemistry and Chemical Biology, University of California, San Francisco, USA), 293T (ATCC-CRL3216), and 293TGFP1-10 cells (kind gift from Manual Leonetti, Dept. of Cellular and Molecular Pharmacology, University of California, San Francisco, USA) were grown in High Glucose, Dulbecco's modified Eagle's medium (DMEM) supplemented with 1 mM glutamine and 10% FBS. Cells were passaged regularly and maintained below 80% cell density. Cells were transfected with DNA constructs using Effectene (Qiagen) according to the manufacturer's protocol. Prior to electroporation with Cas9/sgRNA RNP complexes (see below), 293TGFP1-10 cells were arrested at the G2/M phase of the cell cycle by treatment with 200 ng/µl nocodazole (Sigma) for 16 h. Nocodazole-treated cells were washed with serum-free DMEM medium once and then with RNase- and cation-free PBS (137 mM NaCl, 2.7 mM KCl, 10 mM Na_2HpO_4, 1.8 mM KH_2PO_4, 1 mL DEPC). Approximately $2x10^5$ cells were resuspended in 60 µl Gene Pulser Electroporation Buffer (BioRad) and used for electroporation.

Sub-cellular fractionation

For separating mitochondrial and cytoplasmic fractions, cells were washed twice with ice-cold 0.25 M sucrose and then harvested by scraping in 1.5 ml ice-cold Homogenizing Buffer (HB; 250 mM mannitol, 5 mM HEPES-KOH, pH 7.0, 0.5 mM EGTA, 1 mM protein inhibitor cocktail and 0.1 mM PMSF). Cells were homogenized in HB by flushing through a Balch Homogenizer 20-30 times using a 2 ml syringe. The homogenate was centrifuged twice at 600 x g_{max} for 5 min to pellet nuclei. The post-nuclear supernatant was centrifuged at 10.000 x g_{max} for 10 min to pellet mitochondria. Mitochondrial pellets were washed twice in homogenization

buffer to remove contaminating ER membranes and re-suspended in 200 µl Buffer R (10 mM Tris, 0.25 M Sucrose, pH7.4, 1 mM protein inhibitor cocktail and 0.1 M PMSF). Post-mitochondrial fractions were centrifuged at 100,000x g_{max} for 1 h and supernatants were collected as cytosolic fractions.

Design of sgRNA and HDR template

sgRNAs were designed using the web tool Benchling http://benchling.com/crispr. Selected sgRNA sequences were further verified using CHOPCHOP http://chopchop.rc.fas.harvard.edu and Crispr.mit http://crispr.mit.edu. The following parameters were also considered while designing the sgRNA sequence:

1. The length of the sgRNA sequence recognizing the target DNA was approx. ≈ 20 nt (Fu et al., 2014).
2. For selecting the optimal PAM sequence for Cas9 (5'-NGG-3'), GCGG/CGGG was preferred over CTGG/TCGG (Doench et al., 2014).
3. For efficient targeting of sgRNA, 50-60% of the GC content was preferred (Gilbert et al., 2014)
4. The presence of homopolymer regions in sgRNA sequence (GGGG, CCCC, AAAA, TTTT) was avoided (Gilbert et al., 2014).
5. sgRNA targeting either sense or antisense DNA strand were chosen without preference because of their similar efficiency (Gilbert et al., 2014).
6. sgRNAs beginning with 5'-G were preferred as this enhanced T7 polymerase mediated transcription activity (Graham and Root, 2015).

For introducing a GFP11 tag at the desired location in the genome, 200-mer HDR templates were custom synthesized in ssDNA form by Integrated DNA Technologies (Leuven, Belgium). To avoid the Cas9/sgRNA-mediated cleavage of the HDR template and redundant insertion of GFP11 at the target site, we created a silent mutation within the PAM sequence present in the HDR template. The sgRNA and ssDNA sequences used for the experiments described in here are listed in Suppl. Table 1 and Suppl. Table 2, respectively.

sgRNA synthesis

sgRNAs were synthesized as described in (Leonetti et al., 2016), using *in vitro* transcription of a DNA template of the following sequence: 5′-TAA TAC GAC TCA CTA TAG GNN NNN NNN NNN NNN NNG TTT AAG AGC TAT GCT GGA AAC AGC ATA GCA AGT TTA AAT AAG GCT AGT CCG TTA TCA ACT TGA AAA AGT GGC ACC GAG TCG GTG CTT TTT TT-3′ containing a T7 promoter (TAATACGACTCACTATAG), a gene-specific ~20-nt sgRNA sequence starting with a G for optimal T7 transcription (GNNNNNNNNNNNNNNNNNN), and a common sgRNA constant region. The DNA template was generated by overlapping PCR using a set of four primers: three primers common to all reactions (forward primer T25: 5′-TAA TAC GAC TCA CTA TAG-3′; reverse primer BS7: 5′-AAA AAA AGC ACC GAC TCG GTG C-3′ and reverse primer ML611: 5′-AAA AAA AGC ACC GAC TCG GTG CCA CTT TTT CAA GTT GAT AAC GGA CTA GCC TTA TTT AAA CTT GCT ATG CTG TTT CCA GCA TAG CTC TTA AAC-3′) and one gene-specific primer (forward primer 5′-TAA TAC GAC TCA CTA TAG GNN NNN NNN NNN NNN NNG TTT AAG AGC TAT GCT GGA A-3′). For each template, a 100-µl PCR was set using 1x Phusion buffer containing 7.5 mM $MgCl_2$, 2 mM dNTPs, 1 µM T25, 1 µM BS7, 20 nM ML611, 20 nM gene-specific primers and 2 Units of Phusion DNA polymerase (Thermo Fischer Scientific). The thermocycler setting was: 95°C for 30 s, 30 cycles of 95°C for 15 s, 57°C for 15 s, and 72°C for 15 s and 72°C

for 30 s. The PCR product was purified using the QIA quick gel extraction kit (Qiagen) according to the manufacture's instructions and eluted in 20 µl TE buffer (10 mM Tris pH 8.0, 1 mM EDTA). The quality of PCR products was checked by running them on a 2% agarose TBE gel. Next, a 20 µl *in vitro* transcription (IVT) reaction was set using Hi Scribe T7 High Yield RNA synthesis kit (New England Biolabs). To this end, a 20 µl IVT reaction was set using 1 µg of template DNA, 10 mM ATP, 10 mM GTP, 10 mM UTP, 10 mM CTP, 20 Units of RNase Inhibitor - Murine (New England Biolabs) and 2 µl T7 RNA polymerase Reaction Mix in T7 RNA Pol Reaction Buffer (40 mM Tris-HCl pH 7.9, 6 mM $MgCl_2$, 1 mM DTT, 2 mM spermidine) and incubated at 37°C for 2.5 h. sgRNA was precipitated by adding 2 µl 0.5 M EDTA, 2.4 µl 6 M LiCl and 75 µl ice-cold absolute EtOH and overnight incubation at -20°C followed by centrifugation at 10,000 rpm for 15 min at 4˚C. The sgRNA pellet was washed with 70% ice-cold EtOH and dissolved in 30 µl RNase-free buffer (10 mM Tris pH 7.0 in DEPC treated water). sgRNA quality was checked by mixing 5 µl of the sample with 5 µl of RNA loading dye (47.5% formamide, 0.01% SDS, 0.01% bromophenol blue, 0.005% Xylene Cyanol, 0.5 mM EDTA) followed by heating at 70°C for 10 min and running on a 2% agarose TBE gel.

Cas9 purification

Rosetta BL21 *E. coli* cells were freshly transformed with pMJ915 plasmid and a single ampicilin-resistant colony was inoculated in 100 ml of 2xTY media (16 g/L Tryptone, 10 g/L Yeast Extract, 5.0 g/L NaCl) containing 100 µg/ml ampicillin and incubated overnight at 37°C on a shaker at 180 rpm. The overnight culture was used to inoculate 4 L of 2xTY medium containing 100 µg/ml ampicillin and incubated at 37°C on a shaker at 180 rpm until mid-log phase (OD_{600}: 0.6-0.8). Next, the temperature was shifted to 20°C and 50 mM IPTG was added to the culture to induce Cas9 protein expression for 16 h. Cells were harvested by centrifugation at 5000 rpm for 10 min at 4°C and the cell pellet was re-suspended in 1x Lysis Buffer (LB: 50 mM HEPES-NaOH, pH 7.5, 1 M NaCl, 20% glycerol, 1 mM TCEP-HCl, 0.05xPIC, 1 mM PMSF) and lysed using a microfluidizer (Newton, MA). The disrupted cells suspension was collected by centrifugation at 15.000 rpm in a JA25.50 rotor for 30 min. The supernatant was applied onto a Protino Ni-NTA (Macherey nagel) resin equilibrated with 1 x LB and incubated for 1 h at 4°C to capture Cas9 protein on the beads. Beads were washed with 100 ml Washing Buffer (50 mM HEPES-NaOH pH 7.5, 1 M NaCl, 20% glycerol, 1 mM TCEP-HCl, 0.02 M imidazole) and Cas9 protein was eluted in fractions of 1 ml by adding 1x Elution Buffer (50 mM HEPES-NaOH pH 7.5, 100 mM NaCl, 20% glycerol v/v, 1 mM TCEP-HCl, 0.3 M imidazole). TEV-protease (1.6 mg/ml) was added to digest the eluted protein overnight at 4°C. The digested protein was applied onto a HiTrap SP FF Column (GE Healthcare) that was equilibrated with 1x HiTrap Loading Buffer (50 mM HEPES-NaOH pH 7.5, 100 mM NaCl, 20% glycerol, 1 mM TCEP-HCl). The bound protein was washed with 1x HiTrap Washing Buffer (50 mM Hepes pH 7.5, 100 mM KCl, 20% Glycerol, 1 mM TCEP-HCl) and eluted with a salt gradient of up to 1 M KCl. Protein fractions were analyzed by SDS-PAGE and protein in peak fractions was concentrated to ~4 mg/ml using Amicon spin columns (100 kDa MWCO). The purified protein was passed through a 0.22 micron filter unit to remove any contaminations and aliquots were flash frozen in liquid nitrogen before storage at -80°C.

In vitro DNA cleavage assay

To analyze purified Cas9 for catalytic activity, 2.4 pmol sgRNA containing the target sequence 5'-GCAAACCGCTAACAATACCT-3' was pre-heated for 5 min at 70°C and then incubated with 1.2 pmol of Cas9 protein in Cas9 buffer (150 mM KCl, 20 mM Tris, pH 7.5, 1 mM TCEP-HCl, 1 mM $MgCl_2$, 10% glycerol v/v) for 10 min at 37°C. The Cas9/sgRNA RNP compex formed was next incubated with 160 ng of SacI-linearized pRS406 plasmid and incubated for 1 h at 37°C. Cas9-mediated cleavage of DNA was stopped by adding 6x DNA loading dye (10 mM Tris-HCl pH 7.6, 0.03% bromophenol blue, 0.03% xylene cyanol FF, 60% glycerol, 60 mM EDTA, 1.2% SDS). Samples were run on the 1% agarose-TBE gel and visualized after Syber safe staining.

Preparation and electroporation of Cas9/sgRNA RNP complexes

Cas9/sgRNA RNP complexes were prepared as described by Leonetti et al. 2016 with some modifications. For RNP assembly, 390 pmol of sgRNA was pre-heated at 70°C for 5 min in 16 µl Cas9 buffer (150 mM KCl, 20 mM Tris, pH 7.5, 1 mM TCEP-HCl, 1 mM MgCl2, 10% glycerol v/v), mixed with 20 µl of Cas9 protein (16 µM stock in Cas9 buffer), and incubated at 37°C for 10 min. Next, 3 µl of HDR template (100 µM stock in Cas9 buffer) was added to the RNP solution. 43 µl of RNP solution was mixed with 60 µl nocodazole-treated 293T-GFP1-10 cells in Gene Pulser Electroporation Buffer (Biorad). The mixture was transferred to a 0.2 cm electroporation cuvette (Biorad) and electroporation was carried out using a square wave protocol (pulse length -25 msec at 110 V) in a Gene-Pulser X-Cell Electroporation System (Biorad). Cells were transferred onto glass coverslips coated with poly-L-lysin-polyethyleneglycol-arginine-glycine-aspartate (PLL-PEG-RGD) (VandeVondele et al., 2003) in a 6-well culture plate containing high-glucose DMEM supplemented with 10% FBS, 1 mM glutamine and 10,000 I.U./ml penicillin-streptomycin, and cultured for 4 days before analysis.

Imaging

Cells grown on coverslips were fixed with 2% paraformaldehyde in PBS for 10 min and then quenched in 50 mM NH_4Cl/PBS for 10 min at RT. Cells were permeabilized in PM buffer (0.1% saponin and 0.2% BSA in PBS), immuno-labeled with primary antibodies and Cy3- or Cy5-conjugated secondary antibodies, counterstained with DAPI (300 nM in PBS) and mounted in Prolong Gold Antifade Mountant (Thermo Fisher Scientific). Images presented in Fig. 3, 5A, 5B, and 8 were acquired using a Delta Vision Elite (GE healthcare) equipped with an inverted Olympus IX-71 microscope, a 60X NA 1.42, Plan ApoN UIS2 objective, a sCMOS camera (PCO, Kelheim, Germany), an InsightSSI illumination system and SoftWoRx, 6.0, beta27 software (Applied precision, Issaquah, WA). The standard-1 filter set was used with fluorochromes, DAPI, λex=390 nm and λem=435 nm; GFP, λex=475 nm and λem=525nm; mCherry, λex=542 nm and λem=594 nm. Usually, z-stacks of 0.2 µm in 20 optical slices to cover a total of 4 µm were acquired, followed by deconvolution using SoftWoRx software. Images presented in Fig. 4 and 2 were also captured using Leica DM5500 B microscope, 40X NA 1.40 Plan Apo oil objective, and a SPOT Pursuit camera. Fluorochromes used were DAPI, λ ex=360 nm and λem=460 nm; FITC/Alexa Fluor488, λex=488 nm and λem=515 nm; Texas Red/Alexa Fluor568, λex=568 nm and λem=585 nm. All images were processed using Fiji software (NIH, Bethesda, USA).

Flow cytometry

To analyze the efficiency of endogenous GFP11 tagging, trypsinized 293TGFP1-10 cells were centrifuged and re-suspended in 1XPBS buffer containing HEPES (25 mM, pH 7.5). Cells were immediately analyzed and GFP-positive cells were collected by BD FACSAria IIu cell sorter. Immediately after collection the cells were transferred to 1 mL supplemented DMEM in a 24-well culture dish. The sorted GFP positive cells were cultured for 5 days before analysis. To analyze the cell cycle stages of control and Nocodazole treated 293T-GFP1-10, cells were collected and washed once with 1XPBS. Approximately $2X10^6$ cells were fixed with 1% Para-formaldehyde solution (in H2O) for 1 h at 4°C. Fixed cells were permeabilized by adding ice chilled 70% ethanol (in H2O) drop wise and incubated overnight at 4°C. In permeabilized cells, 100 µg/mL RNAse A (Qiagen) was added and cells were stained with 40 µg/mL Propidium Iodide (Life technologies) at 37°C for 30 min. PI staining was excited by the 488 nm wavelength of light with broad emission centered around 617 nm using flow cytometer (BD Calibur). The flow cytometry data were analyzed using the Flowing software (Cell Imaging Core, Turku Centre for Biotechnology). To determine the mitochondrial membrane potential, approximately $2X10^5$ cells were stained with 50 µM tetramethylrhodamine ethyl ester (TMRE) (Abcam) by incubating it with cells for 30 min in the absence or presence of the mitochondrial oxidative phosphorylation uncoupler FCCP to induce apoptosis and analyzed for GFP and TMRE fluorescence using flow cytometer (Attune NxT; Life technologies).

REFRENCES

Allen, J. W. A. (2011). Cytochrome c biogenesis in mitochondria - Systems III and V. *FEBS J.* **278**, 4198–4216.

Budihardjo, I., Oliver, H., Lutter, M., Luo, X. and Wang, X. (1999). Biochemical Pathways of Caspase Activation During Apoptosis. *Annu. Rev. Cell Dev. Biol.* **15**, 269–290.

Chipuk, J. E., McStay, G. P., Bharti, A., Kuwana, T., Clarke, C. J., Siskind, L. J., Obeid, L. M. and Green, D. R. (2012). Sphingolipid metabolism cooperates with BAK and BAX to promote the mitochondrial pathway of apoptosis. *Cell* **148**, 988–1000.

Czabotar, P. E., Lessene, G., Strasser, A. and Adams, J. M. (2013). Control of apoptosis by the BCL-2 protein family: implications for physiology and therapy. *Nat. Rev. Mol. Cell Biol.* **15**, 49–63.

Doench, J. G., Hartenian, E., Graham, D. B., Tothova, Z., Hegde, M., Smith, I., Sullender, M., Ebert, B. L., Xavier, R. J. and Root, D. E. (2014). Rational design of highly active sgRNAs for CRISPR-Cas9–mediated gene inactivation. *Nat. Biotechnol.* **32**, 1262–1267.

Edlich, F. (2015). The great migration of Bax and Bak. *Mol. Cell. Oncol.* **2**, e995029.

Ferrer, P. E., Frederick, P., Gulbis, J. M., Dewson, G., Kluck, R. M., Lindsten, T., Ross, A., King, A., Zong, W., Rathmell, J., et al. (2012). Translocation of a Bak C-Terminus Mutant from Cytosol to Mitochondria to Mediate Cytochrome c Release: Implications for Bak and Bax Apoptotic Function. *PLoS One* **7**, e31510.

Fu, Y., Sander, J. D., Reyon, D., Cascio, V. M. and Joung, J. K. (2014). Improving CRISPR-Cas nuclease specificity using truncated guide RNAs. *Nat. Biotechnol.* **32**, 279–84.

Gilbert, L. A., Horlbeck, M. A., Adamson, B., Villalta, J. E., Chen, Y., Whitehead, E. H., Guimaraes, C., Panning, B., Ploegh, H. L., Bassik, M. C., et al. (2014). Genome-Scale CRISPR-Mediated Control of Gene Repression and Activation. *Cell* **159**, 647–61.

Graham, D. B. and Root, D. E. (2015). Resources for the design of CRISPR gene editing experiments. *Genome Biol.* **16**, 260.

Große, L., Wurm, C. A., Brüser, C., Neumann, D., Jans, D. C. and Jakobs, S. (2016). Bax assembles into large ring-like structures remodeling the mitochondrial outer membrane in apoptosis. *EMBO J.* **35**, 402–413.

Hannun, Y. A. and Obeid, L. M. (2008). Principles of bioactive lipid signalling: lessons from sphingolipids. *Nat. Rev. Mol. Cell Biol.* **9**, 139–150.

Hollville, E. and Martin, S. J. (2012). Greasing the Path to BAX/BAK Activation.

Jacobson, M. D., Weil, M. and Raff, M. C. (1997). Programmed cell death in animal development. *Cell* **88**, 347–54.

Jain, A., Beutel, O., Ebell, K., Korneev, S. and Holthuis, J. C. M. (2016). Diverting CERT-mediated ceramide transport to mitochondria triggers Bax-dependent apoptosis. *J. Cell Sci.*

Kamiyama, D., Sekine, S., Barsi-Rhyne, B., Hu, J., Chen, B., Gilbert, L. A., Ishikawa, H., Leonetti, M. D., Marshall, W. F., Weissman, J. S., et al. (2016). Versatile protein tagging in cells with split fluorescent protein. *Nat. Commun.* **7**, 11046.

Kim, S., Kim, D., Cho, S. W., Kim, J. and Kim, J.-S. (2014). Highly efficient RNA-guided genome editing in human cells via delivery of purified Cas9 ribonucleoproteins. *Genome Res.* **24**, 1012–9.

Lackner, D. H., Carré, A., Guzzardo, P. M., Banning, C., Mangena, R., Henley, T., Oberndorfer, S., Gapp, B. V., Nijman, S. M. B., Brummelkamp, T. R., et al. (2015). A generic strategy for CRISPR-Cas9-mediated gene tagging. *Nat. Commun.* **6**, 10237.

Leonetti, M. D., Sekine, S., Kamiyama, D., Weissman, J. S. and Huang, B. (2016). A scalable strategy for high-throughput GFP tagging of endogenous human proteins .

Manuscript 1–23.

Li, G.-W., Burkhardt, D., Gross, C. and Weissman, J. S. (2014). Quantifying Absolute Protein Synthesis Rates Reveals Principles Underlying Allocation of Cellular Resources. *Cell* **157**, 624–635.

Lin, S., Staahl, B., Alla, R. K. and Doudna, J. a (2014). Enhanced homology-directed human genome engineering by controlled timing of CRISPR/Cas9 delivery. *Elife* **3**, 1–13.

Lindsten, T., Ross, A. J., King, A., Zong, W. X., Rathmell, J. C., Shiels, H. A., Ulrich, E., Waymire, K. G., Mahar, P., Frauwirth, K., et al. (2000). The combined functions of proapoptotic Bcl-2 family members bak and bax are essential for normal development of multiple tissues. *Mol. Cell* **6**, 1389–99.

MacFarlane, M. and Williams, A. C. (2004). Apoptosis and disease: a life or death decision. *EMBO Rep.* **5**, 674–678.

Makarova, K. S., Wolf, Y. I., Alkhnbashi, O. S., Costa, F., Shah, S. A., Saunders, S. J., Barrangou, R., Brouns, S. J. J., Charpentier, E., Haft, D. H., et al. (2015). An updated evolutionary classification of CRISPR–Cas systems. *Nat. Rev. Microbiol.* **13**, 722–736.

Morad, S. A. F. and Cabot, M. C. (2012). Ceramide-orchestrated signalling in cancer cells. *Nat. Rev. Cancer* **13**, 51–65.

Nechushtan, A., Smith, C. L., Hsu, Y.-T. and Youle, R. J. (1999a). Conformation of the Bax C-terminus regulates subcellular location and cell death. *EMBO J.* **18**, 2330–2341.

Nechushtan, A., Smith, C. L., Hsu, Y. T. and Youle, R. J. (1999b). Conformation of the Bax C-terminus regulates subcellular location and cell death. *EMBO J.* **18**, 2330–41.

Nechushtan, A., Smith, C. L., Lamensdorf, I., Yoon, S.-H. and Youle, R. J. (2001). Bax and Bak Coalesce into Novel Mitochondria-Associated Clusters during Apoptosis. *J. Cell Biol.* **153**,.

Ott, M., Robertson, J. D., Gogvadze, V., Zhivotovsky, B. and Orrenius, S. (2002). Cytochrome c release from mitochondria proceeds by a two-step process. *Proc. Natl. Acad. Sci. U. S. A.* **99**, 1259–63.

Pastorino, J. G., Chen, S. T., Tafani, M., Snyder, J. W. and Farber, J. L. (1998). The overexpression of Bax produces cell death upon induction of the mitochondrial permeability transition. *J. Biol. Chem.* **273**, 7770–5.

Perera, M. N., Ganesan, V., Siskind, L. J., Szulc, Z. M., Bielawska, A., Bittman, R. and Colombini, M. (2016). Ceramide channel: Structural basis for selective membrane targeting. *Chem. Phys. Lipids* **194**, 110–116.

Salvador-Gallego, R., Mund, M., Cosentino, K., Schneider, J., Unsay, J., Schraermeyer, U., Engelhardt, J., Ries, J. and Garcia-Saez, A. J. (2016). Bax assembly into rings and arcs in apoptotic mitochondria is linked to membrane pores. *EMBO J.* **35**, 389–401.

Schellenberg, B., Wang, P., Keeble, J. A., Rodriguez-Enriquez, R., Walker, S., Owens, T. W., Foster, F., Tanianis-Hughes, J., Brennan, K., Streuli, C. H., et al. (2013). Bax exists in a dynamic equilibrium between the cytosol and mitochondria to control apoptotic priming. *Mol. Cell* **49**, 959–71.

Siskind, L. J., Kolesnick, R. N. and Colombini, M. (2006). Ceramide forms channels in mitochondrial outer membranes at physiologically relevant concentrations. *Mitochondrion* **6**, 118–125.

Tait, S. W. G. and Green, D. R. (2010). Mitochondria and cell death: outer membrane permeabilization and beyond. *Nat. Rev. Mol. Cell Biol.* **11**, 621–632.

Todt, F., Cakir, Z., Reichenbach, F., Emschermann, F., Lauterwasser, J., Kaiser, A., Ichim, G., Tait, S. W., Frank, S., Langer, H. F., et al. (2015). Differential retrotranslocation of mitochondrial Bax and Bak. *EMBO J.* **34**, 67–80.

VandeVondele, S., Vörös, J. and Hubbell, J. A. (2003). RGD-grafted poly-l-lysine-graft-(polyethylene glycol) copolymers block non-specific protein adsorption while

promoting cell adhesion. *Biotechnol. Bioeng.* **82**, 784–790.

Wakimoto, Y., Jiang, J. and Wakimoto, H. (2014). Isolation of Single-Stranded DNA. In *Current Protocols in Molecular Biology*, p. 2.15.1-2.15.9. Hoboken, NJ, USA: John Wiley & Sons, Inc.

Wei, M. C., Zong, W. X., Cheng, E. H., Lindsten, T., Panoutsakopoulou, V., Ross, A. J., Roth, K. A., MacGregor, G. R., Thompson, C. B. and Korsmeyer, S. J. (2001). Proapoptotic BAX and BAK: A Requisite Gateway to Mitochondrial Dysfunction and Death. *Science (80-.).* **292**, 727–730.

Wilson, R. (2011). Preparation of Single-Stranded DNA from PCR Products with Streptavidin Magnetic Beads. *Nucleic Acid Ther. (Formerly Oligonucleotides)* **21**, 437–440.

Zetsche, B., Gootenberg, J. S., Abudayyeh, O. O., Slaymaker, I. M., Makarova, K. S., Essletzbichler, P., Volz, S. E., Joung, J., van der Oost, J., Regev, A., et al. (2015). Cpf1 Is a Single RNA-Guided Endonuclease of a Class 2 CRISPR-Cas System. *Cell* **163**, 759–771.

SUPPLEMENTARY INFORMATION

Supplementary Figure 1

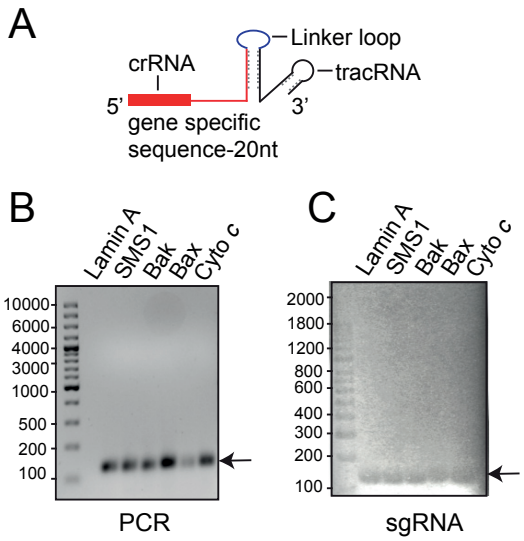

Suppl. Figure 1. sgRNA synthesis using in vitro transcription. (**A**) Schematic outline of sgRNA produced by in vitro transcription using T7 polymerase. (**B**) PCR products used as templates for production of gene-specific sgRNAs. (**C**) sgRNAs synthesized by *in vitro* transcription of PCR products shown in (B).

Supplementary Figure 2

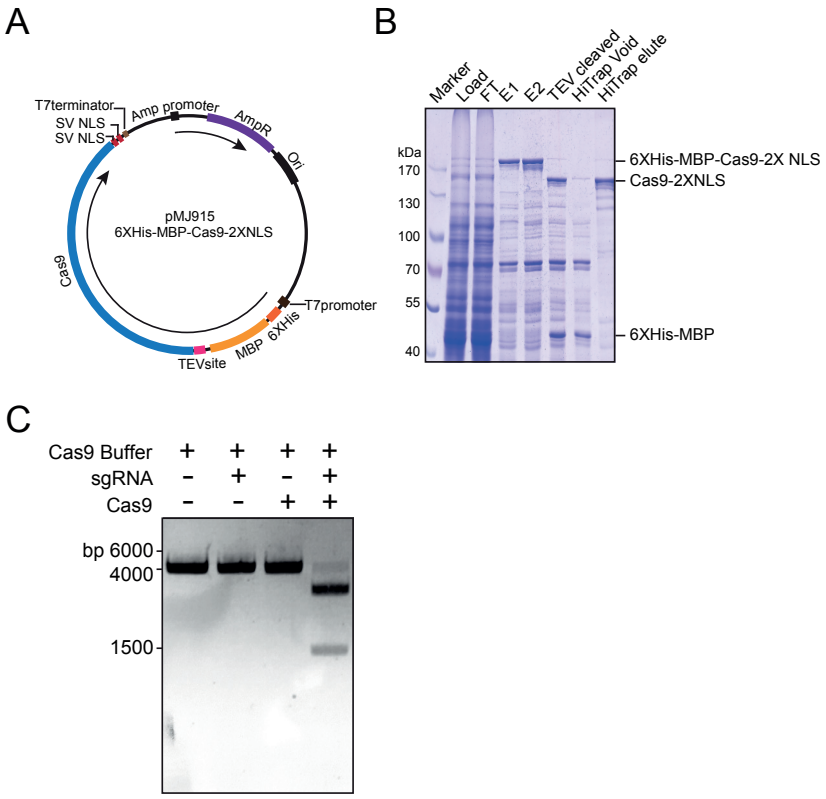

Suppl. Figure 2. Purification of functionally active recombinant Cas9 protein. (**A**) Schematic outline of bacterial expression construct pMJ915, encoding *S. pyogenes* Cas9 with two *C*-terminal Simian Virus 40 (SV40) T-antigen nuclear localization sequences (NLS) and TEV protease-cleavable *N*-terminal poly-histidine and maltose-binding protein (MBP) domains. (**B**) Cas9 protein was expressed in Rosetta BL21 *E coli* cells, affinity-purified from 6X-His- MBP fusion by TEV protease digestion. (**C**) RNPs containing purified Cas9 protein and site-specific sgRNA were incubated with pRS406 plasmid DNA. Cas9-mediated digestion of plasmid DNA was visualized by agarose gel electrophoresis and Syber Safe staining.

Supplementary Figure 3

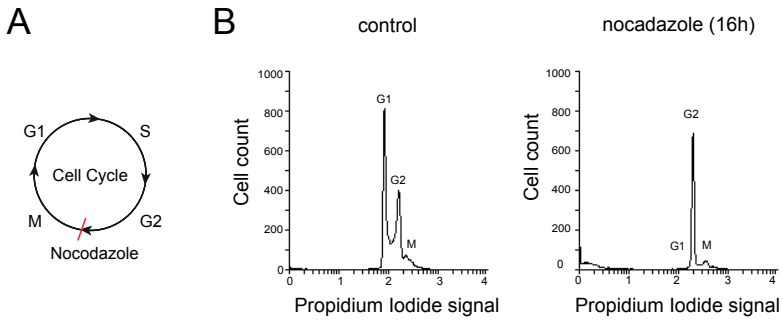

Suppl. Figure 3. Cell cycle synchronization of 293T-GFP1-10 cells. (**A**) 293T-GFP1-10 cells were treated with 200 pmol nocodazole for 16 h to trigger a cell cycle arrest at G2/M. (**B**) Control and nocodazole-treated cells were labeled with the DNA binding dye propidium iodide (PI) and analyzed by flow cytometry.

Suppl. Table 1. Gene-specific oligos for sgRNA synthesis

Gene (Accession ID)	**Terminus**	**Oligo sequence**
LaminA/C (LMNA)	N	TAA TAC GAC TCA CTA TAG GCC ATG GAG ACC CCG TCC CAG GTT TAA GAG CTA TGC TGG AA
SMS1 (SGMS1)	N	TAA TAC GAC TCA CTA TAG GCT GTC TGC CAG TAC AAT GAG TTT AAG AGC TAT GCT GGA A
BAX (BAX)	N	TAA TAC GAC TCA CTA TAG GGA GGC GGC GGC GGG AGC GGG TTT AAG AGC TAT GCT GGA A
BAK1 (BAK1)	N	TAA TAC GAC TCA CTA TAG GGA GAC CTG AAA AAT GGC TTG TTT AAG AGC TAT GCT GGA A
Cyto *c* (CYCS)	C	TAA TAC GAC TCA CTA TAG GTT TGT AAT AAA TAA GGC AGG TTT AAG AGC TAT GCT GGA A

Suppl. Table 2. HDR template sequences

Gene (Accession ID)	**HDR template sequence**
LaminA/C (LMNA)	TCCTTCGACCCGAGCCCCGCGCCCTTTCCGGGACCCCT GCCCCGCGGGCAGCGCTGCCAACCTGCCGGCCATGCG TGACCACATGGTCCTTCATGAGTATGTAAATGCTGCTGG GATTACAGGTGGCGGCGAGACCCCGTCCCAGCGGCGC GCCACCCGCAGCGGGGCGCAGGCCAGCTCCACTCCGC TGTCGCCCACCC
SMS1 (SGMS1)	GCCCTGTCGGAACAGTGACTGCTGACCTGCCAAGAGAG AGCTGGGGACTGCCTGCTGTCTGCCAGTACAatgCGTGA CCACATGGTCCTTCATGAGTATGTAAATGCTGCTGGGAT TACAGGTGGCGGCAAAGAAGTGGTTTATTGGTCACCCAA GAAGGTGGCAGACTGGCTGCTGGAGAATGCTATGCCAG AATACTG
BAX (BAX)	CTCACGTGACCCGGGCGCGCTGCGGCCGCCCGCGCGG ACCCGGCGAGAGGCGGCGGCGGGAGCGGCAGTGatgCG TGACCACATGGTCCTTCATGAGTATGTAAATGCTGCTGG GATTACAGGTGGCGGCGACGGGTCCGGGGAGCAGCCC AGAGGCGGGGGTGAGGCGGGAGGCAGACGGGCGGGA GGAGGGCGAGCCC
BAK1 (BAK1)	GTCACCCCCATCTCTGCTTTTTCTCGCCCTTCCCCGCAG GCTGATCCCGTCCTCCACTGAGACCTGAAAAatgCGTGAC CACATGGTCCTTCATGAGTATGTAAATGCTGCTGGGATT ACAGGTGGCGGCGCTTCAGGGCAAGGCCCAGGTCCTCC CAGGCAGGAGTGCGGAGAGCCTGCCCTGCCCTCTGCTT CTGGTA
Cyto *c* (CYCS)	GTCGGCATTAAGAAGAAGGAAGAAAGGGCAGACTTAATA GCTTATCTCAAAAAAGCTACTAATGAGGGTGGCGGCCCG TGACCACATGGTCCTTCATGAGTATGTAAATGCTGCTGG GATTACATAATAATTGGCCACTGCCTTATTTATTACAAAA CAGAAATGTCTCATGACTTTTTTATGTGTACCATC

Chapter 5

Summarizing Discussion

Amrita Jain[1]

[1]*Molecular Cell Biology Division, Department of Biology/Chemistry, University of Osnabrück, D-49076 Osnabrück, Germany*

Summarizing Discussion

Amrita Jain[1]

[1]*Molecular Cell Biology Division, Department of Biology/Chemistry, University of Osnabrück, D-49076 Osnabrück, Germany*

Apoptosis is a form of programmed cell death, by which damaged or unwanted cells are removed without damaging adjacent cells (Jacobson et al., 1997). In mammalian cells, mitochondria play a central role in initiating apoptosis in response to growth factor withdrawal, DNA damage, and other environmental and cellular stress signals. A point of no-return in mitochondrial apoptosis is an event called mitochondrial outer membrane permeabilization (MOMP) (Chipuk et al., 2006). This selective permeabilization step allows the release of the intermembrane space protein Cyto *c* into the cytosol. Cytosolic Cyto *c* interacts with apoptotic protease activating factor 1 (Apaf-1) and procaspase 9 to form the apoptosome. This complex triggers proteolytic activation of pro-caspase 9, which in turn activates the effector caspases 3, 6 and 7 to execute apoptotic cell death (Budihardjo et al., 1999). B-cell lymphoma-2 (Bcl-2) family members Bcl-2 antagonists X protein (Bax) and Bcl-2 antagonizing killer 1 (Bak) are two core components of the machinery that mediates MOMP (Wei et al., 2001). In the absence of an apoptotic stimulus, Bax and Bak constantly shuttle between the mitochondria and cytosol. Due to different rates in retrotranslocation to the cytosol, Bak predominantly resides in the outer mitochondrial membrane (OMM), whereas the bulk of Bax molecules localizes in the cytosol. Apoptotic stimuli block Bax retrotranslocation, causing Bax to accumulate in the outer mitochondria membrane and resulting in apoptotic pore formation to implement mitochondrial apoptosis (Todt et al., 2015)

While Bax and Bak actively participate in apoptosis induction, accumulating evidence indicates that intermediates of sphingolipid metabolism, notably ceramides, also play a significant role (Hannun and Obeid, 2008). For instance, cellular ceramide levels rise in response to treatment with chemotherapeutic agents such as etoposide and daunorubicin (Bose et al., 1995; Perry et al., 2000). Preventing ceramide accumulation by inhibitors of *de novo* ceramide synthesis or sphingolipid turnover renders cells resistant to these and other apoptotic stimuli. Moreover, external addition of short-chain ceramides triggers apoptotic cell death (Obeid et al., 1993). Some studies suggest that ceramides influence mitochondria-mediated cell death by sensitizing cells to ER stress and activating apoptotic regulators of the unfolded protein response (Liu et al., 2014; Swanton et al., 2007). However, experiments with isolated mitochondria suggest that ceramides, or their down stream metabolites, can initiate MOMP and trigger the release of Cyto *c* (Chipuk et al., 2012; Elrick et al., 2006). At present, the actual contribution of ceramides to the apoptotic response in living cells is unclear.

In this thesis, we set out to define where and how ceramides exert their apoptogenic

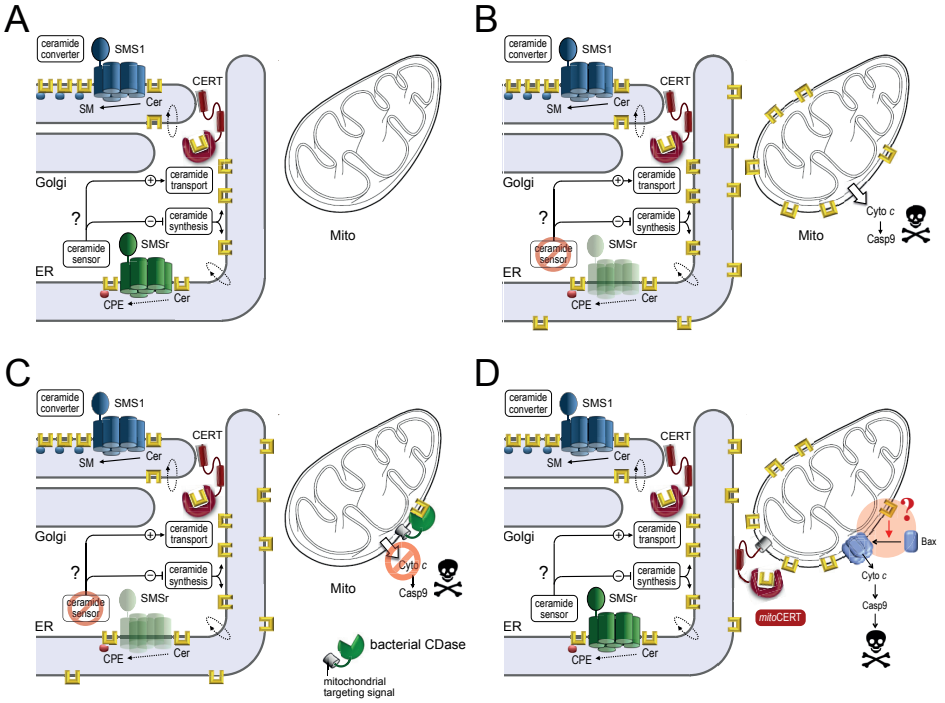

Figure 1. Mitochondrial translocation of ER ceramides triggers Bax-dependent apoptosis. (**A**) In healthy cells, newly synthesized ceramides are exported from the ER to the *trans*-Golgi by CERT for efficient production of sphingomyelin (SM) by SM synthase SMS1. An ER-resident SMS1-related protein, SMSr, produces trace amounts of the SM analog ceramide phosphoethanolamine (CPE) and acts as a negative regulator of ER ceramide levels. (**B**) Disruption of SMSr catalytic activity causes an accumulation of ER ceramides and their mislocalization to mitochondria, triggering the cytosolic release of Cyto *c*, activation of caspase 9 and apoptotic cell death. (**C**) Apoptosis induction in SMSr-deficient cells is suppressed by targeting a bacterial ceramidase (bCDase) to mitochondria. (**D**) Expression of CERT equipped with an *N*-terminal outer mitochondrial membrane anchor (mitoCERT) causes a diversion of the biosynthetic flow of ceramides from the *trans*-Golgi to mitochondria, triggering Bax-dependent apoptotic cell death.

activity in cells. As approach, we applied engineered ceramide transfer proteins and ceramide-metabolizing enzymes to acutely manipulate subcellular ceramide pools and analyze the impact of local fluctuations in ceramide levels on apoptotic signaling. As outlined below, our work provides first *in vivo* proof that intact ceramides act directly on mitochondria to trigger a Bax-dependent pathway of apoptosis. To facilitate a detailed spatiotemporal analysis of the molecular events associated with ceramide-mediated cell death, we also implemented a new strategy for GFP tagging of Bax and other components of the mitochondrial apoptotic machinery.

Ceramides trigger apoptotic cell death by acting directly on mitochondria

Ceramides are central intermediates of sphingolipid metabolism. They are synthesized *de novo* by *N*-acylation of sphingoid long chain bases on the cytosolic surface of the ER (Merrill, 2002). Newly synthesized ceramides are delivered to the *trans*-Golgi by the ceramide transfer protein, CERT. CERT contains an *N*-terminal pleckstrin homology (PH) domain that binds phosphatidylinositol-4-phosphate located on the cytosolic surface of the *trans*-Golgi. Additionally, CERT has a diphenylalanine-in-an-acidic tract (FFAT) motif that binds the ER-resident membrane proteins VAP-A and VAP-B, and a START domain that binds and transfers ceramides (Kawano et al., 2006; Kudo et al., 2008). Equipped with these dual targeting motifs, CERT is believed to shuttle newly synthesized ceramides from the ER to the *trans*-Golgi, where sphingomyelin synthase (SMS) catalyzes their conversion into sphingomyelin (SM) (Hanada, 2010). Mammalian cells contain two SMS isoforms, SMS1 in the *trans*-Golgi and SMS2 at the plasma membrane (Huitema et al., 2004; Tafesse et al., 2007). In addition, mammalian cells contain an ER-localized SMS-related protein, SMSr, which produces the SM analogue ceramide phosphoethanolamine (CPE) (Vacaru et al., 2009). As outlined in Fig. 1, our previous work revealed that acute inactivation of SMSr in mammalian cells causes an accumulation of ceramides in both the ER and mitochondria, triggering a mitochondrial pathway of apoptosis. Moreover, we found that SMSr-deficient cells can be rescued from apoptosis by blocking *de novo* ceramide synthesis or targeting a bacterial ceramidase to mitochondria. These results suggested that ER ceramides are authentic transducers of apoptosis and that their arrival in mitochondria is a critical step in committing cells to death (Tafesse et al., 2014).

In **Chapter 2**, we verified the above hypothesis by analyzing the consequences of diverting the biosynthetic ceramide flow from the *trans*-Golgi to mitochondria on cell viability. To this end, we swapped the Golgi-directed PH domain of CERT for an OMM anchor, yielding mitoCERT. We found that mitoCERT expression promotes ceramide import into mitochondria and triggers cytosolic release of Cyto *c* and activation of caspase-9, two hallmarks of mitochondrial apoptosis (Fig. 1D). Apoptosis induction could be suppressed by addition of *de novo* ceramide synthesis inhibitors (myriosin, fuminosin B12), disrupting the interaction between mitoCERT and ER-localized VAP-A, or removal of its ceramide transfer or START domain. Importantly, these results confirmed our prediction that ER ceramides become apoptogenic upon their arrival in mitochondria. Analogous to the situation in SMSr-deficient cells, apoptosis induction in mitoCERT-expressing cells was blocked by targeting a bacterial ceramidase to mitochondria (Jain et al., 2016). Importantly, the latter finding indicates that MOMP is initiated by intact ceramides. This is in sharp contrast to previous *in vitro* studies, which indicated that not ceramides, but rather their downstream metabolites, sphingosine-1-phosphate (S1P) and hexadecanal, are responsible for activating Bak and Bax to trigger MOMP in isolated mitochondria (Chipuk et al., 2012; Hollville and Martin, 2012). Potential pitfalls of such

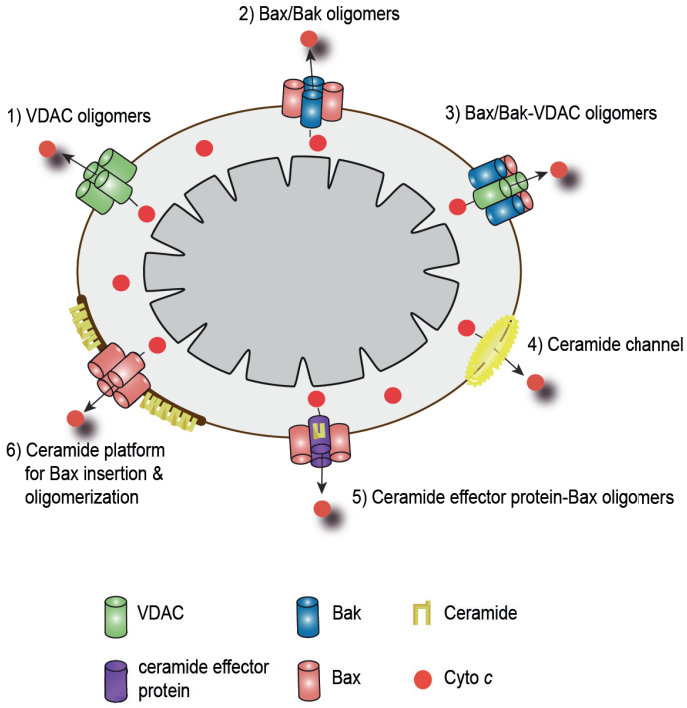

Figure 2. Ceramide-dependent and independent mechanisms for initiating MOMP. Potential mechanisms responsible for triggering mitochondrial outer membrane permeabilization (MOMP) for Cyto *c*, a point of no-return in apoptotic cell death: 1) homo-oligomerization of voltage-dependent anion channels (VDACs) into a protein-conducting pore; 2) homo-oligomerization of activated Bax (or Bak) into a protein-conducting pore; 3) hetero-oligomerization of VDACs and Bax (or Bak) into a protein-conducting pore; 4) self-assembly of ceramides into a stable, protein-conducting channel; 5) formation of Bax oligomers triggered by a ceramide effector protein embedded in the outer mitochondrial membrane (OMM); 6) formation of Bax oligomers triggered by a ceramide-enriched microdomain in the OMM. See text for further details.

studies are that the amount of externally added lipids may not correspond to physiologically relevant levels and that their partial conversion into other bioactive metabolites is hard to exclude.

Ceramide-induced apoptosis requires pro-apoptotic Bcl-2 protein Bax

We previously showed that SMSr inactivation causes a deregulation of ER ceramides and their mislocalization to mitochondria, triggering mitochondrial apoptosis (Tafesse et al., 2014). As ceramides are virtually insoluble in water, this implies the existence of a mechanism that facilitates their transfer from the ER to mitochondria. Addressing whether this

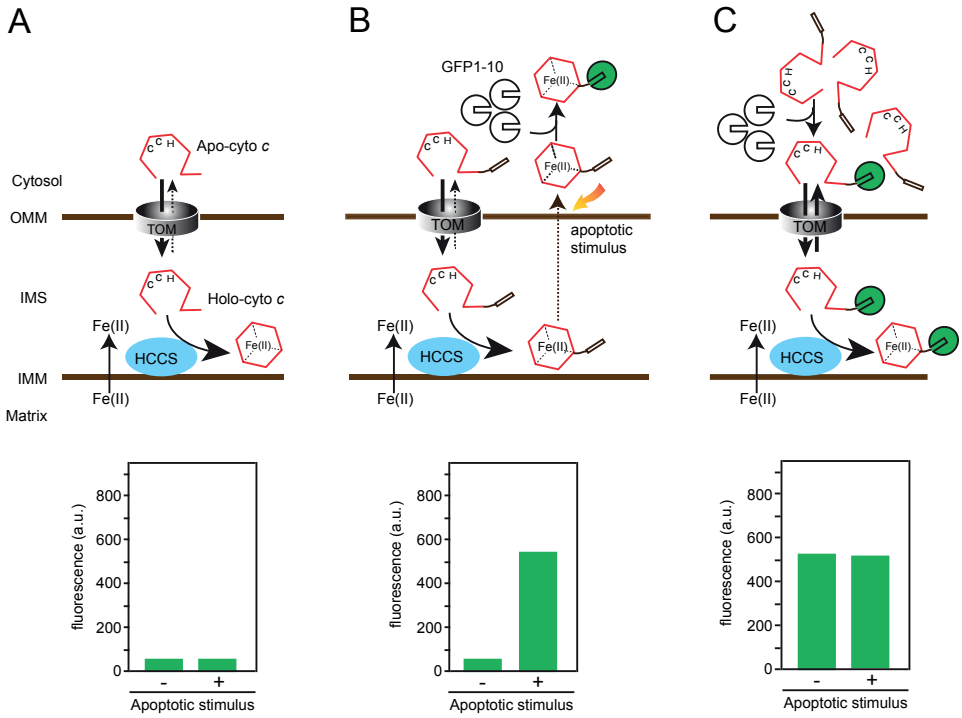

Figure 3. Real-time imaging of Cyto *c* translocation using split-GFP technology. (**A**) Schematic outline of Cyto *c* biosynthesis, which starts with *de novo* production of a polypeptide, termed apocytochrome *c* (Apo-cyto *c*), in the cytosol. Following translocation across the OMM by the TOM complex, Apo-cyto *c* is covalently linked to its ferrous [Fe(II)] heme cofactor, yielding holocytochrome *c* (Holo-cyto *c*). The heme group is attached at the cysteines of a heme-binding sequence C-X-X-C-H in Apo-cyto *c* by holocytochrome *c* synthase (HCCS), an enzyme that resides on the outer surface of the inner mitochondrial membrane. Note that attachment of the heme group traps Cyto *c* in mitochondria by preventing its back diffusion into the cytosol. (**B**) Application of split-GFP technology for real-time imaging of the cytosolic release of Cyto *c* in cells undergoing mitochondrial apoptosis. By introducing a GFP11-tag at the endogenous locus of Cyto *c* in cells expressing cytosolic GFP1-10, GFP fluorescence by functional complementation of the two GFP fragments is expected only upon induction of mitochondrial apoptosis. (**C**) Overproduction of GFP11-tagged Cyto *c* by heterologous expression from a plasmid leads to functional complementation with cytosolic GFP1-10 in the absence of an apoptotic stimulus due to saturation of HCCS, the enzyme responsible for heme attachment.

transfer occurs at intimate contacts between ER and mitochondria, involves a cytosolic transfer protein analogous to CERT, or both, will require further investigations (see also **Chapter 1**). A major outstanding question is how ceramides, upon their arrival in mitochondria, trigger MOMP and commit cells to death. In the literature, several models have been proposed on how ceramides might initiate MOMP (Fig. 2). For instance, ceramides may inhibit phosphoinositide-3 kinase (PI3K) and Akt/PKB signaling, leading to activation of the pro-apoptotic Bcl-2 protein Bad to allow Bax/Bak-mediated MOMP (Bourbon et al., 2002). Another model postulates that ceramides can self-assemble into stable channels that are large enough to allow passage of Cyto *c* (Siskind, Kolesnick, and Colombini 2006). Curiously, formation of these channels appears to be controlled by, but does not require Bcl-2 proteins (Siskind et al., 2008). However, in **Chapter 2** we demonstrate that ceramide-induced mitochondrial apoptosis is critically dependent on the pro-apoptotic Bcl-2 protein Bax, hence ruling out that initiation of MOMP in living cells relies exclusively on self-assembly of ceramides into channels.

To resolve the mechanism by which ceramides trigger Bax-dependent apoptosis, we developed a rapamycin-inducible version of mitoCERT, termed switchable CERT (sCERT). In **Chapter 3**, we showed that in response to rapamycin, sCERT-expressing cells import externally added ceramides into mitochondria. This was accompanied by mitochondrial translocation of Bax. Importantly, Bax translocation required a ceramide-transfer competent form of sCERT, indicating that the arrival of ceramides in mitochondria is key to Bax accumulation on these organelles. Moreover, mitochondrial translocation of Bax also occurred in the presence of a broad-spectrum caspase inhibitor. This indicates that ceramide-induced Bax recruitment occurs independently of a caspase-mediated amplification loop, hence in contrast to the Bax-mediated apoptotic pathways triggered by death receptors and epirubicin (Wendt et al., 2006). Besides substantiating our previous finding that mitochondrial translocation of ER ceramides triggers Bax-dependent apoptosis, the experiments described in **Chapter 3** established sCERT as a suitable new tool to dissect the underlying mechanism in real time. As these experiments relied on immunostaining of Bax in chemically fixed cells, a next challenge was to develop assays that allow one to monitor the spatial-temporal dynamics of Bax and other components of the apoptotic machinery in living cells.

Unraveling the mechanism of ceramide-induced apoptosis using switchable ceramide carriers and split-GFP technology

Several recent studies reported on the visualization of Bax recruitment and assembly in apoptotic mitochondria using heterologous GFP-fusion expression constructs (Große et al., 2016; Salvador-Gallego et al., 2016; Todt et al., 2015). However, a major drawback associated with the heterologous expression of pro-apoptotic proteins like Bax and Bak is that their overproduction is cytotoxic and induces apoptosis. To circumvent this problem, we took advantage of a recent Cas9/sgRNA-mediated knockin strategy for GFP tagging of endogenous proteins

(Leonetti et al., 2016).This approach involves the application of a split-GFP system that separates the superfolder GFP protein into two fragments, namely GFP11 (corresponding to the 11th beta-strand) and GFP1-10 (i.e. GFP without the 11th beta-strand). When co-expressed in the same cell, GFP11 recruits its non-fluorescent GFP1-10 binding partner, allowing spontaneous reconstitution of a functional (i.e. fluorescent) GFP molecule. In **Chapter 4**, we demonstrate that electroporation of Cas9/sgRNA complexes and GFP11 single-stranded DNA donors in cells that constitutively express GFP1-10 enables a functional GFP tagging of endogenous Bax, Bak and a variety of other proteins. Importantly, we also show that complementation of GFP11-tagged Bax does not interfere with its mitochondrial translocation upon apoptosis induction. Together with the establishment of switchable ceramide carriers described in **Chapter 3**, implementation of the split-GFP-based Cas9/sgRNA-mediated knockin strategy paves the way to dissect the mechanism of ceramide-induced cell death in real-time.

As Cyto *c* release from mitochondria marks a key event in the execution phase of apoptosis (Kluck et al., 1997), we also sought to exploit the split-GFP system to monitor this process in living cells. However, we found that a substantial portion of GFP11-tagged Cyto *c* produced in cells transfected with the corresponding expression construct already formed a fluorescent complex with GFP1-10 in the absence of an apoptotic stimulus (**Chapter 4**). Moreover, treatment of cells with staurosporin, a potent inducer of mitochondrial apoptosis, did not lead to the anticipated increase in GFP fluorescence. Cyto *c* biosynthesis requires translocation of a newly synthesized polypeptide, apocytochrome (Apo-cyto *c*), across the OMM followed by covalent linkage of a heme group to the cysteines of the heme-binding sequence C-X-X-C-H in the polypeptide (Thöny-Meyer, 2000). Attachment of the heme group to Apo-cyto *c* is catalyzed by Holo-cyto *c* synthase (HCCS), an enzyme that resides on the outer surface of the inner mitochondrial membrane. Heme attachment by HCCS is essential for retaining Cyto *c* in mitochondria as Apo-cyto *c* is free to diffuse back to the cytosol upon its mitochondrial import (Allen, 2011). Thus, one potential explanation for why heterologous expression of GFP11-tagged Cyto *c* results in functional complementation with GFP1-10 in the cytosol of healthy cells is that overproduction of the protein may saturate the reaction catalyzed by HCCS (Fig. 3). Therefore, our current efforts are aimed at GFP11-tagging of Cyto *c* at its genomic locus.

Model of how ceramides may trigger Bax-dependent apoptosis

In healthy cells, Bax constantly shuttles between the cytosol and mitochondria, maintaining a dynamic equilibrium whereby the bulk of the protein is found in the cytosol (Schellenberg et al., 2013; Todt et al., 2015). Single amino acid substitutions in its *C*-terminal helix can cause Bax to become permanently associated with mitochondria or abolish OMM binding all together (Nechushtan et al., 1999). When Bax retro-translocation is compromised, Bax accumulates on the OMM but still requires further stimulation

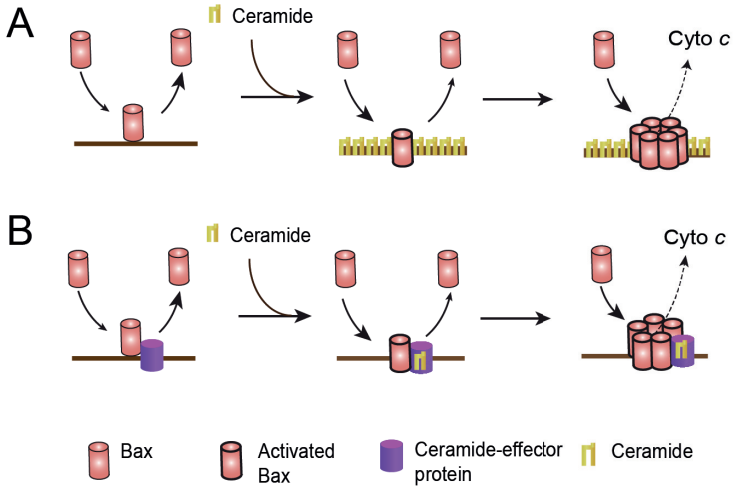

Figure 4. Models of how ceramides may trigger Bax-dependent apoptosis. In healthy cells, pro-apoptotic Bcl-2 protein Bax constantly shuttles between the cytosol and the OMM, with the high rate of retro-translocation being responsible for stabilization of cytosolic Bax. Ceramides arriving in the OMM reduce the rate of Bax retro-translocation by: (**A**) directly promoting its insertion into the bilayer through specific interactions between protein and lipid, or ceramide-induced changes in biophysical properties of the bilayer that favor this process; or (**B**) acting via other OMM-resident proteins like VDAC2, which is known to act as a mitochondrial platform for Bax retro-translocation. See text for further details.

to fully exert its pro-apoptotic activity, which involves membrane insertion and self-assembly into a pore that permeabilizes the OMM for Cyto *c* (Große et al., 2016; Salvador-Gallego et al., 2016). Pro-survival Bcl-2 proteins keep Bax in check by stimulating its retro-translocation into the cytosol through interactions occurring on the OMM (Schellenberg et al., 2013). Based on the data presented in this thesis, we postulate that ceramides arriving in the OMM trigger apoptosis by blocking retro-translocation of Bax. There are at least two potential mechanisms by which this could be accomplished (Fig. 4). First, ceramides may directly facilitate insertion of Bax into the OMM through specific molecular interactions or by altering the lateral organization or intrinsic curvature of the membrane to favor this process. Indeed, ceramide-rich macrodomains in the OMM have been proposed to functionalize Bax during radiation-induced apoptosis (Lee et al., 2011). Alternatively, ceramides could act through other OMM-resident proteins that control Bax retro-translocation. A potential candidate for such ceramide-dependent effector protein is the voltage-dependent anion channel VDAC2, which has recently been reported to serve as a mitochondrial platform for Bax retro-translocation (Lauterwasser et al., 2016). Bax retro-translocation is also subject to regulation by Bak, the adenine nucleotide

transporter (ANT), cyclophilin D and Tom22 (Cartron et al., 2008; Crompton, 2000). Consequently, it would be interesting to explore whether any of these Bax-interaction partners have affinity for ceramides.

Conclusion and future perspectives

In conclusion, the present study provides direct *in vivo* evidence that ceramides are potent transducers of mitochondrial apoptosis that act through a Bax-mediated pathway. The development of drug-inducible ceramide carrier proteins combined with the implementation of a novel approach to visualize apoptotic machinery in action in living cells now provides a great starting point to further unravel the mechanism by which ceramides can commit cells to death.

REFERENCES

Allen, J. W. A. (2011). Cytochrome c biogenesis in mitochondria - Systems III and V. *FEBS J.* **278**, 4198–4216.

Bose, R., Verheij, M., Haimovitz-Friedman, A., Scotto, K., Fuks, Z. and Kolesnick, R. (1995). Ceramide synthase mediates daunorubicin-induced apoptosis: an alternative mechanism for generating death signals. *Cell* **82**, 405–14.

Bourbon, N. A., Sandirasegarane, L. and Kester, M. (2002). Ceramide-induced inhibition of Akt is mediated through protein kinase Czeta: implications for growth arrest. *J. Biol. Chem.* **277**, 3286–92.

Budihardjo, I., Oliver, H., Lutter, M., Luo, X. and Wang, X. (1999). Biochemical Pathways of Caspase Activation During Apoptosis. *Annu. Rev. Cell Dev. Biol.* **15**, 269–290.

Cartron, P.-F., Bellot, G., Oliver, L., Grandier-Vazeille, X., Manon, S. and Vallette, F. M. (2008). Bax inserts into the mitochondrial outer membrane by different mechanisms. *FEBS Lett.* **582**, 3045–3051.

Chipuk, J. E., Bouchier-Hayes, L. and Green, D. R. (2006). Mitochondrial outer membrane permeabilization during apoptosis: the innocent bystander scenario. *Cell Death Differ.* **13**, 1396–1402.

Chipuk, J. E., McStay, G. P., Bharti, A., Kuwana, T., Clarke, C. J., Siskind, L. J., Obeid, L. M. and Green, D. R. (2012). Sphingolipid metabolism cooperates with BAK and BAX to promote the mitochondrial pathway of apoptosis. *Cell* **148**, 988–1000.

Crompton, M. (2000). Bax, Bid and the permeabilization of the mitochondrial outer membrane in apoptosis. *Curr. Opin. Cell Biol.* **12**, 414–419.

Elrick, M. J., Fluss, S. and Colombini, M. (2006). Sphingosine, a Product of Ceramide Hydrolysis, Influences the Formation of Ceramide Channels. *Biophys. J.* **91**, 1749–1756.

Große, L., Wurm, C. A., Brüser, C., Neumann, D., Jans, D. C. and Jakobs, S. (2016). Bax assembles into large ring-like structures remodeling the mitochondrial outer membrane in apoptosis. *EMBO J.* **35**, 402–413.

Hanada, K. (2010). Intracellular trafficking of ceramide by ceramide transfer protein. *Proc. Jpn. Acad. Ser. B. Phys. Biol. Sci.* **86**, 426–37.

Hannun, Y. A. and Obeid, L. M. (2008). Principles of bioactive lipid signalling: lessons from sphingolipids. *Nat. Rev. Mol. Cell Biol.* **9**, 139–150.

Hollville, E. and Martin, S. J. (2012). Greasing the Path to BAX/BAK Activation.

Huitema, K., van den Dikkenberg, J., Brouwers, J. F. H. M. and Holthuis, J. C. M. (2004). Identification of a family of animal sphingomyelin synthases. *EMBO J.* **23**, 33–44.

Jacobson, M. D., Weil, M. and Raff, M. C. (1997). Programmed cell death in animal development. *Cell* **88**, 347–54.

Jain, A., Beutel, O., Ebell, K., Korneev, S. and Holthuis, J. C. M. (2016). Diverting CERT-mediated ceramide transport to mitochondria triggers Bax-dependent apoptosis. *J. Cell Sci.*

Kawano, M., Kumagai, K., Nishijima, M. and Hanada, K. (2006). Efficient trafficking of ceramide from the endoplasmic reticulum to the Golgi apparatus requires a VAMP-associated protein-interacting FFAT motif of CERT. *J. Biol. Chem.* **281**, 30279–88.

Kluck, R. M., Bossy-Wetzel, E., Green, D. R. and Newmeyer, D. D. (1997). The release of cytochrome c from mitochondria: a primary site for Bcl-2 regulation of apoptosis. *Science* **275**, 1132–6.

Kudo, N., Kumagai, K., Tomishige, N., Yamaji, T., Wakatsuki, S., Nishijima, M., Hanada, K. and Kato, R. (2008). Structural basis for specific lipid recognition by CERT responsible for nonvesicular trafficking of ceramide. *Proc. Natl. Acad. Sci. U.*

S. A. **105**, 488–93.

Lauterwasser, J., Todt, F., Zerbes, R. M., Nguyen, T. N., Craigen, W., Lazarou, M., van der Laan, M. and Edlich, F. (2016). The porin VDAC2 is the mitochondrial platform for Bax retrotranslocation. *Sci. Rep.* **6**, 32994.

Lee, H., Rotolo, J. A., Mesicek, J., Penate-Medina, T., Rimner, A., Liao, W.-C., Yin, X., Ragupathi, G., Ehleiter, D., Gulbins, E., et al. (2011). Mitochondrial Ceramide-Rich Macrodomains Functionalize Bax upon Irradiation. *PLoS One* **6**, e19783.

Leonetti, M. D., Sekine, S., Kamiyama, D., Weissman, J. S. and Huang, B. (2016). A scalable strategy for high-throughput GFP tagging of endogenous human proteins . *Manuscript* 1–23.

Liu, J., Gaj, T., Patterson, J. T., Sirk, S. J. and Barbas, C. F. (2014). Cell-penetrating peptide-mediated delivery of TALEN proteins via bioconjugation for genome engineering. *PLoS One* **9**, e85755.

Merrill, A. H. (2002). De novo sphingolipid biosynthesis: a necessary, but dangerous, pathway. *J. Biol. Chem.* **277**, 25843–6.

Nechushtan, A., Smith, C. L., Hsu, Y.-T. and Youle, R. J. (1999). Conformation of the Bax C-terminus regulates subcellular location and cell death. *EMBO J.* **18**, 2330–2341.

Obeid, L. M., Linardic, C. M., Karolak, L. A. and Hannun, Y. A. (1993). Programmed cell death induced by ceramide. *Science* **259**, 1769–71.

Perry, D. K., Carton, J., Shah, A. K., Meredith, F., Uhlinger, D. J. and Hannun, Y. A. (2000). Serine palmitoyltransferase regulates de novo ceramide generation during etoposide-induced apoptosis. *J. Biol. Chem.* **275**, 9078–84.

Salvador-Gallego, R., Mund, M., Cosentino, K., Schneider, J., Unsay, J., Schraermeyer, U., Engelhardt, J., Ries, J. and Garcia-Saez, A. J. (2016). Bax assembly into rings and arcs in apoptotic mitochondria is linked to membrane pores. *EMBO J.* **35**, 389–401.

Schellenberg, B., Wang, P., Keeble, J. A., Rodriguez-Enriquez, R., Walker, S., Owens, T. W., Foster, F., Tanianis-Hughes, J., Brennan, K., Streuli, C. H., et al. (2013). Bax exists in a dynamic equilibrium between the cytosol and mitochondria to control apoptotic priming. *Mol. Cell* **49**, 959–71.

Siskind, L. J., Kolesnick, R. N. and Colombini, M. (2006). Ceramide forms channels in mitochondrial outer membranes at physiologically relevant concentrations. *Mitochondrion* **6**, 118–125.

Siskind, L. J., Feinstein, L., Yu, T., Davis, J. S., Jones, D., Choi, J., Zuckerman, J. E., Tan, W., Hill, R. B., Hardwick, J. M., et al. (2008). Anti-apoptotic Bcl-2 Family Proteins Disassemble Ceramide Channels. *J. Biol. Chem.* **283**, 6622–30.

Swanton, C., Marani, M., Pardo, O., Warne, P. H., Kelly, G., Sahai, E., Elustondo, F., Chang, J., Temple, J., Ahmed, A. A., et al. (2007). Regulators of Mitotic Arrest and Ceramide Metabolism Are Determinants of Sensitivity to Paclitaxel and Other Chemotherapeutic Drugs. *Cancer Cell* **11**, 498–512.

Tafesse, F. G., Huitema, K., Hermansson, M., Ne Van Der Poel, S., Van Den Dikkenberg, J., Uphoff, A., Somerharju, P. and Holthuis, J. C. M. (2007). Both Sphingomyelin Synthases SMS1 and SMS2 Are Required for Sphingomyelin Homeostasis and Growth in Human HeLa Cells * □ S.

Tafesse, F. G., Vacaru, A. M., Bosma, E. F., Hermansson, M., Jain, A., Hilderink, A., Somerharju, P. and Holthuis, J. C. M. (2014). Sphingomyelin synthase-related protein SMSr is a suppressor of ceramide-induced mitochondrial apoptosis. *J. Cell Sci.* **127**,.

Thöny-Meyer, L. (2000). Haem-polypeptide interactions during cytochrome c maturation. *Biochim. Biophys. Acta - Bioenerg.* **1459**, 316–324.

Todt, F., Cakir, Z., Reichenbach, F., Emschermann, F., Lauterwasser, J., Kaiser, A., Ichim, G., Tait, S. W., Frank, S., Langer, H. F., et al. (2015). Differential retrotranslocation of mitochondrial Bax and Bak. *EMBO J.* **34**, 67–80.

Vacaru, A. M., Tafesse, F. G., Ternes, P., Kondylis, V., Hermansson, M., Brouwers, J.

F. H. M., Somerharju, P., Rabouille, C. and Holthuis, J. C. M. (2009). Sphingomyelin synthase-related protein SMSr controls ceramide homeostasis in the ER. *J. Cell Biol.* **185**,.

Wei, M. C., Zong, W. X., Cheng, E. H., Lindsten, T., Panoutsakopoulou, V., Ross, A. J., Roth, K. A., MacGregor, G. R., Thompson, C. B. and Korsmeyer, S. J. (2001). Proapoptotic BAX and BAK: A Requisite Gateway to Mitochondrial Dysfunction and Death. *Science (80-.).* **292**, 727–730.

Wendt, J., Radetzki, S., von Haefen, C., Hemmati, P. G., Güner, D., Schulze-Osthoff, K., Dörken, B. and Daniel, P. T. (2006). Induction of p21CIP/WAF-1 and G2 arrest by ionizing irradiation impedes caspase-3-mediated apoptosis in human carcinoma cells. *Oncogene* **25**, 972–980.

Appendix

Nederlandse Samenvatting

Apoptose is een vorm van geprogrammeerde celdood, met behulp waarvan beschadigde of ongewenste cellen worden verwijderd, zonder daarbij andere cellen in de directe omgeving te beschadigen. In zoogdiercellen spelen mitochondriën een centrale rol bij het initiëren van apoptose. Dit proces kan plaatsvinden als reactie op bijvoorbeeld het ontbreken van groeifactoren, ontstane schade aan het DNA, of andere omgevings- en cellulaire stresssignalen. Een onomkeerbare stap in de mitochondriale apoptose is een gebeurtenis genaamd *mitochondriale buitenmembraanpermeabilisatie* (mitochondrial outer membrane permeabilisation, afgekort MOMP). Deze selectieve permeabilisatiestap veroorzaakt het vrijkomen van *Cytochroom c* in het cytosol. Daar aangekomen vormt *Cytochroom c* met *apoptotische protease-activerende factor 1* (Apaf-1) en *procaspase 9* het zogenaamde apoptosoom. De vorming van dit complex leidt tot proteolytische activering van *pro-caspase 9*, dat op zijn beurt de *effector caspases 3, 6 en 7* activeert, die daarna de apoptose uitvoeren.

Eiwitten van de familie *Bax* (B-cel lymfoom-2 antagonist X-eiwit) en en *Bak* (B-cel lymfoom-2 antagonist Killer) zijn twee kerncomponenten van het mechanisme dat MOMP bewerkstelligt. *Bax* en *Bak* zijn beide in een dynamisch evenwicht tussen localisatie aan het mitochondrion en in het cytosol. Echter, vanwege het verschil in de snelheid van retrotranslocatie naar het cytosol, bevindt Bak zich voornamelijk op de buitenste mitochondriale membraan (mitochondrial outer membrane - MOM), terwijl het grootste deel van Bax-moleculen cytosolisch gelokaliseerd zijn. Apoptotische stimuli echter blokkeren de retrotranslocatie van Bax, waardoor dit aan de MOM accumuleert. Dit resulteert in MOMP en daarmee apoptose. Naast Bax en Bak blijken ook tussenproducten van sfingolipide metabolisme, met name ceramides, een belangrijke rol te spelen in het veroorzaken van apoptose. Tijdens de behandeling van kanker, bijvoorbeeld door toepassing van chemokuren of radioactieve bestraling, is de hoeveelheid ceramide in het endoplasmatisch reticulum (ER) vaak drastisch verhoogd. Wanneer deze verhoging van ceramide concentraties in het ER geblokkeerd wordt, dan worden daarmee de kankercellen resistent tegen de behandeling. Dit geeft aan dat ceramiden noodzakelijk zijn om mitochondriale apoptose te veroorzaken.

Sommige studies wijzen erop dat ceramiden dit proces beïnvloeden door cellen gevoeliger te maken voor ER-stress en door de apoptotische regulatoren van de *ontvouwde eiwitrespons* te activeren. Echter, experimenten met geïsoleerde mitochondriën hebben laten zien dat ceramiden in staat zijn om de uitvoeringsfase van de apoptose te initiëren door MOMP. Hoewel ceramides momenteel veel aandacht trekken als mogelijke tumorsuppressor-lipiden, is nog steeds onvoldoende duidelijk waar en hoe deze biomoleculen hun apoptogene activiteit in cellen uitoefenen.

Het eiwit SMSr (SAMD8), een ER-resident ceramide phosphoethanolamine synthase, functioneert als een repressor van ceramide-gemedieerde apoptose. Het blokkeren van de katalytische activiteit van SMSr veroorzaakt een stijging van ceramiden in het ER

en hun mislokalisatie in het mitochondrion, wat uiteindelijk leidt tot mitochondriale apoptose. Het blokkeren van *de novo* synthese van ceramiden, het stimuleren van ceramide export uit het ER, of de aanwezigheid van een bacteriële ceramidase op mitochondriën, behoeden SMSr-deficiënte cellen voor apoptose. Deze bevindingen suggereren dat ER ceramides authentieke mediatoren van apoptose zijn, en dat hun aankomst in mitochondriën een cruciale stap is om cellen tot apoptose aan te zetten. Het hoofddoel van dit proefschrift was om deze voorspellingen te verifiëren en nieuwe benaderingen te ontwikkelen om het mechanisme te ontrafelen waardoor ceramides de apoptose veroorzaken.

In hoofdstuk 2 analyseerden we, in de levende cel, de gevolgen van het exporteren van nieuw gesynthetiseerde ceramides naar mitochondriën met behulp van een ceramide transfer eiwit uitgerust met een buiten mitochondriaal membraan anker, mitoCERT. We tonen aan dat expressie van mitoCERT ceramide-gemedieerde mitochondriale apoptose veroorzaakt, waarvoor bovendien *Bax* vereist is. Deze bevindingen complementeren eerder gepubliceerde *in vitro* onderzoeken waarin al werd aagetoond dat ceramiden direct op mitochondriën kunnen inwerken en daarmee uiteindelijke permeabilisatie van de buitenmembraan bevorderen.

Van *Bax* en zijn structurele homoloog *Bak* wordt verondersteld dat ze direct betrokken zijn bij MOMP door proteolipide poriën te creëren die verantwoordelijk zijn voor het vrijkomen van *cytochroom c*. Om het mechanisme, hoe ceramiden Bax-afhankelijke apoptose activeren, verder te onderzoeken, ontwikkelden we een omschakelbare versie van CERT, sCERT, met behulp van FKB-FRBP chemische dimeratietechnologie. In hoofdstuk 3 tonen we aan dat in reactie op rapamycine, sCERT aan de mitochondriën gerecruteerd wordt en daar het transport van ceramiden naar mitochondriën bevordert. Deze mitochondriale localisatie van sCERT veroorzaakt translocatie van Bax naar mitochondriën. We laten hier ook zien dat het vermogen van sCERT om mitochondriale translocatie van Bax te veroorzaken compleet afhankelijk is van CERTs ceramide transfer domein, wat bevestigt dat de inkomende stroom van ceramide in mitochondriën specifiek Bax activeert om daarmee de apoptose in te leiden.

Om uiteindelijk te komen tot een een gedetailleerde spatiotemporele analyse van Bax, en van andere eiwitten die bij ceramide-geïnduceerde celdood betrokken zijn, hebben we een strategie onwikkeld, waarbij met behulp van Cas9 / sgRNA techniek endogene eiwitten gelabeled worden met een korte aminozuursequentie. Deze sequentie complementeert een non-fluorescent GFP-molecuul (apart in de cel tot expressie gebracht), wat daardoor fluorescent wordt en zodoende gedetecteerd kan worden. In hoofdstuk 4 rapporteren we over de GFP-labeling van Bax en van andere componenten van de mitochondriale apoptose. Hiermee kunnen de verschillende eiwitten in de (nog) levende cel gevolgd worden en kan zodoende het mechanisme verder in kaart worden gebracht.

In hoofdstuk 5 bespreken we de algemene implicaties van de gegevens die in dit proefschrift zijn gepresenteerd, en wordt een model voorgesteld dat verklaart hoe ceramides van het ER de associatie van Bax met de MOM bewerkstelligen, en hoe daarna de porie in de MOM wordt gevormd waardoor mitochondriale eiwitten in het cysosol terchtkomen en daar de caspases activeren. Ook wordt vooruitgeblikt naar een experiment, gericht op het identificeren van de ceramide effectoren of -sensoren in de MOM, die betrokken zijn mitochondriale apoptose.

Deutsche Zusammenfassung

Apoptose ist eine Form des programmierten Zelltods, durch die beschädigte oder unerwünschte Zellen entfernt werden, ohne dabei benachbarte Zellen zu schädigen. In Säugetierzellen spielen Mitochondrien bei der Initiierung von Apoptose eine zentrale Rolle. Apoptose wird dabei als Reaktion auf den Entzug von Wachstumsfaktoren, DNA-Schädigungen und durch Umwelt- und zelluläre Stresssignale ausgelöst. Ein irreversibles Ereignis in der mitochondrialen Apoptose ist die Permeabilisierung der äußeren Membran (MOMP). Dieser selektive Permeabilisierungsschritt ermöglicht die Freisetzung des Intermembranproteins Cytochrom c (Cyto c) in das Zytosol. Zytosolisches Cyto c interagiert mit dem apoptotischen Proteaseaktivierungsfaktor 1 (Apaf-1) und Procaspase 9, um das Apoptosom zu bilden. Dieser Komplex löst die proteolytische Aktivierung von Pro-Caspase 9 aus, die wiederum die Effektor-Caspasen 3, 6 und 7 aktiviert, die den apoptotischen Zelltod initiieren. Die B-Zell-Lymphom-2 (Bcl-2) Familienmitglieder Bcl-2-Antagonisten X-Protein (Bax) und Bcl-2-Antagonistenkiller 1 (Bak) sind zwei Kernkomponenten der apoptotischen Maschinerie, die MOMP vermittelt. In Abwesenheit eines apoptotischen Reizes pendeln Bax und Bak stetig zwischen den Mitochondrien und dem Cytosol. Aufgrund unterschiedlicher Raten bei der Retrotranslokation zum Cytosol liegt Bak überwiegend in der äußeren mitochondrialen Membran (OMM) vor, während der Großteil der Bax-Moleküle im Cytosol lokalisiert ist. Apoptotische Stimuli blockieren die Bax-Retrotranslokation, wodurch Bax in der äußeren mitochondrialen Membran akkumuliert, die apoptotische Porenbildung initiiert und schließlich zur mitochondrialen Apoptose führt.

Während Bax und Bak aktiv an der Initiierung von Apoptose beteiligt sind, zeigen andere Untersuchungen, dass Zwischenprodukte des Sphingolipid-Metabolismus, insbesondere Ceramide, auch eine bedeutende Rolle spielen. Eine Abnahme des Ceramidspiegels im ER wird häufig mit der Induktion der mitochondrialen Apoptose in Reaktion auf Chemotherapeutika, Strahlen- und anderen Anti-Krebs-Therapien in Verbindung gebracht.

Interventionen, die Ceramid-Akkumulation unterdrücken, führen dazu, dass die Zellen resistent gegen diese apoptotischen Reize sind. Dies weist darauf hin, dass Ceramide allein ausreichend sowie notwendig sind, um den mitochondrial vermittelten Zelltod auszulösen. Einige Studien zeigen, dass Ceramide diesen Prozess beeinflussen, indem sie Zellen auf ER-Stress sensibilisieren und apoptotische Regulatoren der ungefalteten Proteinantwort aktivieren. Allerdings zeigen Experimente mit isolierten Mitochondrien, dass Ceramide in der Lage sind, Apoptose zu initiieren, indem sie durch eine Permeabilisierung der äußeren mitochondrialen Membran, direkt die Freisetzung von pro-apoptotischen Intermembranproteinen ermöglichen. Während Ceramide derzeit eine starke Aufmerksamkeit als mutmaßliche Tumorsuppressor-Lipide erhalten, ist noch unklar wie diese Biomoleküle ihre apoptogene Aktivität in Zellen ausüben.

Wir haben vor kurzem SMSr (SAMD8), eine ER-residente Ceramid-Phosphoethanolamin-Synthase, als Suppressor des Ceramid-vermittelten Zelltods identifiziert. Die Störung der katalytischen Aktivität von SMSr bewirkt einen Anstieg der ER-Ceramide und deren Fehlleitung zu den Mitochondrien, wo sie eine mitochondriale Apoptose auslösen. Infolge einer Blockierung der *de novo* Ceramidsynthese, der Stimulierung des Ceramid-Export aus dem ER oder die Translokation einer bakteriellen Ceramidase zu den Mitochondrien, werden SMSr-defiziente Zellen vor Apoptose gerettet.

Diese Ergebnisse deuten darauf hin, dass ER-Ceramide Signalgeber der Apoptose sind und dass ihr Eintritt in Mitochondrien ein entscheidender Schritt ist, der zum Zelltod führt. Das Hauptziel dieser Arbeit war es, diese Hypothesen zu verifizieren und neue Ansätze zu entwickeln, um den Mechanismus zu entschlüsseln, durch den Ceramide den apoptotischen Zelltod auslösen.

In Kapitel 2 analysieren wir die Konsequenzen der Fehlleitung von neu synthetisierten Ceramiden zu den Mitochondrien. Dies erfolgt unter Verwendung eines Ceramid-Transferproteins, das mit mitoCERT, einem äußeren mitochondrialen Membrananker, ausgestattet ist. Wir zeigen, dass die MitoCERT-Expression einen Ceramid-vermittelten mitochondrialen Weg der Apoptose aktiviert, der das pro-apoptotische Bcl-2-Protein Bax erfordert. Unsere Ergebnisse ergänzen und erweitern die bisherigen *In-vitro*-Studien, die sich mit der Frage beschäftigen, wie Ceramide direkt auf Mitochondrien wirken können und dadurch die äußere Membranpermeabilisierung fördern. Die Permeabilisierung der Membran führt zur Freisetzung von Cytochrom-c-, Caspaseaktivierung und dem Zelltod.

Bax und sein struktureller Homolog Bak scheinen direkten Einfluss auf die Permeabilisierung der äußeren mitochondrialen Membran zu nehmen, indem sie proteolipid Poren ausbilden, die für die Freisetzung von Cytochrom c verantwortlich sind. Um den Mechanismus weiter zu verstehen, durch welchen Ceramide die Bax-abhängige Apoptose aktivieren, haben wir eine schaltbare Version von CERT, sCERT, mit der chemischen Dimerisierungstechnologie von FKB-FRBP entwickelt. In Kapitel 3 zeigen wir, dass sCERT leicht auf Mitochondrien geleitet werden kann, um den mitochondrialen Ceramidimport, als Reaktion auf Rapamycin, zu fördern. Mitochondriale Rekrutierung von sCERT induziert die Translokation von Bax zu Mitochondrien. Die Fähigkeit von sCERT, mitochondriale Translokation von Bax zu induzieren, beruht auf ihrer Ceramid-Transferdomäne. Hierdurch wird bestätigt, dass der Eintritt von Ceramiden in Mitochondrien Bax aktiviert, um Apoptose auszulösen.

Um eine detaillierte räumliche und zeitliche Analyse von Bax und anderen aktiven Teilnehmern am Ceramid-induzierten Zelltod zu ermöglichen, haben wir eine Split-GFP-basierte Cas9 / sgRNA-vermittelte Knockin-Strategie für die GFP-Markierung

von endogenen Proteinen implementiert. In Kapitel 4 berichten wir über die funktionelle GFP-Markierung von Bax und zusätzlichen Komponenten der mitochondrialen apoptotischen Maschinerie und damit den Weg, den Mechanismus des Ceramid-induzierten Zelltods in Echtzeit zu analysieren.

In Kapitel 5 diskutieren wir die allgemeine Bedeutung der in dieser Arbeit präsentierten Daten und schlagen ein Modell vor, in dem erklärt wird, wie ER-Ceramide die Bax-Insertion auf die äußere mitochondriale Membran vermitteln. Hierbei kommt es zur Ausbildung eines apoptotischen Porenkomplexes, der mitochondriale Proteine in das Cytosol freisetzt und zur Aktivierung von Caspase führt. Wir erläutern einige Perspektiven für das zukünftige Experiment, das darauf abzielt, den Ceramideffektor / -Sensor bei der äußeren mitochondrialen Membran zu identifizieren, der an der Ausführungsphase der Ceramid-vermittelten mitochondrialen Apoptose beteiligt ist.

हिंदी सारांश

कोशिका सजीवों के शरीर की रचनात्मक और क्रियात्मक इकाई है और प्राय: स्वत: जनन की सामर्थ्य रखती है। 'कोशिका' का अंग्रेजी शब्द *सेल* लैटिन भाषा के 'शेलुला' शब्द से लिया गया है जिसका अर्थ 'एक छोटा कमरा' है। कुछ सजीव जैसे जीवाणुओं के शरीर एक ही कोशिका से बने होते हैं, उन्हें एककोशकीय जीव कहते हैं जबकि कुछ सजीव जैसे मनुष्य का शरीर अनेक कोशिकाओं से मिलकर बना होता है उन्हें बहुकोशकीय सजीव कहते हैं।

जिस प्रकार शरीर के विभिन्न अंग भिन्न-भिन्न कार्य करते हैं, उसी प्रकार कोशिका के अन्दर स्थित संरचनाएँ विशिष्ट कार्य करती हैं। अतः इन संरचनाओं को कोशिकांग कहते हैं। कोशिका के बाहरी आवरण को कोशिकावरण या कोशिका-झिल्ली कहते हैं यह झिल्ली अवकलीय पारगम्य होती है जिसका अर्थ है कि यह झिल्ली किसी पदार्थ (अणु या आॅयन) को मुक्त रूप से पार होने देती है, सीमित मात्रा में पार होने देती है या बिल्कुल रोक देती है। इसे 'जीवद्रव्य कला' भी कहा जाता है। कोशिका-झिल्ली की संरचना में एक प्रकार की वसा स्फिंगोमाईलिन महत्वपूर्ण है, जो कोशिका को बाहरी हानिकारक तत्वों से सुरक्षा प्रदान करता है। स्फिंगोमाईलिन के संश्लेषण में सिरमाइड प्राथमिक घटक हैं। जहाँ एक ओर स्फिंगोमाईलिन कोशिका की संरचना एवं कार्यविधि के लिए आवश्यक है वहीं इसका प्राथमिक घटक सीरामाईड कोशिका के लिए हानिकारक होता है, इसलिए सीरामाईड का संतुलित स्तर बनाए रखना कोशिका के लिए अत्यंत आवश्यक है।

केन्सर शोध में पाया गया है कि सीरामाईड की मात्रा एवं स्थान सुनिश्चित करना कोशिका के जीवन के लिए अत्यंत आवश्यक है। कई केन्सर निवारक दवाएँ केन्सर कोशिकाओं के कोशिकांग; माईटोकान्ड्रिया में सीरामाईड के स्तर को बड़ा देती है जिससे कोशिका की म्रत्यु हो जाती है। इस तरह सीरामाईड से स्फिंगोमाईलिन के संश्लेषण की प्रक्रिया का अध्यन कर क़ेंसर के निदान के लिए कारगर दवाएँ बनाना सम्भव है।

स्फिंगोमाईलिन का संश्लेषण कोशिकांग- अंतप्रद्रव्य जालिका में प्राथमिक घटक सिरमाइड से होता है। एक सिरमाइड संवाहक प्रोटीन (CERT) सीरामाईड को अंतप्रद्रव्य जालिका से गॉल्जी में ले जाता है। गॉल्जी में स्थित स्फिंगोमाईलिन संश्लेषण प्रोटीन-१, सीरामाईड को स्फिंगोमाईलिन में परिवर्तित करता है। पूर्व समय में हमारी प्रयोगशाला में एक अन्य-स्फिंगोमाईलिन संश्लेषण प्रोटीन की खोज हुई थी, जो अंतप्रद्रव्य जालिका में स्थित होता है और सीरामाईड को सिरमाइड फ़ोस्फो एथनॉलएमीन में बदल देता है जो की स्फिंगोमाईलिन का एक अनुरूप हैं। यदि इस अन्य-स्फिंगोमाईलिन संश्लेषण प्रोटीन की क्रियाविधी बाधित कर दी जाए तो अंतप्रद्रव्य जालिका में सीरामाईड का स्तर अनियंत्रित रूप से कई गुना बढ़ जाता है और कोशिकिय म्रत्यु की प्रक्रिया

प्रारंभ हो जाता हैं। हमारा अनुमान है कि इस तरह अंतप्रद्रव्य जालिका में अनियंत्रित रूप से बढ़े हुए सीरामाईड माईटोकान्ड्रिया में पहुँच कर माईटोकान्ड्रिया-मध्यस्थ कोशिकिय म्रत्यु की प्रक्रिया का आरम्भ करते हैं। इस अनुमान को सत्यापित करने के लिए एवं सीरामाईड-उत्प्रेरित कोशिकिय म्रत्यु की प्रकिया को समझने के लिए हमने सीरामाईड संवाहक प्रोटीन (CERT) में इस तरह परिवर्तन किए ताकि वह सिरमाइड को अंतप्रद्रव्य जालिका से माईटोकान्ड्रिया में कत्रिम रूप से ले जाए। इस परिवर्तरित सीरामाईड संवाहक प्रोटीन को माईटोकान्ड्रिया-सीरामाईड संवाहक प्रोटीन (माईटो-CERT) का नाम दिया गया। हमने माईटो-CERT का प्रयोग गर्भाशय केन्सर कोशिका-हीला में किया।

पाठ-२ में हमने इस माईटो-CERT की कार्यविधि से हुए परिणाम का अध्ययन किया और पाया की यह सिरमाइड को अंतप्रद्रव्य जालिका से माईटोकान्ड्रिया तक परिवहित करने में समर्थ है जिससे केंसर कोशिका की म्रत्यु हो जाती है। इस शोध में इस अनुमान का सत्यापन किया गया कि अंतप्रद्रव्य जालिका में संश्लेतित सीरामाईड, माईटोकान्ड्रिया में पहुँच कर कोशिका म्रत्यु का कारण बनता है। इस शोध में यह भी सामने आया कि इस प्रक्रिया में एक बेक्स नामक जीवद्रव्य में स्थित प्रोटीन की महत्वपूर्ण भूमिका होती हैं।

अब बेक्स एवं सिरमाइड-उत्प्रेरित कोशिकिय म्रत्यु की प्रक्रिया का और अधिक विश्लेषण करने लिए हमने मिटो-CERT में पुनः बदलाव किए ताकि वह सीरामाईड को माईटोकान्ड्रिया तक समय निर्धारित रूप में परिवहित कर सके, इसे स्विच-CERT का नाम दिया गया। **पाठ -३** में हमने पाया कि जिन कोशिकाओं में स्विच-CERT-मध्यस्थ सीरामाईड का माईटोकान्ड्रिया में परिवहन हुआ है, उनमे केन्सर कोशिका की म्रत्यु ८ घंटे के अंदर हो गई। इस अध्ययन में यह भी सामने आया की बेक्स प्रोटीन इस प्रक्रिया में जीवद्रव्य से माईटोकान्ड्रिया में अनुगमित होता हैं जोकि माईटोकान्ड्रिया की बाहरी झिल्ली को पारगामी बना देता है, जिससे माईटोकान्ड्रिया में उपस्थित प्रोटीन जीवद्रव्य में स्थान्तरित हो कर कोशिका म्रत्यु की प्रक्रिया का आरम्भ करते हैं।

इस प्रक्रिया का विश्लेषण समय एवं स्थान-निर्धारित रूप से जीवित कोशिका में करने के उद्देश्य से हमने एक अनुवंशिकी जीन परिवर्तन तकनीक का उपयोग किया। इस प्रक्रिया में हमने कोशिका में उपस्थित बेक्स जीन के संरचना में परिवर्तन किया ताकि वह एक हरे रंग के सूचक प्रोटीन के साथ उत्पादित हो। अब इस सूचक प्रोटीन के साथ लगे बेक्स प्रोटीन को सूक्ष्मदर्शी की सहायता से जीवित कोशिका में भी देखना सम्भव हुआ। इस सफल अनुवंशिकी जीन परिवर्तन तकनीक का उपयोग कर हम सिरमाइड उत्प्रेरित कोशिका म्रत्यु का बेहतर रूप से अध्ययन करने में समर्थ हैं।

पाठ-५ में हम अन्य पाठों में विकसित तकनीको के द्वारा ज्ञात परिणामों पर विचार कर के सीरामाईड-उत्प्रेरित कोशिकिय म्रत्यु की प्रक्रिया का एक मॉडल प्रस्तावित किया है। इस शोध कार्य से सीरामाईड-उत्प्रेरित कोशिकिय म्रत्यु की प्रक्रिया को बेहतर रूप से समझने में मदद मिलीं, साथ ही इस प्रक्रिया के कई महत्वपूर्ण पहलुओं पर प्रकाश पड़ा जो केन्सर के निदान के लिए कारगर दवा बनाने में मददगार साबित हो सकते हैं।

Dankwoord

The time I had spent in the Osnabrück during my PhD gave me the opportunity to develop myself in many ways. I would like to thank some of the people here who helped me throughout this journey and made it a remarkable time of my life. I would also like to thank other people to whom somehow, I could not mention here that contributed in my scientific and personal development.

First of all, I wish to express a sincere thank to my supervisor **Joost** for giving me the opportunity to come to Osnabrück and pursue research on such an exciting topic. Thank you for providing me the support during the ups and down of the research life. I had learned a lot from you over four years both professionally and personally. You have been a source of tremendous energy for me. Your selfless time and care were sometimes all that kept me going. I wish you a lot of success in the future. Thank you!

I am thankful to **Matthijs** for forming the nice working environment in the lab, the fruitful discussions and scientific comments on my work. Thanks for being a super helpful 'Gel-Police'. I greatly appreciate your time for preparing the Dutch translation of the summary of the thesis. Thanks **Svenja** for being there whenever I need words of advice and encouragement, I am grateful for your keen ears for listening all my lab work obstacles. Also, I am thankful for critically assessing the manuscripts of the thesis-chapters. **Birol**, We nearly spent all PhD together in Osna and in the same office. You have been such a pleasant company throughout 4 years. Thanks for always ready to help me. Good luck with all your present and future projects. **RK and Mirjana**, thank you both for being a lovely company in the office with all pranks, big nose smileys and personal and professional discussions. **Sergei**, thanks for supplying the essential chemical for the experiments by your 'chemistry magic' and of course for the much-awaited rapalog☺. **John**, thanks you for always being ready to help me and taking interest in the progress of the projects. **Oli**, you are the colleague everyone wishes for; always ready to help and discuss all the scientific problems in ones mind. Your knowledge about almost everything is inspiring. It was only a short period of time we have been in the same lab, but I had learned a lot from you. **Shashank** in the last few months, we worked together on the switchable CERT project. Thanks for your efforts to improve the chapter 3. Your fresh look to the scientific problems, determination and hard work helped the project go forward. I wish all the best for completing your PhD. Thanks **Jan, Irma, Kristin** for the nice company in the office and best of luck to you all for your future endeavor. Thanks to **Dagma** for spreading happiness in the lab. I really enjoyed our endless discussion about the life, work and about everything else. Thank you for your help with ordering lab stuffs from my unending shopping list and for always ready to help me with a smile. I really enjoyed our cycling trips to Tecklenburg and music concerts in Lutherhaus. Thanks for being one of my *paranimfen*. I will also like to thank, my students, **Katharina and Evan** for their contributions in chapter 2. I would like to thank **Annie, Suzanne and Sigrid** for all the administrative work and recurring reimbursement forms.

The members of the Biochemistry group have contributed greatly to my personal and professional time at Osna. The group has been a source of friendships as well as good advice. **Kathrin, Henning, Jens,** thanks for helping with the microscopes. **Latha, Jieqiong, Pedro** and **Anna,** thanks for your help, nice talks and good times in the microscopy room. **Jannis** my CRISPR-mate in the exciting, frustrating and eureka moment journey of gene editing experiments. It was very great working with you; I wish you all the best for your thesis. I would also like to acknowledge the Biophysics department- group members and students for helping me with confocal, super resolution microscopes and data analysis. Moreover, thanks to **Rainer** for the technical assistant provided for the various microscopes setups. I would like to thank **Dr. Heiko** for his help with chemicals and advice for guided RNA preparation. I also thank **Dr. Hans-Peter** and **Dr.Jörg** for their help during the FACS enrichment experiment discussed in the chapter 4. Also I thank all the members of the **SPHINGONET**, PIs and fellows. It was indeed a great experience to be part of such an excellent scientific community.

During the PhD time people outside the lab also play an important role. I would like to thank my dear 'the Indian Group' for all the parties, amazing Indian food, memorable trips and weekend meet ups to make my life in Osna so much happening and enjoyable. **Mangesh dada** you have one of the kindest heart and fun filled soul in the world. Thanks a lot for all your help and support whenever needed. Thanks for all the great Indian food, beautiful visits to Cologne, Berlin, Hannover, late night parties and of course the casino times and many more nice times to come. **Latha**, Thanks a lot for being such a great friend and joyful time we had spent together. **Meenakshi, Arun, Eva, RK, Leoni, Madhu, Raminta, Vikash, Rajesh, Sandra,** thanks for making my initial years in Osna fun. **Anil and Nisha** you both are such an adorable couple. It was very nice to have you around during the Indian get together. **Deepak bhaiya** and **Reecha bhabhi** thanks for making Diwali celebrations memorable even being far away from home. My dear Pakistani friends in Osna, though India and Pakistan may have separated and have the conflict promoting politics in both the states but it didn't stop us from becoming friends. I am lucky to have my Pakistani friend, **Wajiha**. Thanks a lot for your friendship and firm support. I am grateful for your keen ears to all my highs and lows. I am sure we will be friends for life☺. **Sabeen** and **Farhan bhai** thank you for all amazing desi food, BBQ and special Eid celebrations. You make your life and life of people around you special, thanks for making me part of it. **Shumaila** and **Ehasan bhai** thanks for all the weekend get together at your place and amazing food. **Barbara**, thanks for the lovely company during the language classes and for the tasty Spanish tapas evening. A special thanks to the 'girl-gang' of Osna **Sabeen**, **Wajiha**, **Shumaila**, **Meenakshi**, **Latha**, **Nisha, Ankitha** for the weekend swimming turned gossiping sessions, discount shopping, make-up, dress-ups and photo-shoot sessions and many beautiful trips we had enjoyed over the last years. Thanks you all for making life is Osna such a fun. I would also like to appreciate my friends from Madurai times.

Thanks **Ria**, for the long telephone conversations and catching up about the current happening in our lives, for the beautiful trips to Amsterdam, Freiburg, Colmar and Heidelberg. I wish you all the luck for finishing your PhD and having nice time at Harvard. Thanks **Ajit** and **Ashiwini** for being such a nice friend.

Lieber **Klaus** und **Siegrid** - Meine lieben Gästeeltern! Sie sind beide die schönsten Leute, die ich kenne. Ich wusste, dass ich immer ein zweites Zuhause in Friesyothe haben würde. Vielen Dank für wunderbare X-Mas und Ester Feiern!

My very special word of thanks goes to **Ashish** for his continuous support and encouragement during my PhD. Though, Thank is the right word in this perspective, but it shares a much deeper sense when I express it to you. Thank you for your wise solutions to all my problems and making me a better person everyday. Thank you for accepting to be my *paranimfen*.

Last but not the least, I would like to thank my family for their unconditional love and support to me. I would like to dedicate this thesis to my grandfather, **Shri Vimal Chand Jain**, my **dada**. I have been extremely fortunate in my life to have grandfather who has shown absolute love and support. Thanks you for playing an important role in the development of my identity and shaping the individual that I am today. Dear Mummy (**Shrimati Sujata Jain)**, thank you so much for your unconditional love and boundless care. Though thousands of mile apart but you are always next to me- caring, loving encouraging, and supporting. You are the best mother in the world. I am blessed to be your daughter. Thank you! My dear younger brother and the oldest friend **Rajneesh** (Nanu) Thanks for always believing in me and sharing all sweet and sour time together. I wish you all the success and happiness in the life. My dear aunts, **Deva mousiji**, **Viru mousi ji**, all Mamaji and Mamiji, thank you for all your support and love. **Chintu bhaiya, Pintu Bhaiya, Ballu, Bittu, Rachana Bhabhi, Manisha bhabhi, Namish bhaiya, Tina Bhabhi, Ashwin bhaiya, Jyoti bhabhi** and all my extended family thank you all for your love, care and believing in me.

मैं यह थीसिस अपने **दादाजी (दादा)** को समर्पित करना चाहूंगी । मैं अपने जीवन में बेहद भाग्यशाली रही हूँ कि मेरे पास दादा हैं जिन्होंने मुझे बिना शर्त प्यार और समर्थन दिया। मेरी पहचान और व्यक्तित्व के विकास में एक महत्वपूर्ण भूमिका निभाने के लिए आपका बहुत धन्यवाद **!** प्रिय **मम्मी**, आपके बिना शर्त प्यार और असीम देखभाल के लिए बहुत बहुत धन्यवाद**!** हालांकि आप मुझसे हजारो मील अलग हैं लेकिन आप हमेशा मेरे पास हैं - मुझे प्रोत्साहित करने, समर्थन देने और देखभाल करने के लिए। आप दुनिया में सबसे अच्छी मां हैं मुझे आपकी बेटी होने का गर्व हैं । धन्यवाद**!** मेरे प्रिय छोटे भाई और सबसे पुराने दोस्त **रजनीश (नानू)** मुझे हमेशा प्यार करने के लिए और सभी अच्छा और बुरा समय एक साथ साझा करने के लिए धन्यवाद। मैं आशा करती हूँ कि तुम्हारे जीवन में बहुत सारी ख़ुशियाँ और सफलता आए। मेरी प्रिय देवा मोसीजी, वीरू मोसीजी, मोसाजी एवं सभी मामाजी और मामीजी

आप सभी को समर्थन और प्रेम के लिए धन्यवाद। चिटू भैया, पिटू भैया, बल्लु, बिट्टू, रचना भाभी, मनीषा भाभी, नमिष भैया, टीना भाभी और मेरे समस्त परिवार को आपके असीम प्यार के लिए धन्यवाद ।

Overall, many thanks to all who had one way or another influenced the development of the thesis. Thank you all!

About the Author

Amrita Jain was born on March 1, 1988 in Khandwa, Madhya Pradesh, India. After her pre-university schooling in Khandwa, she obtained s Bachelor of Science in the year 2009 (Biotechnology, Zoology, Chemistry) from Holkar Science collage (Affiliated to Devi Ahilya University) Indore. Her post graduation studies were done at Madurai Kamaraj University, Tamilnadu. During her studies, she was awarded with Indian Academy of Science Summer Research fellowship 2010 to pursue an internship at the International Centre for Genetic Engineering and Biotechnology, New Delhi. After receiving her Master of Science (Genomics) in the year 2011, she then spent a year as Junior Research Fellow in the Eukaryotic Gene Expression laboratory at the National Institute of Immunology, New Delhi. In September 2012, she started her PhD as a Marie Curie Initial Training Network SPHINGONET, Early stage researcher under the supervision of Prof. Joost Holthuis at the Department of Molecular Cell Biology at University of Osnabrück, Germany. The results of this research have been unified in this thesis. Below are the scientific publication related to the work presented here and her previous work.

Publications:

Jain A., Holthuis J.C.M. (2017) Membrane contact sites, ancient and central hubs of cellular lipid logistics. Invited review by BBA - Molecular Cell Research (Submitted)

Jain, A., Beutel, O., Ebell, K., Korneev, S. and Holthuis, J. C. M. (2016). Diverting CERT-mediated ceramide transport to mitochondria triggers Bax-dependent apoptosis. *J. Cell Sci.*

Periasamy, J., Muthuswami, M., Ramesh, V., Muthusamy, T., Jain, A., Ch, Karthikeyan, rabose, Trivedi, P., Kumar, R. S., Gunasekaran, P., et al. (2013). Nimesulide and Celecoxib Inhibits Multiple Oncogenic Pathways in Gastric Cancer Cells. *J. Cancer Sci. Ther.* **5**,.

Tafesse, F. G., Vacaru, A. M., Bosma, E. F., Hermansson, M., Jain, A., Hilderink, A., Somerharju, P. and Holthuis, J. C. M. (2014). Sphingomyelin synthase-related protein SMSr is a suppressor of ceramide-induced mitochondrial apoptosis. *J. Cell Sci.* **127**,.

Manuscripts in preparations:

Jain A., Dadsena S., Holthuis, J. C. M. (2017) Resolving the sequence of events in ceramide-induced apoptosis using switchable ceramide transfer proteins. (In prepration)